

CR-180827

THE BRADLEY DEPARTMENT OF ELECTRICAL ENGINEERING

VIRGINIA TECH

STUDY OF SPREAD SPECTRUM MULTIPLE ACCESS SYSTEMS FOR SATELLITE COMMUNICATIONS WITH OVERLAY ON CURRENT SERVICES

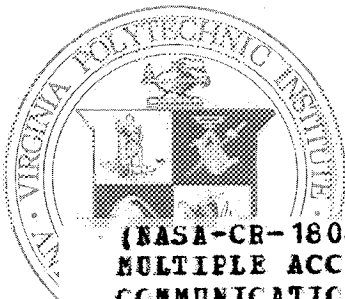
by Tri T. Ha and Timothy Pratt

VIRGINIA POLYTECHNIC INSTITUTE AND STATE UNIVERSITY
BLACKSBURG, VA 24061

prepared for

NATIONAL AERONAUTICS AND SPACE ADMINISTRATION

NASA Lewis Research Center



Contract NAS 3-24887

(NASA-CR-180827) STUDY OF SPREAD SPECTRUM
MULTIPLE ACCESS SYSTEMS FOR SATELLITE
COMMUNICATIONS WITH OVERLAY ON CURRENT
SERVICES (Virginia Polytechnic Inst. and
State Univ.) 255 p

N89-23757

Unclas
CSCL 17B G3/32 0211548

VIRGINIA POLYTECHNIC INSTITUTE AND STATE UNIVERSITY
Blacksburg, Virginia 24061 (703)961-6646

Final Report

1. Report No. CR 180-827		2. Government Accession No.		3. Recipient's Catalog No.	
4. Title and Subtitle Final Report on Contract NAS3-24887: "A Study of Spread Spectrum Multiple Access Systems for Satellite Communications with Overlay on Current Service."				5. Report Date December 1987	
				6. Performing Organization Code	
7. Author(s) Tri T. Ha, Timothy Pratt				8. Performing Organization Report No.	
				10. Work Unit No.	
9. Performing Organization Name and Address Virginia Polytechnic Institute and State University, Blacksburg, VA 24061				11. Contract or Grant No. NAS3-24887	
				13. Type of Report and Period Covered Contractor Report	
12. Sponsoring Agency Name and Address NASA Lewis Research Center Cleveland, OHIO 44135				14. Sponsoring Agency Code	
15. Supplementary Notes Project Manager: John E. Zuzek, NASA Lewis Research Center, 21000 Brookpark Rd.; Cleveland, OH 44135					
16. Abstract <p>This report investigates the feasibility of using spread spectrum techniques to provide a low-cost multiple access system for a very large number of low data terminals.</p> <p>Part A of this report presents two applications of spread spectrum technology to very small aperture terminal (VSAT) satellite communication networks. It describes two spread spectrum multiple access systems which use a form of noncoherent M-ary FSK (MFSK) as the primary modulation and analyzes their throughput. The analysis considers such factors as satellite power constraints and adjacent satellite interference. It considers the effect of on-board processing on the multiple access efficiency and investigates the feasibility of overlaying low data rate spread spectrum signals on existing satellite traffic as a form of frequency reuse.</p> <p>Part B of the report examines the use of chirp for spread spectrum communications. In a chirp communication system, each data bit is converted into one or more up or down sweeps of frequency, which spread the RF energy across a broad range of frequencies. Several different forms of chirp communication systems are considered, and a multiple-chirp coded system is proposed for overlay service. The mutual interference problem is examined in some detail and a performance analysis undertaken for the case of a chirp data channel overlaid on a video channel.</p>					
17. Key Words (Suggested by Author(s)) Spread Spectrum Multiple Access Satellite Communications Overlay Service				18. Distribution Statement	
19. Security Classif. (of this report) Unclassified		20. Security Classif. (of this page) Unclassified		21. No. of pages 236	22. Price*

Abstract

This report investigates the feasibility of using spread spectrum techniques to provide a low-cost multiple access system for a very large number of low data terminals.

Part A of this report presents two applications of spread spectrum technology to very small aperture terminal (VSAT) satellite communication networks. It describes two spread spectrum multiple access systems which use a form of noncoherent M-ary FSK (MFSK) as the primary modulation and analyzes their throughput. The analysis considers such factors as satellite power constraints and adjacent satellite interference. It considers the effect of on-board processing on the multiple access efficiency and investigates the feasibility of overlaying low data rate spread spectrum signals on existing satellite traffic as a form of frequency reuse.

Part B of the report examines the use of chirp for spread spectrum communications. In a chirp communication system, each data bit is converted into one or more up or down sweeps of frequency, which spread the RF energy across a broad range of frequencies. Several different forms of chirp communication systems are considered, and a multiple-chirp coded system is proposed for overlay service. The mutual interference problem is examined in some detail and a performance analysis undertaken for the case of a chirp data channel overlaid on a video channel.

Table of Contents

Part A. SPREAD SPECTRUM MULTIPLE ACCESS AND OVERLAY SERVICE

	PAGE
I. Introduction	2
Spread Spectrum Multiple Access	3
Overlay Service	4
II. Overview of Multiple Access and Spread Spectrum Techniques	5
Conventional Multiple Access Techniques	5
On-Board Processing	11
Overlay Systems	12
III. MFSK Spread Spectrum Multiple Access	13
Preliminaries	13
Performance Analysis	16

Multiple Access Systems	22
System 1: MFSK/DS/FDM	22
System 2: MFSK/DS/FH	23
Numerical Examples	26
Example 1: C Band System	27
Example 2: Ku Band System	27
Sample Link Analyses	32
C-band System-968 users at 1.2kbps	34
Ku-band System-57 users at 56 kbps	35
Conclusions	37
IV. Spread Spectrum Overlay Service	38
Overview	38
Comparison of Spread Spectrum Overlay Systems	39
Frequency Hopped Spread Spectrum	39
MFSK/DS Spread Spectrum Overlay	40
Direct Sequence Overlay	41
Interference Modeling	41
Modeling of Wideband Signals Passed Through Narrowband Filters	43
Modeling of Interference PSK Signals by Multiple PSK Interferers	43
Overlay System Performance Analysis	44
Overview	44
Description of Existing Signals	44
Overlay on FDM/FM/FDMA Telephone Traffic	45
FDM Overlay System: C-Band	51
Overlay of Digital SCPC System	52
SCPC Overlay System: C-band	56
Analog Television Overlay	57

Analog Television Overlay: C-band	61
Extension to Multiple Overlay Signals	62
Conclusions	62
V. On Board Processing for Multiple Access Systems	64
Introduction	64
Simple Procession Transponder	68
Dual Modulation Systems	68
MFSK/TDM Processing Transponder System	71
Ku Band MFSK/DS-TDM System: 110 users	72
VI. VSAT Networks-An Overview	74
Introduction	74
Architectures	75
Ku-Band versus C-Band	76
Power-Limited Networks	81
Spread Spectrum VSAT Networks	86
Epilogue	92
VII. Conclusions	94
IIIX. References	96
Appendix A. Performance of Noncoherent MFSK in Colored Noise	99
Appendix B. Derivation of Interference PSD	103
Appendix C. MFSK/DS/FDM Performance Analysis Program	108
Table of Contents	v

Appendix D. MFSK/DS/FH Performance Analysis Program

111

Part B. Chirp Spread Spectrum System and Overlay

Service

	PAGE
1. Introduction	117
2. Review of Chirp Spread Spectrum Systems	120
3. Coded Multiple Chirp Spread Spectrum System	127
3.1. Basic System Concept	127
3.2. Performance Analysis	131
3.2.1. System Parameters and Waveform Definitions	131
3.2.2. Cross-correlation of Up Chirp and Down Chirp	132
3.2.3. Cross-correlation between Code(Word) Sequence	136
3.2.4. Chip Error Probability(Dechirper BER)	137
3.2.5. Performance of Digital Code Correlator	142
3.2.6. Chirp Spread Spectrum Multiple Access	146
4. Overlay Service—An Overview	148
5. Interference Analysis I (General Approach)	150
5.1. Analog FM-TV Demodulation	151
5.2. Chirp Interference to Analog FM-TV Signal	151
5.3. Simulation of FM-Discriminator Output	162
5.4. Analog FM-TV Signal Interference on Chirp Demodulation	169

6. Interference Analysis II (Modeling and Simulation)	174
6.1. Analog FM-TV Signal Modeling I -- Without Preemphasis	175
6.2. Simulation of Wideband FM-TV Signal and Chirp I -- No Preemphasis	178
6.3. Analog FM-TV Signal Modeling II -- With Preemphasis	189
6.3.1. Preemphasis Characteristic	189
6.3.2. Modeling of FM-TV Video Signal	195
6.4. Wideband FM-TV Signal Simulation II -- With Preemphasis	200
6.5. Overlay System Link Analysis	203
6.5.1. FM-TV Overlay Link Analysis	204
6.5.2. Chirp S.S. Overlay Link Analysis	206
7. Performance Analysis of Overlay Service I -- Without Preemphasis	209
7.1. Signal Power Calculation	210
7.2. Interference Power Calculation	213
7.2.1. Chirp Interference to FM-TV	213
7.2.2. FM-TV Interference to Chirp	214
8. Performance Analysis of Overlay Service II -- With Preemphasis	222
8.1. Signal Power	222
8.2. Interference of Chirp to FM-TV	225
8.3. Interference of FM-TV to Chirp	225
9. Conclusions	232
10. References	233

List of Illustrations — Part A

	PAGE
Fig. 1. FDMA Signal Organization[2]	6
Fig. 2. Typical TDMA System[5]	8
Fig. 3. SSMA System Model	15
Fig. 4. SSMA System Model-N users	17
Fig. 5. MFSK Receiver Model	18
Fig. 6. Interference PSD Model	21
Fig. 7. MFSK Slot Bandwidth	24
Fig. 8. Hybrid MFSK/DS/FH SSMA System	25
Fig. 9. Performance of MFSK/DS/FDM System(C band)	28
Fig. 10. Performance of MFSK/DS/FH Systems(C band)	29

Fig. 11.	Performance of MFSK/DS/FDM Systems(Ku band)	30
Fig. 12.	Performance of MFSK/DS/FH Systems(Ku band)	31
Fig. 13.	Full Mesh Network Architecture	33
Fig. 14.	DS Overlay System	42
Fig. 15.	FDMA Existing Signal	46
Fig. 16.	DS Overlay Signal	47
Fig. 17.	Interference PSD caused by the FDMA Signal	49
Fig. 18.	SCPC Existing Signal	53
Fig. 19.	Interference PSD caused by the SCPC Signal	55
Fig. 20.	BPSK Signal Passed Through an FM Demodulator	59
Fig. 21.	Interference PSD Caused by a TV Signal	60
Fig. 22.	Classical Transponder	65
Fig. 23.	Processing Transponder	66
Fig. 24.	Multipoint to Point Network Architecture	70
Fig. 25.	Single Hop Architecture	77
Fig. 26.	Hybrid Architecture	78

Fig. 27. Full Mesh Architecture

79

Fig. 28. SSMA Modem

87

List of Illustrations — Part B

	PAGE
Fig. 1. Within Chirp Modulations	123
Fig. 2a. Multiple Chirp Modulations	124
Fig. 2b. Typical Waveforms of Multiple Chirp Modulations	125
Fig. 3a. Coded Multiple Chirp S.S. System	129
Fig. 3b. Typical Waveforms of Coded Multiple Chirp S.S. System (proposed)	130
Fig. 4. Autocorrelation (matched case) and Crosscorrelation (mismatched case)	135
Fig. 5a. Chip Error Probability of Dechirper	140
Fig. 5b. BER Comparison of Noncoherent FSK and Chirp for different BT product	141
Fig. 6. Word Miss Probability vs. Dechirper BER	144
Fig. 7. Word False Alarm Probability vs Miss Probability	145

Fig. 8.	Time waveform of FM-discriminator output error voltage for unmodulated TV carrier plus chirp interference	153
Fig. 9.	Time waveform of FM-discriminator output error voltage for FM-TV carrier plus chirp interference ($m(t) = 0.5V$ dc)	154
Fig. 10.	Simulated 9 step staircase function (time plot)	164
Fig. 11.	Received and lowpass filtered simulated 9 step staircase function	165
Fig. 12.	Error output voltage of FM-discriminator after bandpass filtering	166
Fig. 13.	Spectrum of error output after bandpass filtering (3-4 MHz)	167
Fig. 14.	Spectrum of 9 step staircase function	168
Fig. 15.	Typical compression filter output for chirp signal input	172
Fig. 16.	Compression filter output for FM-TV signal with amplitude = 0.1V	173
Fig. 17.	Time plot of simulated 200 step staircase function model for video signal	177
Fig. 18.	Time plot of simulated 256 step random amplitude model for video signal	182
Fig. 19.	Transmitted FM-TV signal time plot (random)	183
Fig. 20.	Frequency spectrum of Fig. 19 (random)	184
Fig. 21.	Transmitted FM-TV signal time plot (linear)	185
Fig. 22.	Frequency spectrum of Fig. 21 (linear)	186

Fig. 23.	Transmitted chirp signal time plot	187
Fig. 24.	Frequency spectrum of Fig. 23	188
Fig. 25.	Typical NTSC modem structure with preemphasis/deemphasis	191
Fig. 26.	TV preemphasis characteristics (525, 625, 819 and 405 lines)	192
Fig. 27.	NTSC 525 line - CCIR REC.405 preemphasis characteristics	193
Fig. 28.	Simulated preemphasis filter for NTSC 525 line TV system	194
Fig. 29.	TV message $m(t)$ before preemphasis (time plot); random amplitude	196
Fig. 30.	TV message $m(t)$ after preemphasis (time plot); random amplitude	197
Fig. 31.	TV message $m(t)$ before preemphasis (time plot); linear staircase f_n	198
Fig. 32.	TV message $m(t)$ after preemphasis (time plot); linear staircase f_n	199
Fig. 33.	Transmitted FM-TV spectrum ($m(t)$ = random, preemphasis version)	201
Fig. 34.	Transmitted FM-TV spectrum ($m(t)$ = linear, preemphasis version)	202
Fig. 35.	36dB attenuated chirp signal spectrum	212
Fig. 36.	Overlapped spectrum of FM-TV (staircase $m(t)$) and 36dB atten chirp	217
Fig. 37.	Overlapped spectrum of FM-TV (random amplitude $m(t)$) and 36dB atten chirp	218
Fig. 38.	C/I ratio vs IF offset frequency (random amplitude message and linear staircase)	221

Fig. 39.	Overlapped spectrum of FM-TV (preemphasis) and 36dB atten chirp (random)	223
Fig. 40.	Overlapped spectrum of FM-TV (preemphasis and 36dB atten chirp (linear staircase)	224
Fig. 41.	C/I ratio vs IF offset frequency (preemphasis case)	229
Fig. 42.	C/I ratio vs IF offset frequency (preemphasis case and no preemphasis case)	230
Fig. 43.	Offset (IF) frequency vs chip error rate for some compression gain	231

Summary

The major objective of this study is to investigate the feasibility of using spread spectrum techniques to provide a low-cost multiple access system for a very large number of low data rate terminals. In addition, the study also examines the feasibility of overlaying spread spectrum transmissions onto existing communications and the use of on-board processing to improve the system throughput. The report considers three spread spectrum techniques; 1) MFSK/DS, 2) hybrid MFSK/DS-FH, 3) Chirp. Part A of the report addresses mainly the first two techniques and Part B addresses the third technique.

The MFSK/DS and hybrid MFSK/DS-FH systems proposed can achieve a throughput of approximately 6-8% for Ku-band satellites and 2-3% for C-band satellites. The advantage of spread spectrum systems is that they make very small aperture terminal (VSAT) networks possible with antenna diameter less than 1.8 meters for C-band operation and when the angular satellite spacing is small, situations which makes VSAT networks infeasible for other modulations. At Ku-band, spread spectrum systems may offer a cost saving advantage over single-channel-per-carrier (SCPC) systems in a full mesh architecture. This is possible because an MFSK/DS or a PSK/DS VSAT does not require a frequency synthesizer as an SCPC VSAT does. This advantage is lost in a star architecture operating at Ku-band. The principal conclusion reached here is that VSAT networks are inherently power-limited and not bandwidth-limited, therefore it makes little difference whether non-spread spectrum or spread

**ORIGINAL PAGE IS
OF POOR QUALITY**

spectrum technology is used at Ku-band. At C-band, the use of spread spectrum technology for VSAT networks is almost unavoidable for antenna diameters less than 1.8 meters.

The use of PSK/DS overlay signals on existing traffic is also feasible. When convolutional coding is used, a data rate of 10 to 20 kbps for an overlay signal may be achieved per satellite transponder.

On-board processing has the ability to dramatically increase the throughput of spread spectrum systems (almost twice as much). But the future of on-board processing in the commercial market, however, is probably not bright because the complex on-board electronics required would make the satellite very expensive and less reliable. Furthermore, the transponder becomes dedicated to a certain type of service and hence less flexible in handling different kinds of traffic.

Chirp communication systems use swept frequency techniques to spread the RF energy across a much wider bandwidth than that occupied by the data signal. Each data bit is converted to one or more chirps, and each chirp is a linearly increasing or decreasing sweep across a predetermined RF band of frequencies. Thus all chirp systems are inherently spread spectrum. The chief advantage which chirp offers over other spread spectrum techniques is passive synchronization. All direct-sequence spread spectrum system must first synchronize the receiver to the transmitted sequence before any data can be extracted. In a chirp system, the despreading operation is achieved with a pulse-compression filter, which is a passive device requiring no synchronization at its input. This is a major advantage in a system which employs many transmitters and receivers with low duty cycles and low data rates.

A simple chirp spread spectrum offers good compatibility with other modulated signals; however, for multiple access to a common channel orthogonal between different chirp signals is needed. This report examines several ways in which such orthogonality can be provided, by using within-chirp and multiple-chirp coding. Multiple-coded chirp was selected as a candidate system for a low bit rate overlay service, and its performance was studied to derive the parameters of working system.

Multiple-coded chirp can be used successfully for spread-spectrum overlay on an existing channel. This report examines in detail the mutual interference resulting from overlaying a multiple-coded chirp signal on an occupied FM-TV satellite channel. The performance, in terms of interference ratios for the

TV signal and BER for the overlay data channel, has been derived for a variety of bit rates and C/I ratios.

Finally, a typical application is presented in which data from a VSAT earth station is sent back to a large earth station over a TV channel using a C-band satellite transponder. It is shown that a data rate of 2.4 kbps can be achieved with a low power transmitter(300mW), with no significant interference at adjacent satellites.

***Part A. Spread Spectrum Multiple Access and Overlay
Service***

I. Introduction

Spread spectrum signals have been used in military satellite communications for years because of their ability to reject interference and jamming. In commercial satellite systems, where there is no intentional jamming, spread spectrum techniques were thought to provide no advantage.

For high-capacity point to point communications, satellite and fiber optic communications are cost efficient, since the substantial cost of several large earth stations or the installation of miles of optical fiber can be divided among many users. In large "thin route" networks, where the terminals are widely separated and the data rates are relatively low, the network overhead cost becomes prohibitive. The geographical spacing increases installation and networking costs for an optical fiber system dramatically. In satellite communication, the main problem would be the large number of users. The high cost of many large earth stations could not be justified for terminals transmitting low rate data.

Recently there has been a great deal of interest in satellite communication from very small aperture terminals. This paper analyzes the performance of two types of satellite communication from such terminals using spread spectrum techniques and shows that spread spectrum provides some unique advantages that make these services feasible. In addition, a small aperture terminal network using a processing transponder is presented and analyzed.

Spread Spectrum Multiple Access

The majority of current satellite traffic consists of analog television or medium to high data rate signals transmitted from a small number of large aperture earth stations. Mainly because of their large antenna diameter, these earth stations are very expensive. When there are many users, the cost of this type of earth station would make the network prohibitively expensive. Since the earth station cost is most dependent on the antenna diameter, the obvious way to reduce its cost is to reduce the antenna diameter. Earth stations that use small diameter antennas have become known as "Very Small Aperture Terminals", or VSATs.

Reducing the antenna diameter affects the system performance in two ways. First the antenna gain is reduced, lowering the link carrier to noise ratio. Second, the antenna beamwidth is broadened, increasing both the interference received from and transmitted to adjacent satellites. The signal transmitted from a small aperture earth station interferes with the operation of adjacent satellites more than the signal from a large aperture terminal on the uplink. Signals transmitted from adjacent satellites will not be attenuated significantly, increasing the interference level in the VSAT receiver. The interference rejection capabilities of spread spectrum signals make multiple access from small earth terminals feasible for a large number of low data rate users. Chapter 3 analyzes the performance of two spread spectrum multiple access systems which use a form of noncoherent M-ary FSK as their primary modulation. These performance results are then applied to practical example satellite systems using small diameter antennas.

Overlay Service

Overlay service is a method of frequency reuse which involves adding a signal to a transponder already considered to be full by overlaying the new signal within the bandwidth of the existing signal. For this type of service to work, the overlay signal must not interfere appreciably with the existing signal, and vice-versa. A spread spectrum signal with a wide, flat power spectral density (PSD) can appear noiselike to the existing signal, and will not disturb the existing signal if the power is low enough. Since the overlay signal power will be much lower than that of the existing signal, the overlay signal must be able to reject the strong interference caused by the existing signal. The VSAT receiver can use the processing gain of spread spectrum systems to achieve the required interference rejection. Chapter 4 compares various types of spread spectrum signals to find the type most suitable for overlay systems. It finds the maximum overlay data rate for three types of existing signals and calculates the improvement in overlay data rate achieved by using a representative convolutional code.

II. Overview of Multiple Access and Spread Spectrum Techniques

Conventional Multiple Access Techniques

The two major multiple access techniques in commercial use today are 1) frequency division multiple access, and 2) time division multiple access. Frequency division multiple access (FDMA) is the most mature of the multiple access technologies. In this system, each user is allocated a specific part of the transponder bandwidth for its exclusive use [1]. Figure 1 illustrates a typical four channel system.

FDMA systems require a low level of coordination among users, with only frequency band assignments to be made. The transmitting and receiving equipment is essentially the same as when there is no multiple access.

The major disadvantage of FDMA systems is that the transponder output power must be reduced, or "backed-off", to ensure that the transponder is operating in its linear region. If the transponder is sufficiently nonlinear, intermodulation interference between different users will result [3].

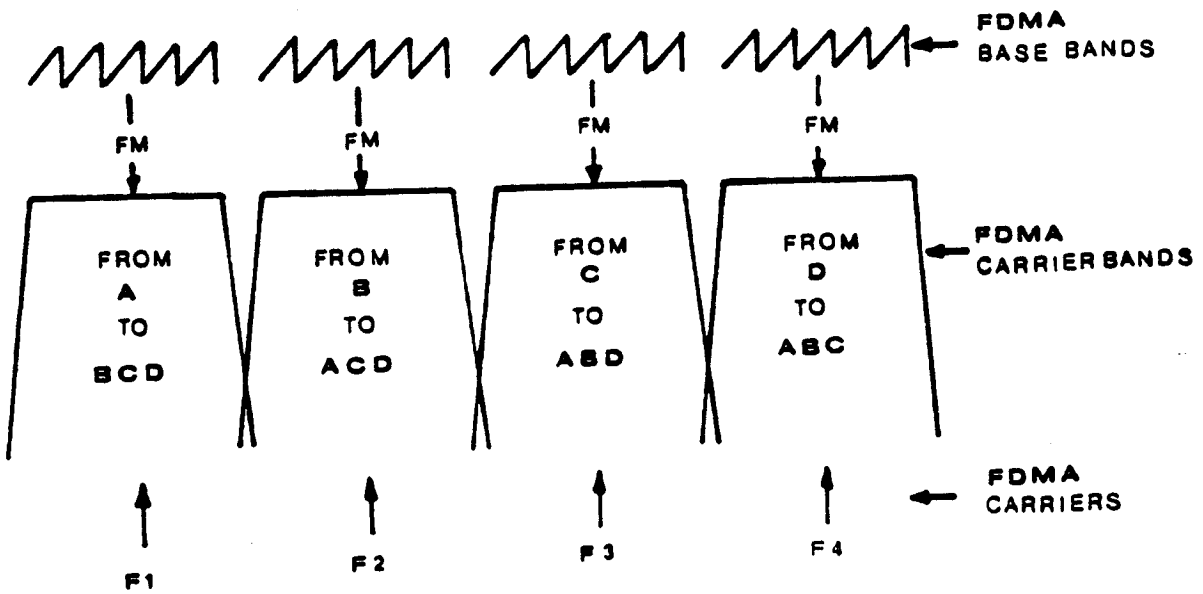


Figure 1. FDMA Signal Organization [2]

Time division multiple access (TDMA) avoids the backoff problem inherent in FDMA systems by allowing only one user to occupy the transponder at a time, so that no interference between users is possible. Each user is allowed to use the entire transponder bandwidth in sequence for a short period of time. This requires accurate time synchronization between all users. Synchronization requirements make the earth terminals expensive and complicated [4]. Figure 2 illustrates the time multiplexing of TDMA signals transmitted from a three channel system.

As mentioned previously, to construct a network of small aperture earth terminals, which have wide antenna beamwidths, a modulation type which reduces adjacent satellite interference is needed. The FDMA and TDMA systems described above use conventional modulation types, such as FM for analog signals, and QPSK for digital signals. These systems use these modulations for reasons other than interference rejection. Interference control is achieved primarily by reducing the antenna gain in the direction of the adjacent satellites, several degrees off axis, by using very large diameter antennas. The interference transmitted to adjacent satellites in VSAT networks can be reduced if the PSD of the transmitted signals is relatively low and flat.

Spread spectrum signals have features which can effectively reduce these problems. Some spread spectrum signals have relatively flat PSDs. In addition the correlation of the received signals with spreading codes in spread spectrum receivers effectively distributes the energy of uncorrelated interfering signals over a large bandwidth while simultaneously compressing the bandwidth of the desired signal. This "processing gain" is a significant source of interference rejection. In addition, most spread spectrum multiple access systems have little network overhead. Transmitters can operate asynchronously, unlike TDMA systems, and do not need to coordinate the operating frequencies as in FDMA systems.

Any type of spread spectrum signal can be used in a spread spectrum multiple access system. The two major classifications of spread spectrum signals are direct sequence and frequency hopped. Direct sequence systems spread a signal's bandwidth by mixing the signal with a relatively high rate

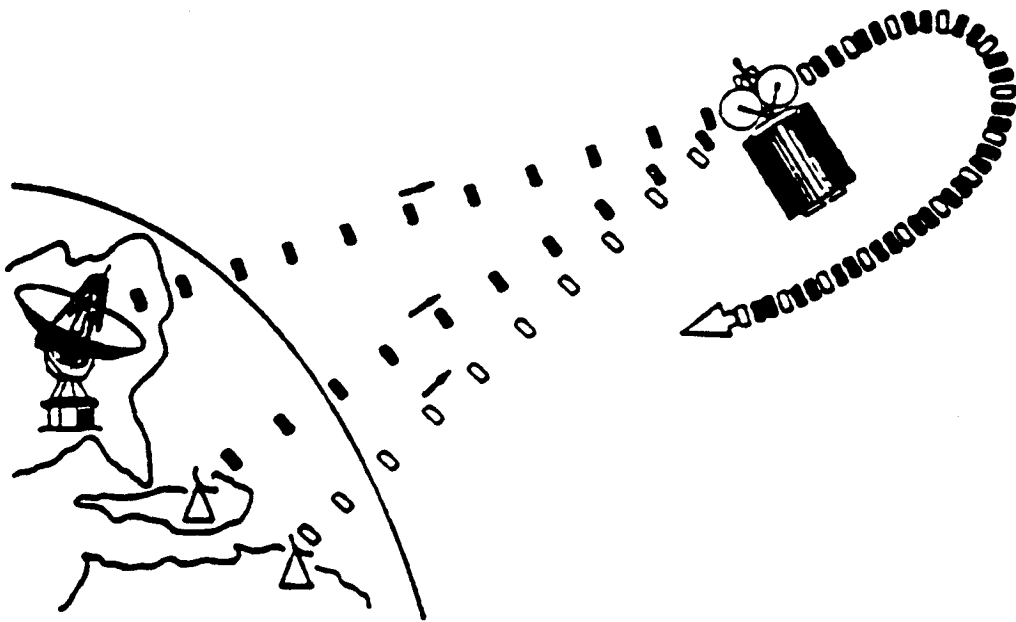


Figure 2. Typical TDMA System [5]

pseudonoise (PN) code [6]. Frequency hopped systems spread the signal by using a carrier signal which hops around the channel bandwidth in a pseudorandom manner [7].

In satellite spread spectrum multiple access, also known as code division multiple access (CDMA), uplink earth stations transmit signals that share the same bandwidth and time. Each transmitter spreads its signal with a unique code. Differentiation between desired and undesired signals is accomplished at the receiver, which correlates the received signal with a synchronized version of the spreading code. The bandwidth of the correlated signal is collapsed to its unspread bandwidth, while the bandwidth of the other users' signals is spread further, decreasing the PSD of the interference [8].

Direct sequence SSMA systems can be either "sequence synchronous" or "sequence asynchronous" [9]. Sequence synchronous systems require the bit transitions of each transmitter's spreading code to be in synchronization when received by the satellite. These systems can achieve very low levels of inter-user interference if orthogonal spreading codes are used, but this limits the number of users to the length of the code [10]. Synchronous systems are impractical for large thin-route networks however. The synchronization of hundreds to thousands of widely spaced transmitters is an overwhelming problem, especially when the earth station cost is a major consideration. Loss of synchronization produces a catastrophic increase in the users' error rate [11].

Sequence asynchronous DS SSMA systems allow completely asynchronous transmissions. Inter-user interference is increased significantly over orthogonal synchronous DS SSMA however. The amount of inter-user interference is dependent on the partial cross-correlations between the different spreading codes [12,13]. Sequence asynchronous DS SSMA systems are promising for practical SSMA small earth terminal systems.

Frequency hopped multiple access (FHMA) is commonly used with M-ary FSK as the primary modulation. The available channel bandwidth is divided into "slots". The MFSK signal hops from slot to slot under the control of its unique PN code. Symbol errors occur when more than one user hops into the same slot. Slow hop FHMA systems hop in frequency no more than once per symbol. Fast

hop FHMA systems hop more than once per information symbol, and the receiver uses a majority logic decision circuit to estimate the transmitted symbol based on the multiple received hops. [14]

While MFSK FHMA receivers can be simplified by using noncoherent detection, the cost of a frequency synthesizer that can produce carrier frequencies over the entire 36 or 54 MHz bandwidth of a satellite transponder may be expensive, and not suitable for large thin-route networks.

One type of sequence asynchronous DS SSMA system that shows promise for multiple access from small earth terminals is an MFSK/DS SSMA system. In this system an MFSK information signal is spread by a PN code. This is the type of system analyzed in Chapter 3.

The performance of individual MFSK/DS signals in the presence of various types of jamming signals is well known [15]. The performance of MFSK/DS multiple access systems, however, has not been thoroughly studied. At the time this research was started, the only work on MFSK/DS spread spectrum multiple access systems is a paper by Yamauchi et al. translated from Japanese [16]. This paper shows that the multiple access efficiency of MFSK/DS SSMA systems improves when the spacing between MFSK symbol frequencies is greater than the symbol rate. The paper presents an analysis of the performance of an MFSK/DS SSMA system which references several sources available only in Japanese. Because of this, their analysis could not be easily verified.

The analysis presented in Chapter 3 is based on the paper by Yamauchi. The MFSK system with modified symbol frequency spacing that he presents, which is called "wideband MFSK" here, is used. The performance equations are completely rederived, with the mathematical details presented in appendices A and B, and do not agree with those in Yamauchi's paper. All the formulas used in this report are derived herein.

In addition, the MFSK/DS SSMA system results are applied to satellite multiple access from small earth terminals. Two original SSMA systems based on the wideband MFSK/DS SSMA system are

presented and analyzed. This analysis considers the power and interference constraints of practical satellite systems.

On-Board Processing

The practice of demodulating the uplink signals at the satellite and retransmitting them is known as "on-board processing". Simply demodulating the uplink signal and retransmitting it with the same modulation can give about a 3 dB improvement in C/N when the uplink C/N and downlink C/N are nearly equal.

Satellite Switched TDMA (SS-TDMA) is a technique that directs each TDMA burst to its particular destination through a narrow, high gain spot beam. The high gain downlink antenna significantly improves the downlink C/N. Since the downlink antenna no longer provides coverage of the entire service area, SS-TDMA requires the satellite to recognize the intended recipient of each uplink burst and direct it to the appropriate spot beam [17].

A processing transponder for multiple access of low data rate mobile users has been proposed [18]. This technique requires the transponder to compute a discrete Fourier transform of its bandwidth to demodulate MFSK uplink signals. Such a technique is said to be much more able to track the doppler shift of the mobile users' signals.

The analysis of satellite links that use processing transponders is easily accomplished by considering the uplink and downlink bit error rates separately [19]. Chapter 5 discusses various on-board processing systems which may improve the throughput of the systems analyzed in Chapter 3 and the conditions under which they may be used. An analysis of the Ku band example from Chapter 3 is

performed to show the possible throughput improvement provided by a particular type of processing transponder.

Overlay Systems

Satellite signal overlay has not been widely studied or practiced. The only type of overlay signal known to be in use is in a system which overlays a DS signal on TDMA traffic for TDMA loop-back synchronization [20].

No analytic work on satellite overlay systems was found. One brief reference to a satellite television overlay experiment gives so few details of the system parameters that it is of no use [21]. The overlay analysis in Chapter 4 is intended to give a rough estimate of the performance of satellite signal overlay from small earth terminals. The possible overlay system performance of several spread spectrum overlay signals is compared. A general methodology for analyzing the overlay performance is presented and applied to three example systems. The methodology and analysis are original.

III. MFSK Spread Spectrum Multiple Access

Many spread spectrum multiple access (SSMA) systems have been studied. Unfortunately the efficiency, measured by the number of users accommodated in a given bandwidth, is usually low. This chapter analyzes two SSMA techniques which use a form of noncoherent M-ary FSK as the primary modulation to improve throughput. It includes a systems level description of the performance of these systems, while mathematical details are kept to a minimum. The following sections describe and analyze two practical SSMA systems. The analysis includes calculations of their bandwidth efficiency and link analyses to assess power and adjacent satellite interference limitations which may occur in practical systems.

Preliminaries

Several features are essential to keep the system as simple as possible and to reduce the equipment cost to a level appropriate to small earth terminals. First, noncoherent detection of the MFSK signal is assumed, simplifying the receiver. Also, all users transmit asynchronously, with no network synchronization. Synchronization of hundreds to thousands of transmitters, even at the millisecond

level, would be extremely difficult. The analysis assumes that all users have the same power at the earth station receiver input. This assumption is valid for satellite communications since some form of power control at the transmitters is necessary to prevent power-hogging in the transponder.

Both of the SSMA systems to be analyzed are based on the system model shown in Figure 3. Information at a bit rate R_b is modulated into MFSK symbols at a rate R_s , where $R_s = R_b / k$ and $k = \log_2 M$. The spectrum of this MFSK signal is spread when mixed with a PN code at a code rate R_c . The j^{th} user's signal can be described by

$$s_j(t) = \sqrt{2C} \sum_{k=1}^{\infty} \text{rect}(t - kT_s) \cos(2\pi f_j t) PN_j(t) \quad (3.1)$$

where $PN_j(t)$ is a full period of a bipolar NRZ rectangular pseudonoise pulse sequence at a rate R_c , C is the signal power, and $T_s = 1/R_s$.

In a conventional MFSK system the signal is represented by M tones separated in frequency by R_s . This frequency spacing minimizes the total signal bandwidth while maintaining the orthogonality between the symbols. Minimizing the signal bandwidth is of no concern here since we intend to spread the signal bandwidth anyway. The modulation can be generalized to allow frequency spacing between MFSK symbols of

$$\Delta f = pR_s \quad (3.2)$$

where p is an integer. $p=1$ corresponds to the conventional narrowband MFSK. When $p > 1$ the system will be referred to as *wideband* MFSK. It has been shown that using values of $p > 1$ increases the multiple-access efficiency by whitening the co-channel interference PSD at the receiver [22]. Since p is an integer, the symbols are still orthogonal and noncoherent detection is still possible.

Figure 4 depicts this system in a multiple-access context, with N one way transmissions. Each of the N transmitters spreads its signal with its own unique PN code, labelled PN_1 through PN_N . Transmitter

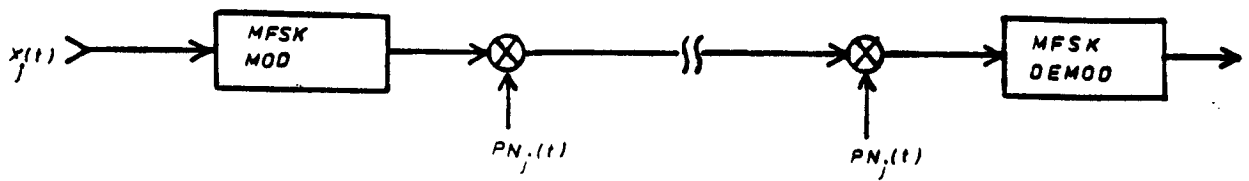


Figure 3. SSMA System Model

j intends to communicate with receiver j . At the input to receiver j are N user signals plus thermal noise. When the receiver correlates the j^{th} transmitted signal with a properly synchronized version of the j^{th} PN code, the wideband MFSK signal s_j is recovered. Added to the recovered information signal is a co-channel interference signal which consists of the correlation of the j^{th} PN code with $N-1$ signals spread by $N-1$ different, unsynchronized PN codes.

Up to this point, nothing has been said about the type of PN spreading code to be used. Though it will not be discussed here, the co-channel interference caused by an asynchronous interfering user is dependent upon the partial cross-correlations between the two PN codes [23]. Therefore it is desirable to choose a family of codes with a low cross-correlation between any two members, such as the well known Gold or Kasami codes. Since the number of interfering users will be large, and they will all be transmitting asynchronously, a central-limit theorem argument can be used to model the co-channel user interference as a Gaussian process [24]. Doing so gives an ensemble average measure of the system performance. In practice some channels will exceed the average performance, and others will fare worse. Making this Gaussian assumption reduces the performance analysis of this system to that of wideband noncoherent MFSK in colored Gaussian noise.

Performance Analysis

Assume that Gaussian noise exists with a PSD given by $I(f)$. The form of the MFSK signal is

$$\sqrt{2C} \sum_{j=1}^{\infty} \text{rect}(t - jT_b) \cos(2\pi f_j t) \quad i \in [1, M] \quad (3.3)$$

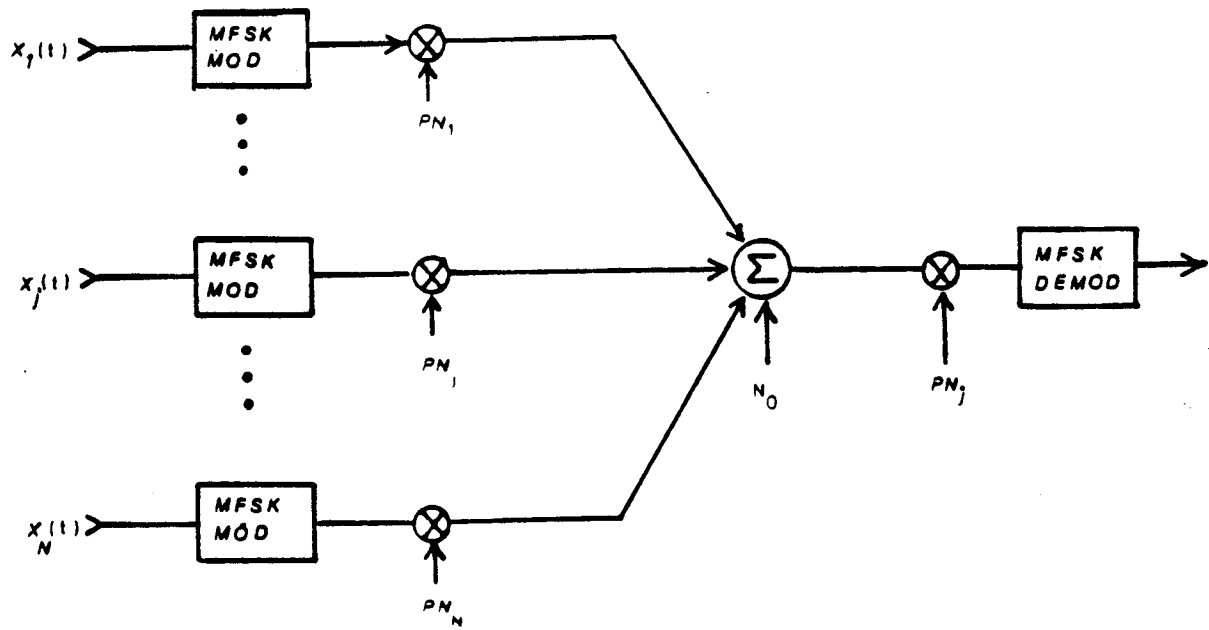


Figure 4. SSMA System Model - N Users

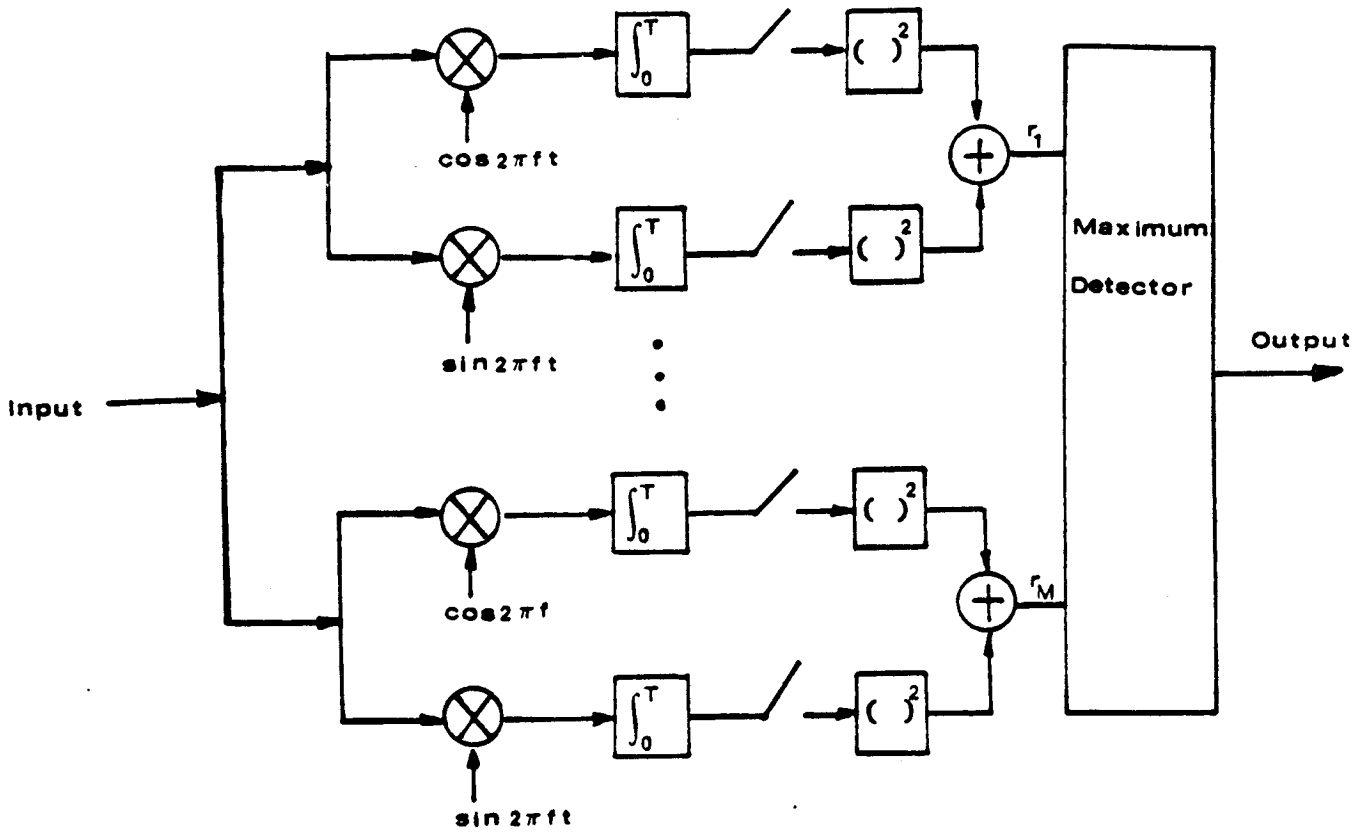


Figure 5. MFSK Receiver Model

Figure 5 shows the model of the MFSK receiver. Letting s_p denote that an MFSK symbol at frequency f_p was transmitted, the probability that the receiver incorrectly chooses symbol q given that symbol p was sent is given by [Appendix A]

$$\Pr(r_q > r_p | s_p) = \frac{N_q}{N_p + N_q} \exp\left[-\frac{E_s}{N_p + N_q}\right] \quad (3.4)$$

where E_s is the symbol energy ($= kCT_b$) and $N_p = I(f_p)$, $N_q = I(f_q)$. The probability that an error is not made in this decision is

$$\Pr(r_q < r_p | s_p) = 1 - \Pr(r_q > r_p | s_p) \quad (3.5)$$

The probability that no errors are made over all of the incorrect symbols is

$$\prod_{\substack{q=1 \\ q \neq p}}^M [1 - \Pr(r_q > r_p | s_p)] \quad (3.6)$$

Therefore the probability of a symbol error given symbol p is transmitted is

$$1 - \prod_{\substack{q=1 \\ q \neq p}}^M [1 - \Pr(r_q > r_p | s_p)] \quad (3.7)$$

Since the interference is not white, the probability of a symbol error is symbol dependent. The average symbol error rate is found by averaging over all of the symbols

$$P_{se} = \frac{1}{M} \sum_{p=1}^M \left[1 - \prod_{\substack{q=1 \\ q \neq p}}^M [1 - \Pr(r_q > r_p | s_p)] \right] \quad (3.8)$$

The corresponding bit error probability can be approximated by using the relation

$$P_{be} = \frac{M/2}{M-1} P_{se} \quad (3.9)$$

All that remains to be done is to find the form of the PSD of the interference, $I(f)$. An individual MFSK symbol from an interfering user is spread twice by two different asynchronous PN codes (Figure 6). The PSD of the resulting signal is centered at the symbol frequency f_p and has a shape determined by the convolution of the PSDs of the two PN codes. Using an envelope approximation to the PSD of a PN sequence, the resulting interference PSD can be approximated by [Appendix B]

$$I(f) = \frac{2CR_c}{4R_c^2 + \pi^2(f - f_p)^2} \quad (3.10)$$

Since there are $N-1$ transmitters and each is transmitting any of the M symbols with equal probability, on average there are $(N-1)/M$ users transmitting each symbol. Assuming all of the users' signals are uncorrelated and $R_s \ll R_c$, the powers add, and including thermal noise (N_b) the expression becomes

$$I(f) = N_b + \frac{(N-1)C}{M} \sum_{j=1}^M \frac{2R_c}{4R_c^2 + \pi^2(f - f_j)^2} \quad (3.11)$$

With a frequency spacing between MFSK symbols of Δf , the interference at the i^{th} symbol frequency is

$$N_i = I(f_i) = N_b + \frac{(N-1)C}{M} \sum_{j=1}^M \frac{2R_c}{4R_c^2 + \pi^2\Delta f^2(i-j)^2} \quad (3.12)$$

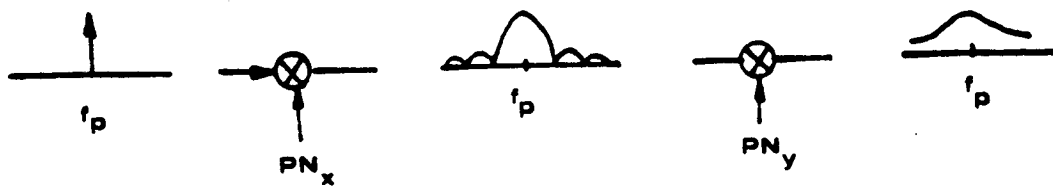


Figure 6. Interference PSD Model

Multiple Access Systems

Using the described system to spread the energy of a low data rate MFSK signal over the entire bandwidth of a satellite transponder is impractical for several reasons. First of all, the high chip-rate needed to spread the bandwidth to 36 MHz or more requires expensive hardware. A high chip-rate also greatly complicates the code synchronization problem over low chip-rate systems. Two alternate methods of spreading the bandwidth in the channel will be presented. In both cases part of the channel bandwidth must be allocated to a control channel. A simple control station can use this channel to limit the number of users to a preset maximum and to assign PN codes to users when they initiate communication.

System 1: MFSK/DS/FDM

One possible multiple access technique is to divide the available channel bandwidth into several "FDM" slots, each containing a separate MFSK/DS SSMA system. The approximate bandwidth of one slot is (Fig 7)

$$(M - 1) \Delta f + 2R_c \quad (3.13)$$

If the number of FDM "slots" that can fit in the channel bandwidth is denoted by Z, the number of allowable users is simply Z times the number of users able to use one slot as given by equation (3.9).

System 2: MFSK/DS/FH

Figure 8 shows a block diagram of hybrid SSMA transmitter and receiver which uses a frequency hopped carrier to spread an MFSK/DS signal over the transponder bandwidth.

Only slow hopping systems, with one frequency hop per symbol time will be considered. In a conventional slow-hop FHMA FSK system, if two (or more) users hop into the same FH slot simultaneously an error will occur (except for the case where all users are transmitting the same symbol). Fast-hopping (multiple hops per symbol) eliminates the certain occurrence of a symbol error from a single collision. In a sense the hybrid SSMA system behaves like a fast-hop system, in that a single FH collision does not necessarily cause a symbol error. The PN codes provide the differentiation between intended and interfering users.

The performance of the hybrid system can be calculated by applying the total probability theorem:

$$P_{be} = \sum_{n=1}^N \Pr(\text{bit error} | n \text{ users colliding}) \Pr(n \text{ users colliding}) \quad (3.14)$$

where N = the total number of users .

If the user hops randomly among Z frequency slots, the probability that the user is in a given slot is $1/Z$, and the probability that n users out of N are using that slot is given by the Bernoulli trials formula

$$\Pr(n \text{ users colliding}) = \binom{N}{n} \left[\frac{1}{Z} \right]^n \left[1 - \frac{1}{Z} \right]^{N-n} \quad (3.15)$$

The probability of a bit error given n interfering users is calculated using formula (2.14) with $\Pr(\text{bit error} | n \text{ users colliding})$ calculated using equation (3.9) with N replaced by n in the interference formula (3.12).

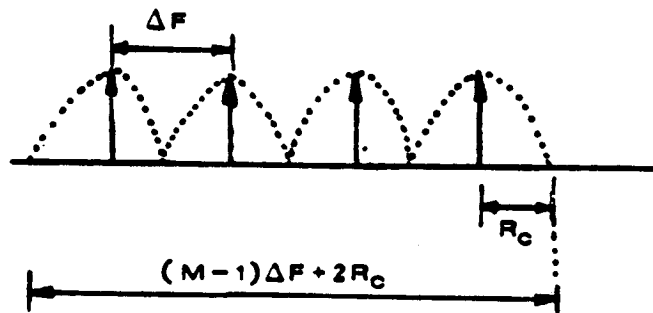


Figure 7. MFSK Slot Bandwidth

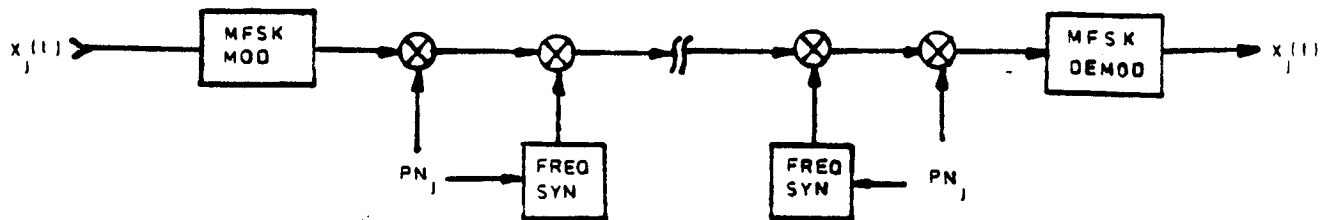


Figure 8. Hybrid MFSK/DS/FH SSMA System

Numerical Examples

The following tables list the parameters of sample C and Ku band satellite SSMA systems. The tabulated parameters are:

- M - the number of MFSK symbol frequencies ($= 2^k$)
- R_s - the symbol rate ($= R_b / k$)
- R_c - the PN code rate
- Δf - the frequency spacing between symbol frequencies
($= p R_s$)
- Z - the number of frequency hop slots in the FH system or
the number of FDM slots in the FDM system

Example 1: C Band System

Transponder Bandwidth = 36 MHz
 Data Rate (R_b) = 1200 bps
 $p = 46$
 BER = 10^{-6}
 $R_c = 31 R_b$

M	R_b	R_c	Δf	Z
2	1200	37,200	55,200	277
4	600	18,600	27,600	300
8	400	12,400	18,400	234
16	300	9,300	13,800	159

Example 2: Ku Band System

Transponder Bandwidth = 54 MHz
 Data Rate (R_b) = 56 kbps
 $p = 22$
 BER = 10^{-6}
 $R_c = 15 R_b$
 $R_b, R_c, \Delta f$ are in kbps and kHz

M	R_b	R_c	Δf	Z
2	56	840	1,232	18
4	28	420	616	20
8	18.66	280	410.66	15
16	14	210	308	10

Figures 9-12 show the performance both multiple access systems for the C and Ku band examples. The choice of parameters is not optimized. Considerable flexibility exists in the choice of parameters and considerations such as hardware complexity and cost may dictate certain choices. The above examples serve only to illustrate the general behavior of the systems' performance. Δf is an integer multiple of R_b and is set to approximately 1.5 times R_c since this choice empirically gives good performance.

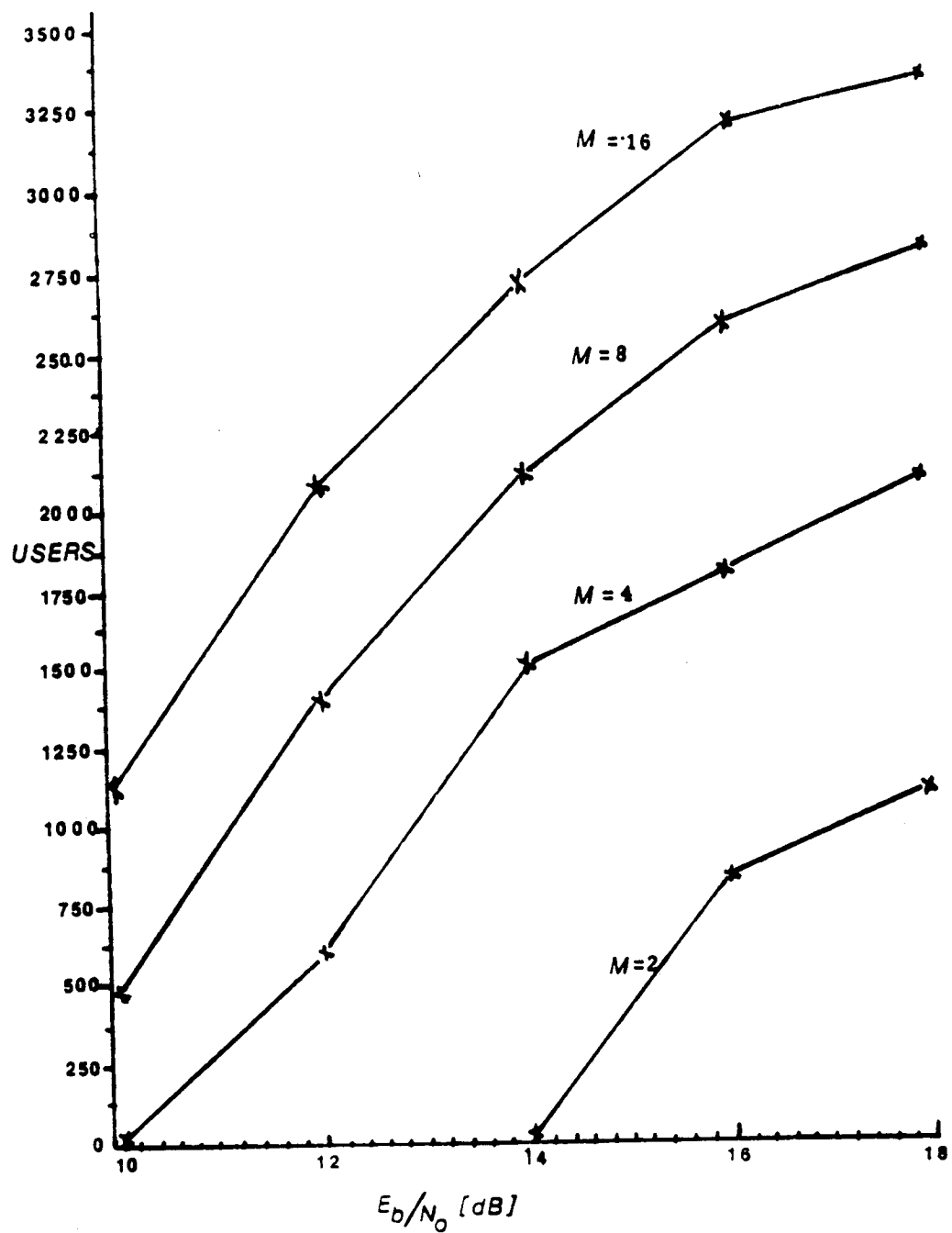


Figure 9. Performance of MFSK/DS/FDM Systems (C band)

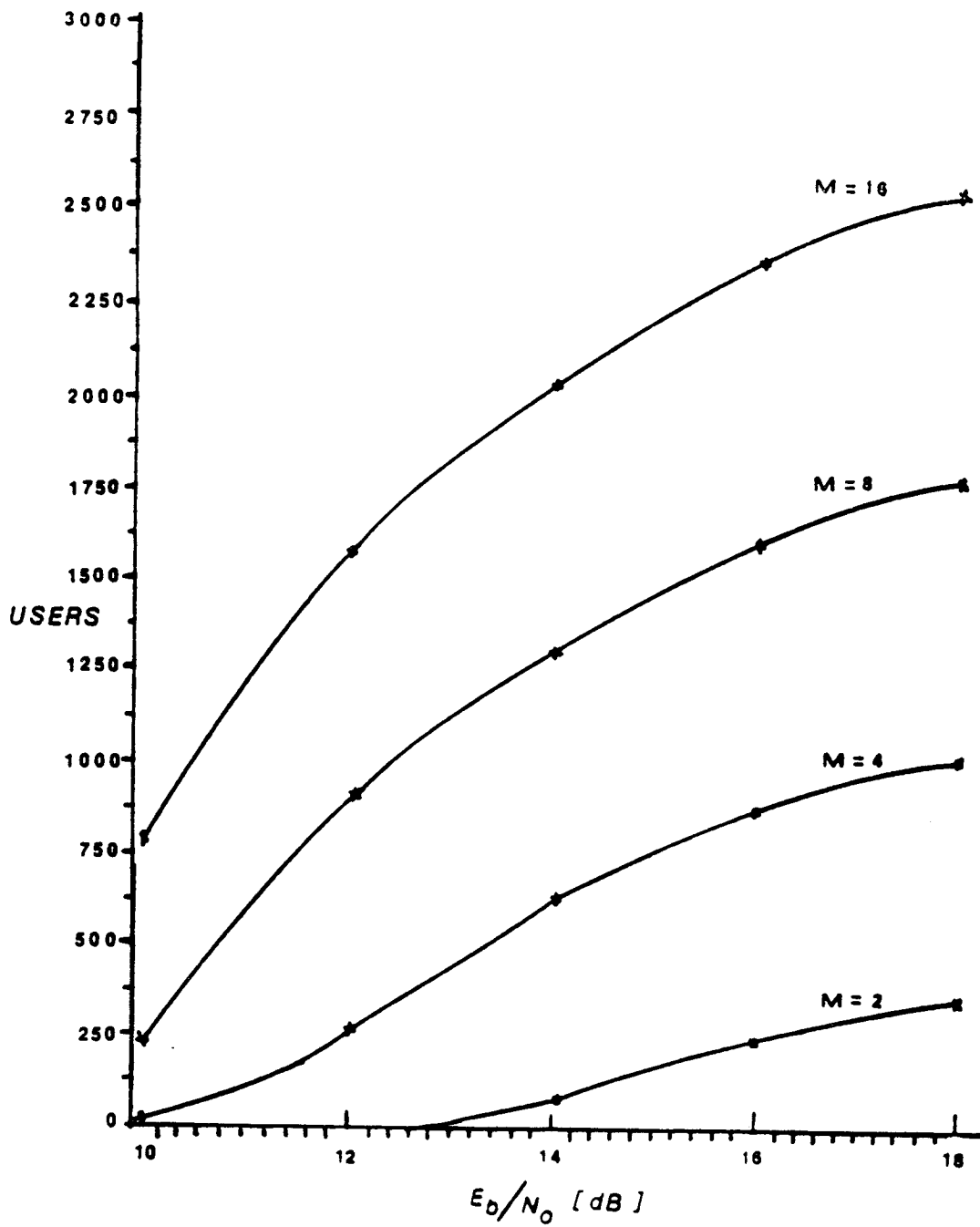


Figure 10. Performance of MFSK/DS/FH Systems (C band)

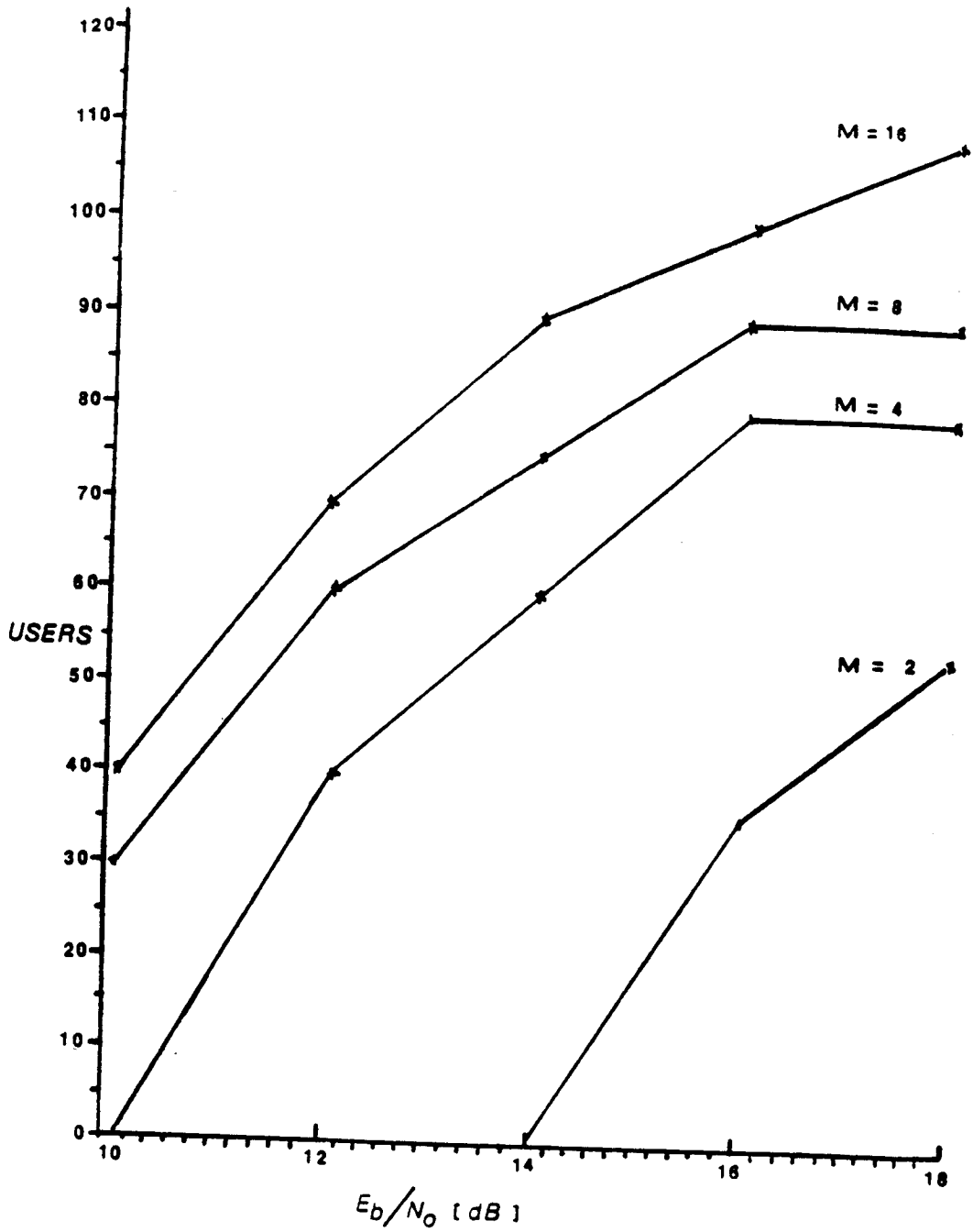


Figure 11. Performance of MFSK/DS/FDM Systems (Ku band)

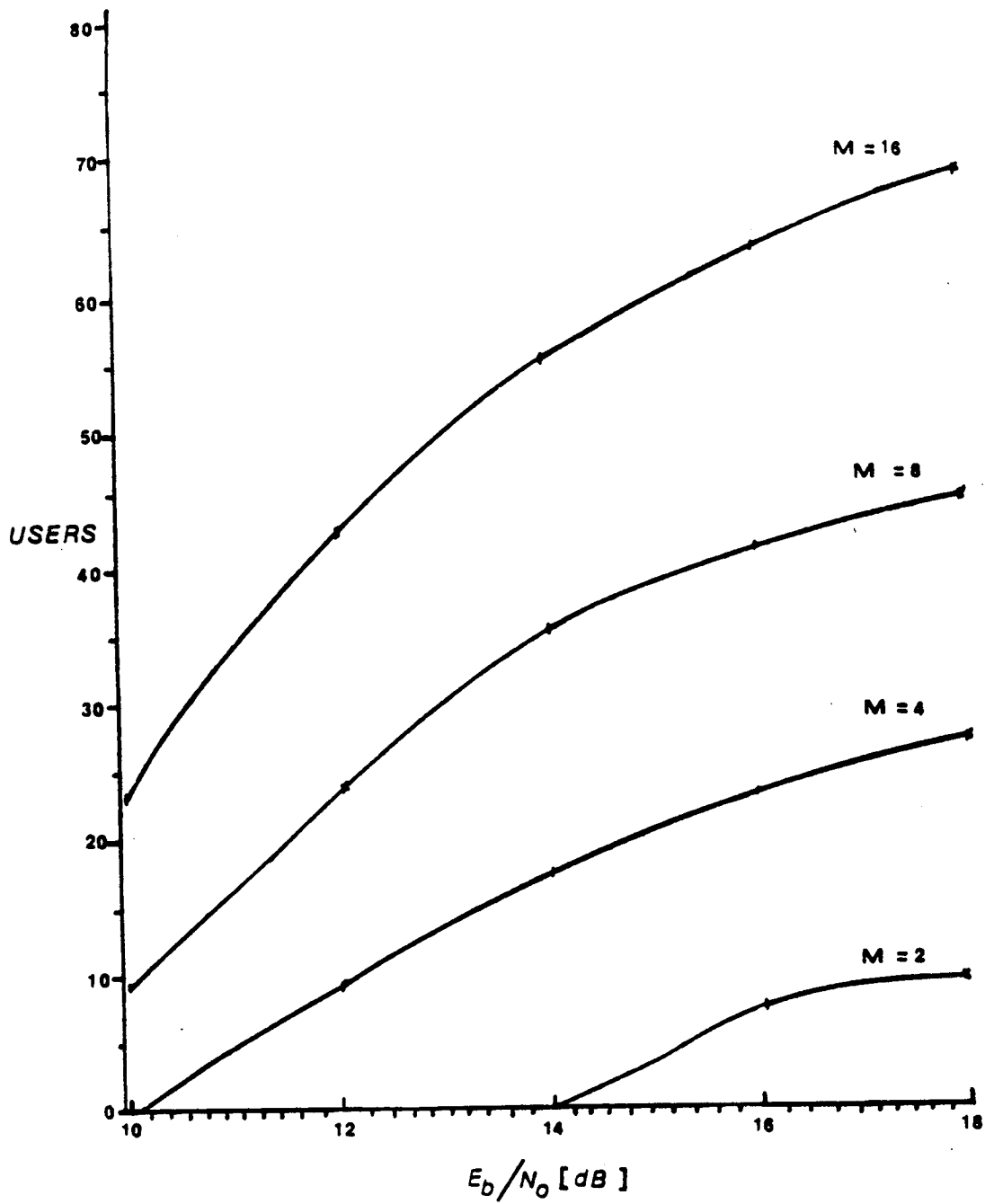


Figure 12. Performance of MFSK/DS/FH Systems (Ku band)

Sample Link Analyses

Shown in Table 3.1 and Table 3.2 are link analyses for the C band and Ku band systems described previously with earth station parameters chosen to be those of the common small earth terminals. The network architecture is the "full mesh" type where direct communication between two small earth terminals via the satellite, as in Figure 13, is assumed.

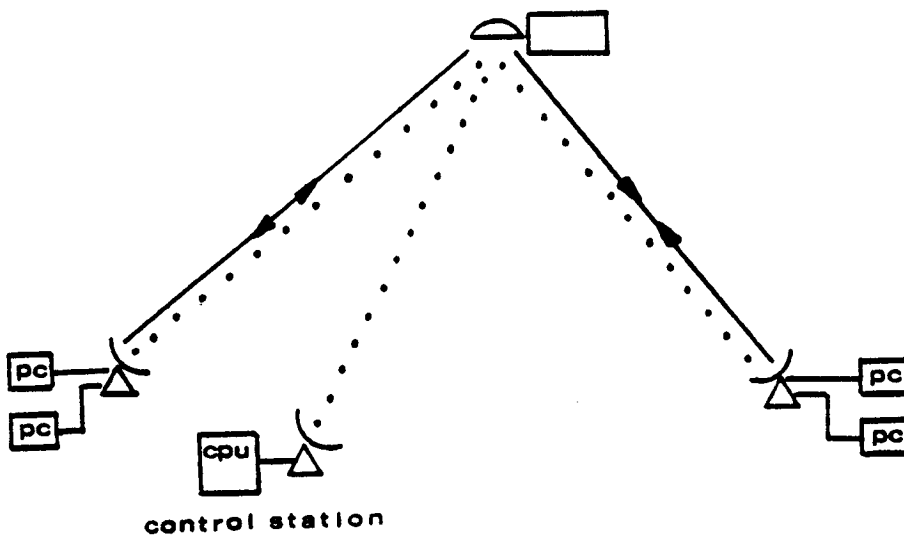


Figure 13. Full Mesh Network Architecture

Table 3.1. C-band System - 968 users at 1.2 kbps

Satellite Parameters

EIRP	=	36 dBW
G/T	=	-3 dB/K
Bandwidth	=	36 MHz

Earth Station Parameters

Antenna Diameter	=	1.2 m
Aperture Efficiency	=	65
Transmit Gain (6 GHz)	=	35.6 dB
Receive Gain (4 GHz)	=	32.2 dB
R_b	=	1200 bps
T_s	=	170 K

Downlink

Propagation and pointing loss	=	196.3 dB
Earth Station G/T	=	9.1 dB/K
$(C/N_o)_d$	=	45.0 dB-Hz

Uplink

Propagation and pointing loss	=	200.2 dB
Earth station power	=	3.65 dBW
$(C/N_o)_u$	=	64.7 dB-Hz

Overall Link

Carrier to Interference and Intermodulation Ratio	=	18 dB
Overall E_b/N_o	=	12.2 dB
BER	=	10^{-6}
Throughput	=	3.2

Table 3.2. Ku-band System - 57 users at 56 kbps

Satellite Parameters

EIRP	=	38.5 dBW
G/T	=	2 dB/K
Bandwidth	=	54 MHz

Earth Station Parameters

Antenna Diameter	=	1.8 m
Aperture Efficiency	=	65
Transmit Gain (14 GHz)	=	46.6 dB
Receive Gain (11 GHz)	=	44.5 dB
R_b	=	56 kbps
T_s	=	370 K

Downlink

Propagation and pointing loss	=	206.8 dB
Earth Station G/T	=	18.78 dB/K
$(C/N_o)_d$	=	61.5 dB-Hz

Uplink

Propagation and pointing loss	=	208.5 dB
Earth station power	=	-3.0 dBW
$(C/N_o)_u$	=	65.7 dB-Hz

Overall Link

Carrier to Interference and Intermodulation Ratio	=	20 dB
Overall E_b/N_o	=	11.9 dB
BER	=	10^{-6}
Throughput	=	5.9

The available downlink power limits the number of users to 968 for both the FDM and FH systems. The Ku band system, with its higher antenna gain, is power limited for the FDM system to 57 users, but is bandwidth limited for the FH system to approximately 43 users (Figure 11).

To determine the effect of such networks on adjacent satellites, the flux density they present to adjacent satellites will be compared to that produced by a typical large earth station with a 9 meter dish antenna (which meets the new FCC antenna gain specifications) transmitting 27 dBW. Such an earth station presents a flux density of approximately -112 dBW/m² to a satellite at 2° off axis. Assuming a uniform aperture illumination, at 6 GHz a 1.2 meter antenna's gain is down 6 dB relative to its maximum gain at 2° off axis. The flux density of the C band system (with 968 users transmitting simultaneously) at an adjacent satellite is approximately -100 dBW/m². Reducing the flux density to -112 dBW/m² limits the network to only 81 users. Alternatively, the diameter of the earth station antenna can be doubled to 2.4 meters. This brings the antenna gain down 17 dB at 2° off axis, reducing the interference flux density to -111 dBW/m² with no reduction in the number of users. At Ku band the adjacent satellite interference problem is much less severe. At 14 GHz, a 1.8 meter antenna's gain is down 24 dB at 2° off axis.

The wide beamwidth of these small antennas guarantees that signals from adjacent satellites will interfere with the network operation. In the link analysis, conservative carrier to interference ratio values are included for this reason. Spread spectrum systems, unlike other multiple access systems, have the ability to reject interfering signals due to their processing gain. This capability, and the relatively flat PSD presented to adjacent satellites as interference, are the major advantages of spread spectrum multiple access systems.

Conclusions

Both the MFSK/DS/FDM and MFSK/DS/FH SSMA systems provide reasonable multiple access performance. Considering bandwidth constraints only, the FDM SSMA system performs better than the FH SSMA system, providing bandwidth efficiencies of approximately 11 (0.11 bps/Hz) for the C band examples (1200 bps), and for the Ku band examples (56 kbps).

Downlink power limitations prevent the full capability of these systems from being realized in the satellite SSMA context. Considering both the power and bandwidth constraints present in the example systems presented, the C band system throughput was reduced to 3.2 , and the Ku band system to 5.9 . Since these systems are essentially power limited, coding could be used to trade power for bandwidth to increase system performance if the additional cost is tolerable. The link analyses show that a small earth terminal satellite network using wideband MFSK SSMA is feasible. Other types of multiple access systems are power limited but do not have the interference rejection capability and flat PSD of a SSMA system and may therefore become interference limited.

Because of its superior bandwidth efficiency and much simpler and faster synchronization, the FDM SSMA system is best suited for a practical SSMA small earth terminal network.

IV. Spread Spectrum Overlay Service

Overview

Overlay service is the practice of adding or *overlaying* a usually low rate data signal to an existing channel which is generally thought to be filled to capacity. This practice, a form of "frequency reuse", can further increase the capacity of satellite transponders and provide new services and functions to existing satellite users.

The primary consideration in the design overlay systems is that they do not interfere significantly with the operation of the signal which is already using the transponder. This will be called the "existing" signal. The existing signal can be any one of many types of satellite signals currently in use such as analog television, FDM/FM telephone traffic, or digital data. These signals already experience interference from adjacent satellites and terrestrial sources. The addition of the overlay signal to the transponder introduces another source of interference with which the existing signal must contend.

The performance degradation experienced by the existing signal can be kept to an arbitrarily low level by simply lowering the transmitted power of the overlay signal sufficiently. This obviously places

severe limitations on the performance of the overlay link, lowering its carrier to noise density ratio C/N_0 . Theoretically, any E_b/N_0 can be achieved by the overlay link, for a fixed transmitted power C , if the data rate of the overlay signal is sufficiently low, since $E_b = C/R_b$. The relationship between the overlay signal power and data rate illustrates the general characteristics of overlay systems. The overlay signal will be a low data rate signal transmitted at a very low power relative to that of the existing signal. Just as the overlay signal interferes with the existing signal, the existing signal interferes with the overlay signal. The only difference is that the overlay signal must reject a relatively high level interferer. Spread spectrum signals, which have the ability to reject large interferers, are a natural choice for the overlay signal.

The performance of the overlay system is also highly dependent on the type of existing signal being used. This chapter compares the performance of several spread spectrum signals used as overlay signals for three types of existing signals: 1) analog television, 2) FDM/FM/FDMA telephone, and 3) digital SCPC signals. Link analyses are given to assess the feasibility of the overlay systems. The analysis includes calculations of the improvement from forward error correction.

Comparison of Spread Spectrum Overlay Systems

Frequency Hopped Spread Spectrum

In general, spread spectrum systems fall into two categories: 1) direct sequence systems, where the signal is spread by being mixed directly with a pseudo-noise sequence, and 2) frequency hopped systems, where the signal's carrier frequency is changed in a pseudo-random manner. Combinations of these two systems, such as the hybrid spread spectrum multiple access system presented in the previous chapter, also exist. Direct sequence systems are known as "noise averaging" systems.

because their interference rejection, or processing gain, is achieved by spreading the interference signal power over a larger bandwidth, reducing its power spectral density. Frequency hopped systems are known as "avoidance" systems, because they achieve interference rejection by hopping their carrier into areas of the spectrum where there is no interference, thereby "avoiding" the interference. Since the existing signal occupies virtually the entire transponder bandwidth, it appears as wideband interference to the overlay signal. In essentially no portion of the transponder bandwidth will a frequency hopped signal avoid the existing signal. Therefore, pure frequency hopped overlay signals provide no rejection of the existing signal, and are not suitable for overlay service.

MFSK/DS Spread Spectrum Overlay

The MFSK/DS spread spectrum system proposed in Chapter 3 for multiple access has a direct sequence component, and therefore achieves interference rejection through noise averaging. Since the frequency hopping component of the hybrid system provides no interference rejection, the discussion will be confined to systems in which an MFSK signal is simply spread by multiplication with a pseudonoise sequence.

If a large number of MFSK tones are used, i.e. M is large, the energy of the signal will be spread fairly evenly over the transponder bandwidth. This relatively flat power spectral density is a desirable feature in overlay signals, since it is the peaks in the signal spectrum which would cause the most interference to the existing signal. Nevertheless, there are several disadvantages to an MFSK/DS system. First of all, noncoherent detection of the MFSK is required. The synchronization and general hardware complexity of a coherent MFSK/DS system would make this system expensive and complicated. Noncoherent detection schemes suffer a 3 dB penalty in signal to noise ratio relative to coherent detection schemes. Because the interference level is high, this penalty will have a strong effect on the overlay system BER. Also, if many MFSK tones are used to flatten the overlay signal PSD, then the spreading sequence bit rate must be reduced to keep the overlay signal power within

the transponder bandwidth. Reducing the chip rate reduces the bandwidth the interference is spread over. This lowers the ability of the system to reject interference.

Direct Sequence Overlay

From the preliminary analysis of the MFSK/DS and frequency hopped overlay signals, it is evident that an ideal overlay signal would have a flat PSD, use coherent detection, and have as large a chip rate as possible. A pure direct sequence spread spectrum system comes as close to this ideal as any spread spectrum system can. Figure 14 illustrates this system.

Such a system achieves a high processing gain, using a chip rate up to half the transponder bandwidth, and can easily be detected coherently, providing a 3 dB advantage over noncoherent systems. While the PSD of the signal is not as flat as some other spread spectrum systems, the advantages just mentioned more than make up for this disadvantage. This system seems to have the most promise for overlay service, and will be analyzed exclusively.

Interference Modeling

Appropriate statistical models of the interference that the overlay signal presents to the existing signal, and vice-versa, are an important part of the overlay system performance analysis. It will be shown that with a reasonable degree of certainty these interference sources are adequately represented as Gaussian noise. The following sections describe two results which are useful in justifying this treatment.

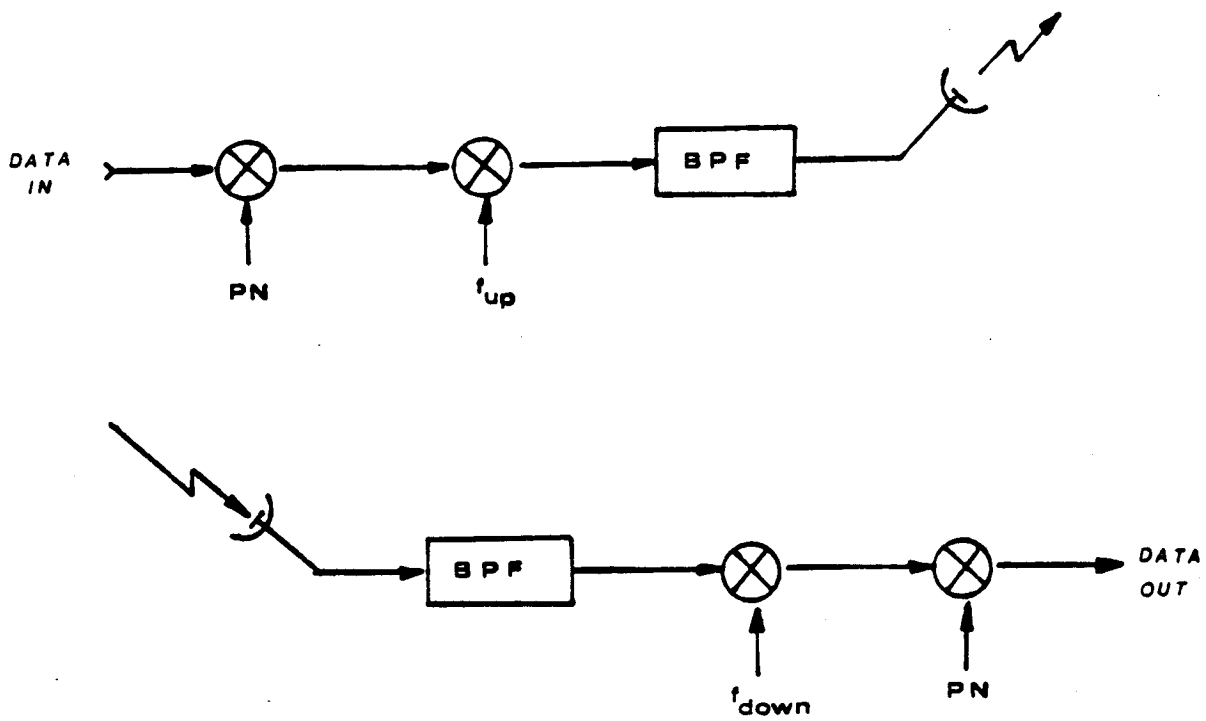


Figure 14. DS Overlay System

Modeling of Wideband Signals Passed Through Narrowband Filters

The statistics of an arbitrary signal passed through a filter with a bandwidth much narrower than the signal bandwidth approach a Gaussian distribution. This is a result of the central limit theorem and the related Berry-Esseen theorem [25,26]. In the overlay systems to be analyzed the interference bandwidth is often much greater than the a receiver's bandwidth. This result can then be used to model the interference in the receiver as a Gaussian process.

Modeling of Interference PSK Signals by Multiple PSK Interferers

In his classic paper V.K. Prabhu considers the error rate performance of a phase shift keyed signal in the presence of Gaussian noise and co-channel interference consisting of K identical phase shift keyed signals [27]. He shows that the error rate increases monotonically as K increases (with the total interference power constant and equally distributed among the K interferers). As K approaches infinity, the error rate reaches its maximum and is identical to the error rate calculated assuming the total interference was white Gaussian noise. The significance of this is that for the practical case, where K is finite, assuming that the interference is Gaussian noise is conservative: this assumption overestimates the bit error rate. This result is directly applicable to one of the cases to be analyzed, where the existing and overlay signals are phase shift keyed signals. One may argue that the worst kind of interference a signal may experience is from a signal of the same type, since the receiver detects this signal just as well as the intended signal. If using a white noise model overestimates the error rate in this case, as Prabhu has shown, it should also overestimate the error rate for a non-identical signal.

Overlay System Performance Analysis

Overview

The analysis of the performance of the overlay signals will be done in three steps. First the maximum overlay signal power that can be transmitted from a small earth terminal (transmitting a BPSK overlay signal) without causing significant interference to the existing signal will be determined. Next the bit error rate performance of the overlay link must be calculated. This is done by determining the PSD of the interference that the overlay signal receiver sees. Since the existing signal is spread at the overlay receiver, the PSD is found by numerically convolving the PSD of the existing signal with that of the spreading signal in the receiver. This PSD is used to calculate the overlay link carrier to interference density ratio. Finally a complete link analysis for the overlay signal is performed. It uses the transmitted power calculated in the first step, and the carrier to interference density ratio calculated in the second step. For a specified BER, a maximum data rate for the overlay signal can be calculated. This will be the measure of performance of the overlay system. The improvement provided by various forward error correction codes will also be calculated.

Description of Existing Signals

As mentioned previously, the overlay system performance depends on the type of traffic existing in the satellite transponder: the existing signal. Since all type of existing signals can not be considered, the analysis will be limited to the three signals described below.

- 1) An FDM/FM/FDMA telephone signal consisting of eight 4 MHz channels in an FDMA mode,
- 2) An SCPC system consisting of two hundred 64 kbps channels using QPSK

modulation.

- 3) A single FM analog television signal occupying virtually an entire 36 MHz transponder.

All signals are assumed to be transmitted from a "typical" large earth station with a 9 meter diameter dish antenna, and approximately 200 watts of total power.

Overlay on FDM/FM/FDMA Telephone Traffic

Figure 15 shows the first existing signal to be considered. It consists of 8 FDMA channels with a bandwidth of 4 MHz each. An earth station with 9 meter diameter antenna transmits each FDMA channel with a power of 25 Watts.

Figure 16 shows the PSD of the overlay signal. It is a simple BPSK signal with a chip rate of 18 MHz. The overlay earth station has a two meter diameter dish antenna. The transmit power is to be determined. The analysis assumes a transponder bandwidth of 36 MHz and operation at C band.

The total bandwidth of the overlay signal is 36 MHz. Any one of the 8 FDM channels will receive only a portion of the overlay signal power. The bandwidth of one of these channels, 4 MHz, is only one ninth of the overlay signal bandwidth. The wideband overlay signal therefore passes through a relatively narrowband filter before being detected by the FM receiver. As discussed previously, when a wideband signal passes through such a filter the output has Gaussian statistics. For this reason the interference to any one of the eight channels of the existing signal caused by the overlay signal will be modeled as Gaussian noise.

To calculate the maximum allowable transmitted power for the overlay signal, the power which causes the signal to interference ratio in the worst case channel to be 25 dB must be determined. Since the

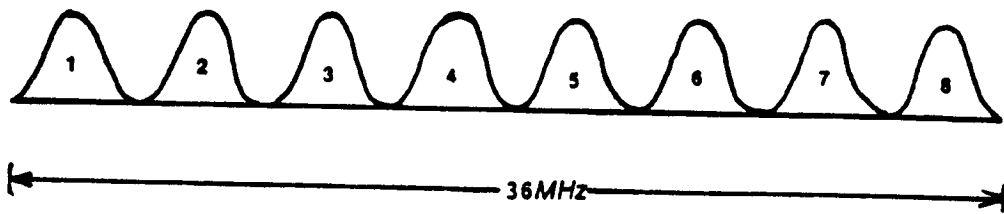


Figure 15. FDMA Existing Signal

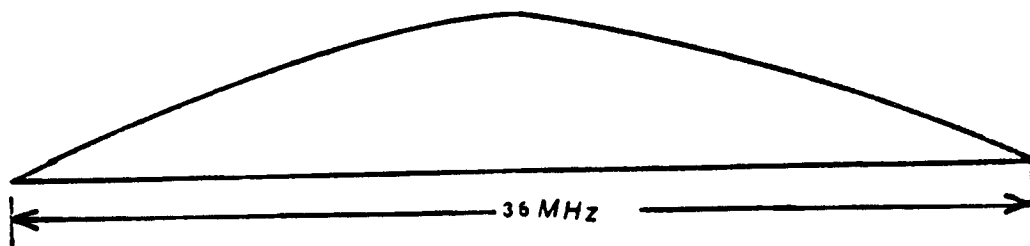


Figure 16. DS Overlay Signal

PSD of the overlay signal is at its highest in the center of the transponder, channels 4 and 5 in Figure 15 experience the most interference. The fraction of the overlay signal power contained in a 4 MHz band around its center is approximately 22%. For the signal to interference ratio at the transponder to be 25 dB in channel 4 or 5, the overlay signal power (again at the satellite) needs to be

$$-25 \text{ dB} - 10 \log(.22) = -19 \text{ dB}$$

The overlay signal power at the transponder must be 19 dB below the power of a single FDMA channel at the satellite. The FDMA signal has a transmitted power of 14 dBW (=25 watts) and its earth station antenna has a gain of 48.2 dB, giving it a total EIRP of 62.2 dBW. The overlay signal EIRP must be 19 dB below this, and since its 2 meter antenna has a gain of 40.1 dB, it must transmit 3 dBW, or 2 watts.

Now that a transmitted power constraint has been placed on the overlay signal so that the performance of the FDMA telephone system is not degraded appreciably, the performance of the overlay link must be analyzed. The interference of the existing signal to the overlay signal must first be considered, then a conventional link analysis using the parameters of the overlay link and earth station can be performed.

As can be seen from Figure 14, the signal received by the overlay receiver is despread by mixing it with a replica of the spreading signal, an 18 MHz chip rate BPSK signal. To calculate the signal to interference ratio for the overlay link (the interference being the existing signal), the effect of this despreading must be calculated. This is done by convolving the PSD of the existing signal with that of the spreading signal, with the PSD of each FDM signal approximated by a Gaussian curve with a standard deviation of 546 kHz [28]. Figure 17 shows the result, with the power of a single FDMA signal normalized to 1.

The matched filter in the overlay receiver has a bandwidth approximately equal to the bit rate of the overlay signal. If the overlay signal data rate is on the order of several kilobits per second, and since the bandwidth of the interference is at least as large as the spreading signal bandwidth of 36 MHz, the statistics at the output of the matched filter are very nearly Gaussian. Since the overlay signal power

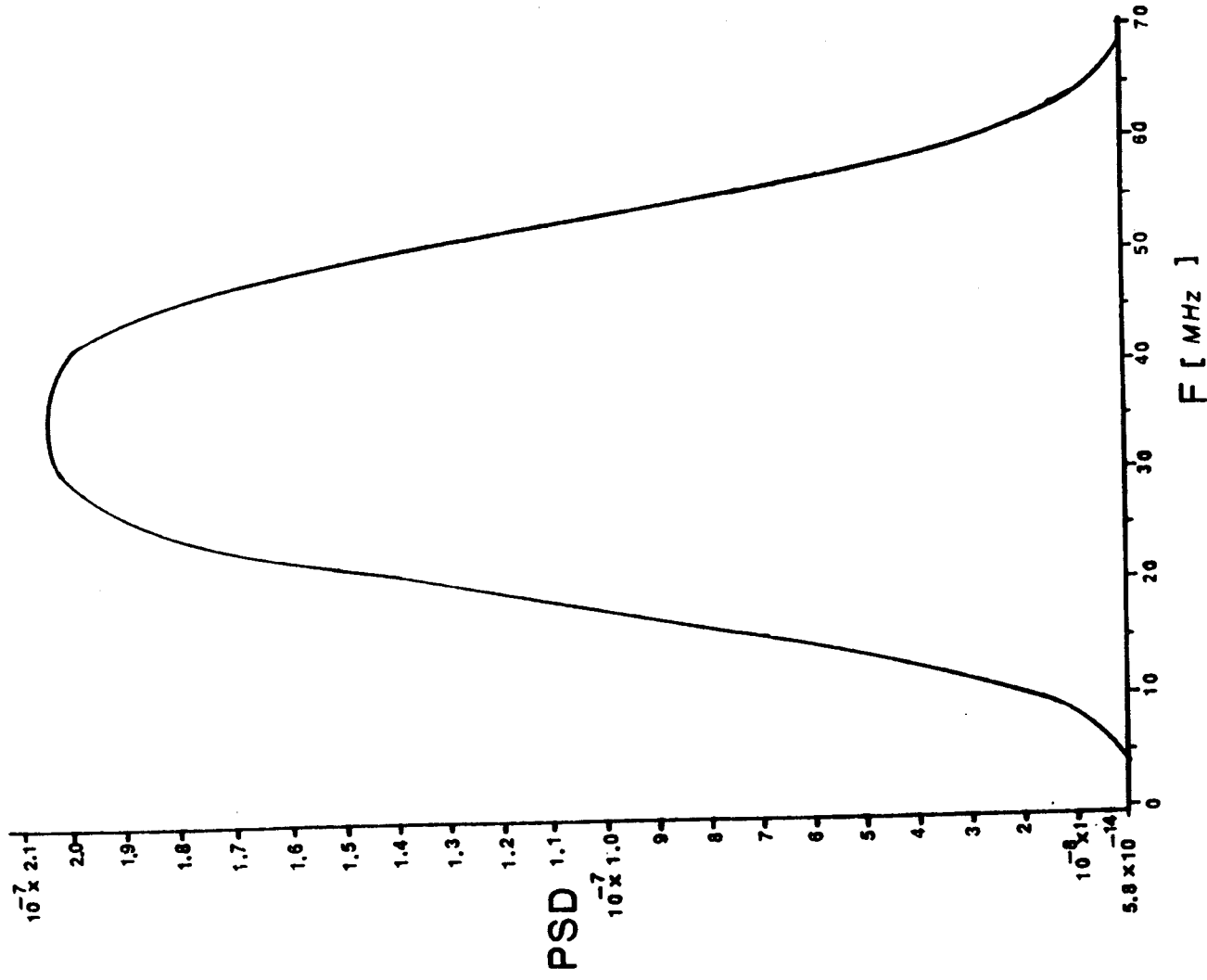


Figure 17. Interference PSD caused by the FDMA Signal

is 19 dB below that of the FDM signal, or 12.6 mW normalized, and the noise spectral density at the center of the transponder bandwidth is 2×10^{-7} Watts/Hz, the carrier to interference density ratio at the overlay receiver is

$$\frac{0.126 \text{ W}}{2 \times 10^{-7} \text{ W/Hz}} \rightarrow 48.0 \text{ dB-Hz}$$

The following link analysis combines this carrier to interference density ratio with the carrier to noise density ratios of the uplink and downlink to determine the link E_b/N_0 (Table 4.1).

Table 4.1. FDM Overlay System: C- Band

<i>Satellite Parameters</i>	
EIRP	= 36 dBW
G/T	= 0 dB/K
Bandwidth	= 36 MHz

<i>Earth Station Parameters</i>	
Antenna Diameter	= 2.0 m
Aperture Efficiency	= 65
Transmit Gain (6 GHz)	= 40.1 dB
G/T	= 14 dB/K

<i>Downlink</i>	
Propagation and pointing loss	= 196.3 dB
$(C/N_o)_e$	= 47.9 dB-Hz

<i>Uplink</i>	
Propagation and pointing loss	= 200.2 dB
Earth station power	= 3.00 dBW
$(C/N_o)_e$	= 76.6 dB-Hz

<i>Overall Link</i>	
Carrier to Interference Density Ratio	= 48.0 dB-Hz
Overall C/N_o	= 44.9 dB-Hz

With an overall link carrier to noise density ratio of 44.9 dB-Hz, and a E_b/N_0 of 11 dB needed to achieve a 10^{-6} bit error rate, the maximum bit rate achievable is

$$44.9 \text{ dB-Hz} - 11 \text{ dB} = 33.9 \text{ dB-bps}$$

or

$$R_{b \text{ max}} = 2475 \text{ bps}$$

While this data rate is quite low, it can be increased by using forward error correction. The chip rate can be held constant at 18 MHz regardless of the data rate by changing the length of the code. If the chip rate is held constant, all of the interference PSDs and link parameters mentioned previously are unchanged.

A rate 1/2, constraint length 7 Viterbi decoded convolutional code gives a 6 dB improvement in E_b/N_0 at a bit error rate of 10^{-6} [29]. Therefore the achievable data rate is increased by 6 dB by using this coding scheme. With this coding:

$$R_{b \text{ max}} = 9855 \text{ bps}$$

Overlay of Digital SCPC System

Figure 18 illustrates the digital SCPC system to be considered. It consists of 200 QPSK signals at 64 kbps each transmitted at 1 Watt through a 9 meter diameter earth station, frequency division multiplexed in a 36 MHz transponder. The RF bandwidth of each of these signals with a 50% rolloff Nyquist filter is approximately 45 kHz. The overlay signal is unchanged from the previous section.

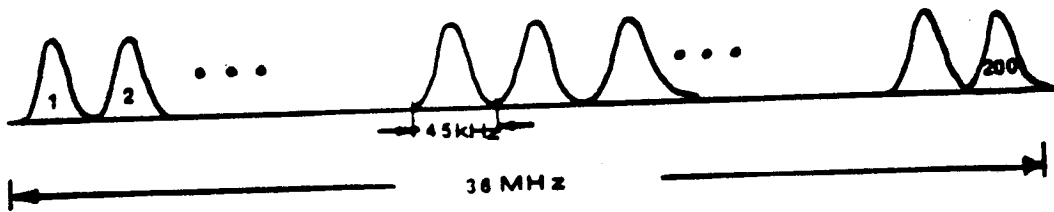


Figure 18. SCPC Existing signal

Using the same arguments as before, the statistics of the interference at the SCPC and overlay signal receivers will be treated as Gaussian. The 36 MHz bandwidth of the overlay signal is much wider than that of the SCPC receiver, causing the interference at the SCPC receiver to have Gaussian statistics. Furthermore, the multiplication of the 200 SCPC signals by the despreading signal in the overlay receiver creates an interference signal with a bandwidth much larger than 36 MHz, which is much larger than the bandwidth of the overlay receiver. Therefore the interference to the overlay system is also Gaussian.

The analysis of the overlay system performance is identical to that for the FDM system. The fraction of the overlay signal power contained in the bandwidth of any SCPC signal is less than 1%. One percent will be used as a conservative figure. Therefore for the signal to interference ratio in the bandwidth of one SCPC signal to be greater than 25 dB, the overlay signal power relative to the power of an SCPC signal (at the satellite) must be $-25 - 10 \log (.01) = -5$ dB. This gives an overlay signal transmit power of 2 Watts. Performing a numerical convolution to determine the interference PSD at the overlay receiver, with the narrowband SCPC signals approximated by impulse functions in the frequency domain, gives an interference spectral density of 5.5×10^{-6} Watts/Hz (see Figure 19). This gives a carrier to interference density ratio of 47.60 dB-Hz. The complete link analysis follows (Table 4.2).

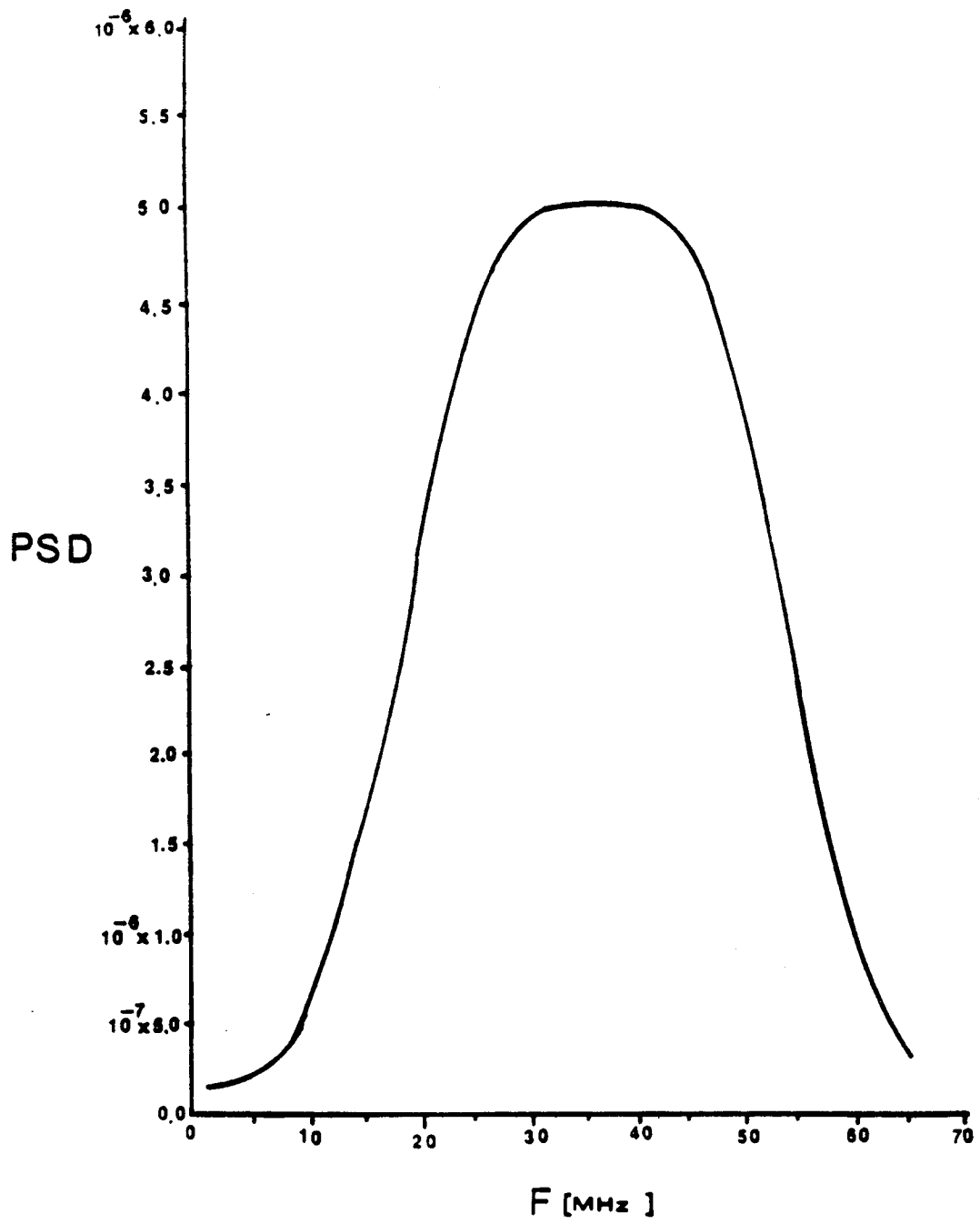


Figure 19. Interference PSD caused by the SCPC signal

Table 4.2. SCPC Overlay System - C Band

<i>Satellite Parameters</i>	
EIRP	= 36 dBW
G/T	= 0 dB/K
Bandwidth	= 36 MHz
 <i>Earth Station Parameters</i>	
Antenna Diameter	= 2.0 m
Aperture Efficiency	= 65
Transmit Gain (6 GHz)	= 40.1 dB
G/T	= 14 dB/K
 <i>Downlink</i>	
Propagation and pointing loss	= 196.3 dB
$(C/N_o)_d$	= 54.3 dB-Hz
 <i>Uplink</i>	
Propagation and pointing loss	= 200.2 dB
Earth station power	= 3.1 dBW
$(C/N_o)_u$	= 76.6 dB-Hz
 <i>Overall Link</i>	
Carrier to Interference Density Ratio	= 47.6 dB-Hz
Overall C/N_o	= 46.75 dB-Hz

**ORIGINAL PAGE IS
OF POOR QUALITY**

Again since an 11 dB E_b/N_0 is needed to achieve a 10^{-6} BER, the maximum data rate of the overlay link is 3758 bps. Using a rate one-half convolutional code with a coding gain of 6 dB increases the data rate to approximately 15 kbps.

Analog Television Overlay

The overlay of data signals on analog television traffic presents some unique problems. First of all the spectrum of the television signal is not known with any degree of certainty. Its shape varies significantly with the type of image being shown. Secondly, in contrast to the FDM and SCPC cases, the television signal is a wideband signal. Essentially the entire overlay signal will be contained within the bandwidth of the television receiver, not only a small portion as is the case with the relatively narrowband FDM and SCPC receivers. Finally, the degree to which an interferer degrades the performance of a television signal is highly subjective, and cannot be quantified. Television is primarily a video signal. Even though an interferer may have a very low power relative to a television signal, if it has certain characteristics, it may produce objectionable images in the received television video. Furthermore, high level interferers with the right parameters may produce little noticeable interference. For these reasons, television interference research is best performed by experiment with human judges. Computer simulation may be useful, but will still fail to include the subjective measures of video quality that are an important part of the system design. This section presents estimates of the acceptable interference levels to provide a crude estimate of the feasibility of signal overlay on analog television signals.

In satellite television transmission, the baseband television signal, with a video bandwidth of approximately 4 MHz, is FM modulated so that its RF bandwidth fills an entire 36 MHz transponder. When the overlay signal, which is a BPSK signal with a data rate of 18 MHz, passes through an ideal FM demodulator, the output would appear as in Figure 20, an impulse at each bit transition. The

impulses would be of random polarity and occur at a maximum rate of 18 MHz. The video receiver is essentially a 4 MHz wide filter. The fact that this wideband (> 18MHz) noiselike signal passes through a filter that has a relatively narrow bandwidth supports the assumption that the amplitude of this interference signal at the output of the video receiver has Gaussian statistics. For this reason it is assumed that the BPSK overlay signal should not produce especially objectional interference to the video signal. Since its distribution should be a nearly Gaussian function, it should not be more objectional than white noise of equal power.

Since the entire overlay signal power is within the television receiver bandwidth, to keep the signal to interference ratio at 25 dB the EIRP of the overlay transmitter should be 25 dB below that of the television transmitter. If we assume a television earth station with a 9 meter diameter antenna transmitting 200 Watts, the overlay transmit power from a 2 meter antenna should be approximately 4 Watts.

If we assume that the PSD of the television signal can be approximated by the following Gaussian curve [30]

$$\frac{1}{\sqrt{2\pi\sigma^2}} \exp\left[-\frac{(f-f_c)^2}{2\sigma^2}\right]$$

where $\sigma = 7.6$ MHz, then the numerical evaluation of the interference PSD at the overlay receiver is shown in Figure 21.

The carrier to interference density ratio is then 49.32 dB-Hz. The analysis of the overlay link is given below (Table 4.3).

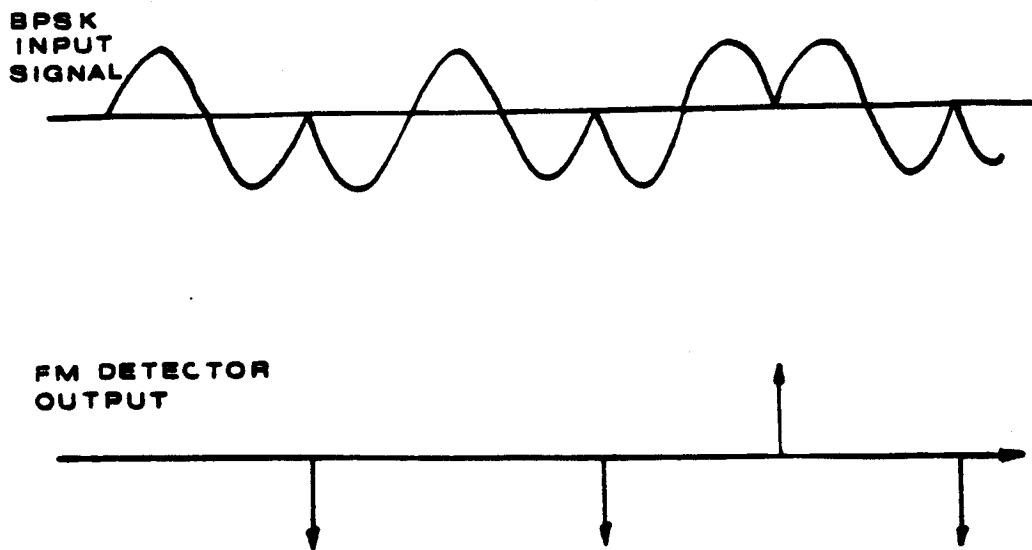


Figure 20. BPSK Signal Passed Through an FM Demodulator

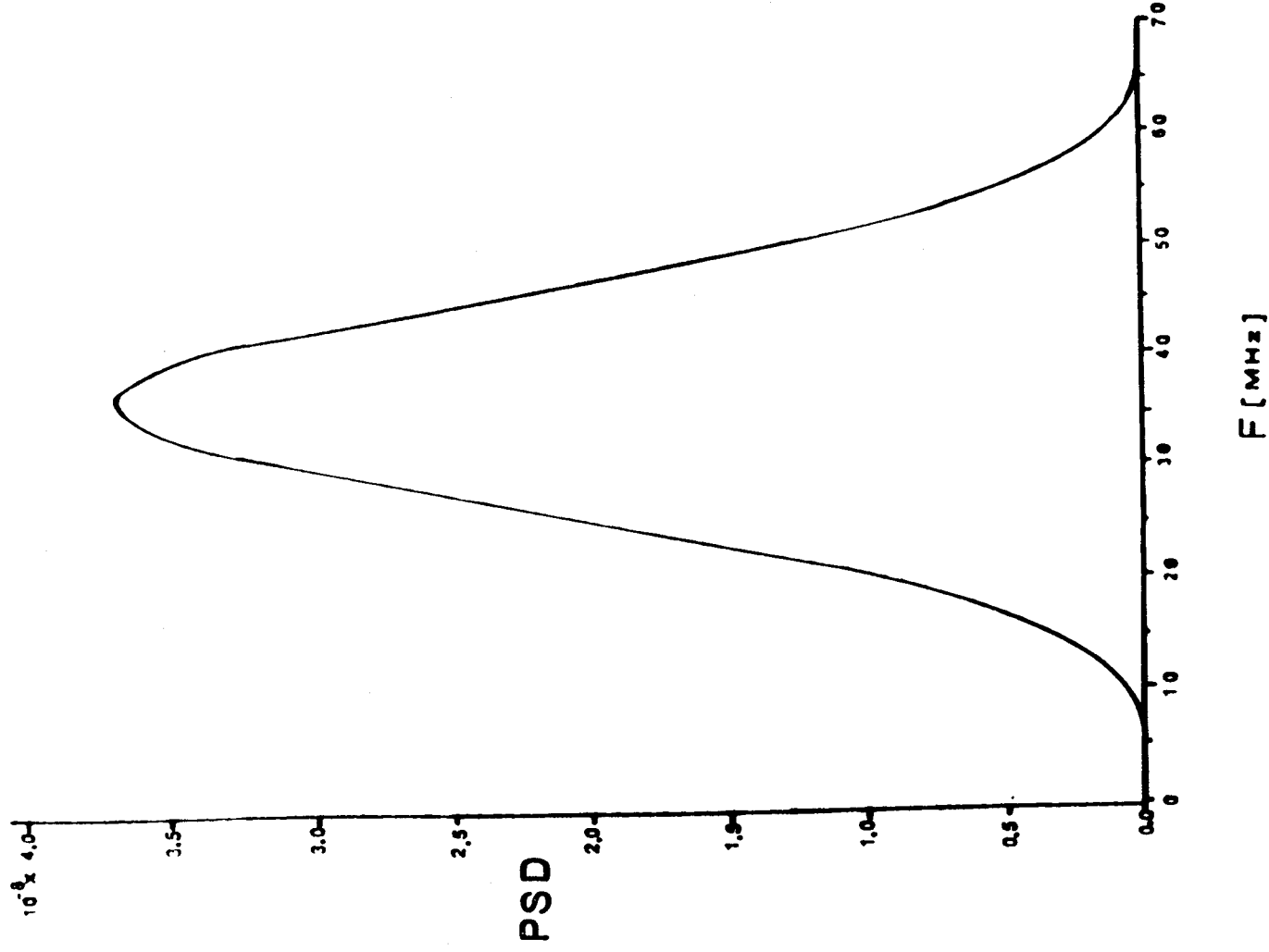


Figure 21. Interference PSD Caused by a TV Signal

Table 4.3. Analog Television Overlay - C Band

<i>Satellite Parameters</i>	
EIRP	= 36 dBW
G/T	= 0 dB/K
Bandwidth	= 36 MHz
<i>Earth Station Parameters</i>	
Antenna Diameter	= 2.0 m
Aperture Efficiency	= 65
Transmit Gain (6 GHz)	= 40.1 dB
G/T	= 14 dB/K
<i>Downlink</i>	
Propagation and pointing loss	= 196.3 dB
(C/N_o) _e	= 57.6 dB-Hz
<i>Uplink</i>	
Propagation and pointing loss	= 200.2 dB
Earth station power	= 8.1 dBW
(C/N_o) _u	= 74.6 dB-Hz
<i>Overall Link</i>	
Carrier to Interference	
Density Ratio	= 49.3 dB-Hz
Overall C/N_o	= 48.7 dB-Hz

The overall link C/N_0 of 48.69 dB-Hz implies a maximum overlay data rate of 5874 bps at a 10^{-4} BER. The 6 dB coding gain from a rate 1/2 convolutional code increases this data rate to approximately 23.5 kbps.

Extension to Multiple Overlay Signals

In the case where N simultaneous overlay signals are desired, the maximum data rate of each must be reduced by a factor of N . For example if the maximum allowable data rate for a single overlay signal is 10000 bps, then two overlay signals of 5000 bps, or 4 signals of 2500 bps, etc., can be accommodated.

The reasoning for this is as follows. If the number of desired signals is N , then to keep the total interference power constant when N signals are used, the power of each must be reduced by a factor of N . This would lower the E_b/N_0 of each signal by a factor of N . To compensate for this decrease to keep the BER at the same level, the data rate must also be reduced by a factor of N to keep E_b/N_0 constant.

Conclusions

This chapter demonstrates that overlay of spread spectrum signals on existing satellite traffic is feasible. The most promising spread spectrum modulation for this purpose appears to be ordinary direct sequence spread spectrum. While this type of service is possible, the modest data rates it is able to support suggest that this service may be impractical. Data rates of less than 20 kbps are generally insufficient to accommodate a single voice channel, unless sophisticated bandwidth

compression schemes are used. However, these data rates can support the operation of several low data rate computer terminals.

V. On Board Processing for Multiple Access Systems

Introduction

All of the systems considered so far and probably all commercial satellites in existence use what is known as a "classical transponder". The classical transponder amplifies the received signal and translates the uplink frequency to the appropriate downlink frequency (Figure 22). While this arrangement has proven itself to be extremely reliable, it has one disadvantage: the satellite retransmits the uplink noise along with the uplink signal increasing the noise received at the earth station. Satellites with "processing transponders" can decouple the effects of the uplink and downlink noise. All of these not only amplify the received signal, but detect it, regenerate the best estimate of the transmitted bit stream, and remodulate the data at the downlink frequency, as shown in Figure 23.

In systems where the uplink and downlink E_b/N_o are nearly equal, this type of system can provide about 3 dB gain. For instance, if the uplink and downlink E_b/N_o for a conventional system are each 10.6 dB, the overall link E_b/N_o determined from the formula

$$\left[\frac{E_b}{N_o} \right]^{-1} = \left[\frac{E_b}{N_o} \right]_{up}^{-1} + \left[\frac{E_b}{N_o} \right]_{down}^{-1} \quad (5.1)$$

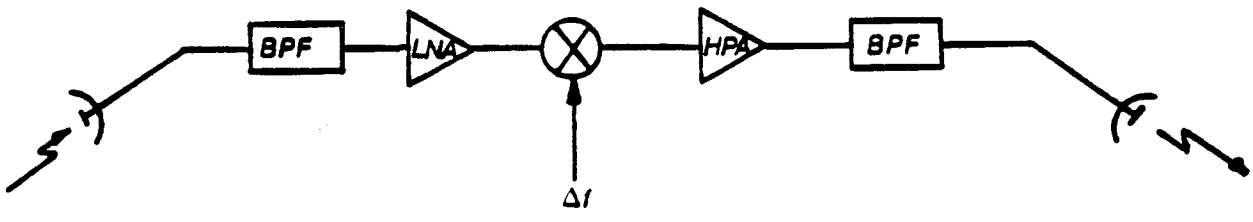


Figure 22. Classical Transponder

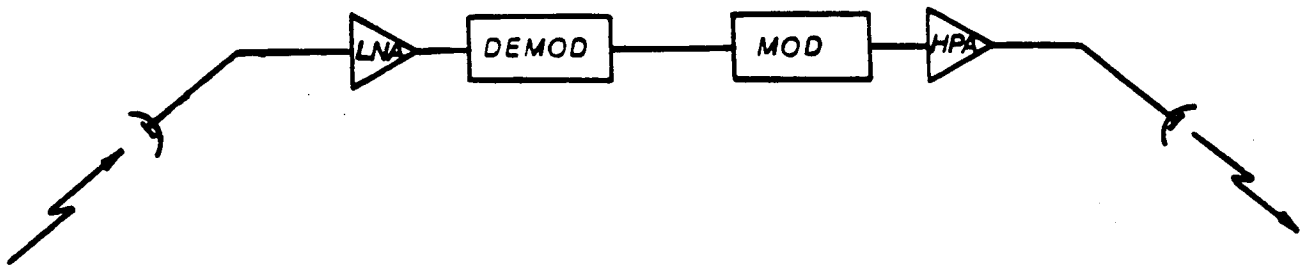


Figure 23. Processing Transponder

is 7.6 dB. For small error rates, the following formula approximates the link bit error rate when a processing transponder is used [31]:

$$P_e = (P_e)_{up} + (P_e)_{down} \quad (5.2)$$

At an E_b/N_o of 10.6 dB, P_e for the uplink and downlink are each 10^{-6} , making the link BER approximately 2×10^{-6} . The link E_b/N_o necessary to achieve this BER without a processing transponder is approximately 10.3 dB. The bit error rate achieved by the processing transponder with an overall link E_b/N_o of 7.8 dB is identical to that achieved by a conventional transponder with a link E_b/N_o of 10.3 dB, a gain of 2.7 dB.

The previous example is not typical. In many applications the uplink and downlink E_b/N_o are very different, meaning that there is little contribution to the overall noise by either the uplink or downlink. In these cases the benefit of a processing transponder is slight.

Processing transponders need not transmit the downlink signal with the same type of modulation as the uplink. In some cases, changing the modulation can provide advantages such as lower interference, reduced hardware complexity, and a lower bit error rate, depending on the application. One commercial satellite system that may be used in the future has an FDMA uplink transformed by a processing transponder to a TDM downlink. This system retains the advantages of FDMA (no time synchronization between users and therefore simple equipment) while eliminating the need for any backoff of the satellite power amplifier since intermodulation interference is not a problem in TDM [32].

In the following sections, the techniques described here are applied to the multiple access problem described in Chapter 3 to determine if and what type of processing transponder would increase the throughput of multiple access from small earth terminals.

Simple Processing Transponder

As mentioned above, simply decoupling the uplink and downlink has little effect if their signal to noise ratios differ appreciably. Unfortunately this is the case for the spread spectrum multiple access systems considered in Chapter 3. Looking at the link analysis in Chapter 3 for the C band multiple access system with 988 users, the uplink C/N_0 is 64.7 dB-Hz while the downlink C/N_0 is 45.0 dB-Hz. The downlink noise determines the link performance. In effect, the difference in C/N_0 , since it virtually negates the effect of the uplink on the link performance, has already decoupled the uplink and downlink. The same is true for the Ku band system. Both systems are downlink limited. The effect of a simple processing transponder on the system performance would be minimal.

Dual Modulation Systems

While simply demodulating the received spread spectrum signals and retransmitting spread spectrum signals would provide little advantage, there are benefits in using non spread spectrum modulations for the downlink. Since the links are downlink limited, anything that would lower the downlink noise, and therefore increase the downlink C/N_0 , would increase the system performance significantly. One obvious source of noise that could be eliminated if a non spread spectrum modulation is used is the inter-user interference. Much of the downlink noise is simply the interference between different users, which are forced to share the same bandwidth at the same time.

Using a spread spectrum uplink is desirable to reduce adjacent satellite interference. On the uplink, the relatively flat PSD of a spread spectrum signal would interfere little with adjacent satellites. As

explained in Chapter 1, this is desirable since the wide beamwidth of the small earth terminal's transmitting antenna would transmit significant power in the direction of adjacent satellites.

While interference to other users is not a problem for the downlink, since the antenna beamwidth is fixed by the desired coverage area on the earth, the use of non spread spectrum modulations would reduce the interference rejection capability of the small earth terminal receiver. Since the wide beamwidth of a small earth terminal's receiving antenna will receive signals from adjacent satellites, some form of rejection of these signals is necessary. Obviously the advantages of a transponder which changes the modulation of the downlink signal can only be realized when the means exist to reduce this interference to an acceptable level.

If the processing gain of a spread spectrum receiver is not available to reject interfering signals, the only means to reject these signals is with the directional gain of the antenna. This immediately excludes the use of non-spread spectrum downlink signals from C band full mesh VSAT networks. The gain of a small dish antenna at several degrees off axis is only reduced by 4 or 5 dB. Signals from adjacent satellites are therefore at a relatively high level, causing severe interference.

One exception to the use of such a system at C band is in multipoint to point networks, as shown in Figure 24. Here many small earth terminals communicate with a single large earth terminal, which may be connected to a central computer or telephone network. Because a narrow beamwidth (large diameter) antenna can be used for reception, signals from adjacent satellites are attenuated sufficiently.

Small earth terminal networks using spread spectrum uplinks and non spread spectrum downlinks are feasible at Ku band and above where a small diameter antenna can provide significant attenuation of signals from adjacent satellites. One such system follows.

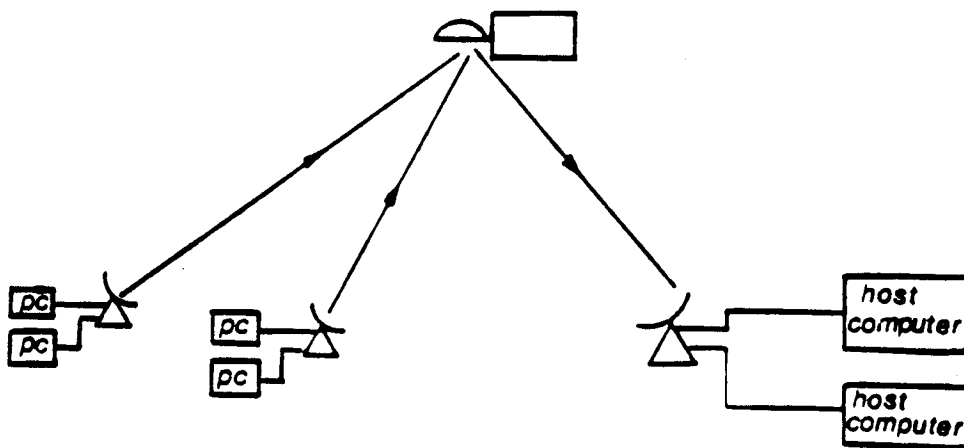


Figure 24. Multipoint to Point Network Architecture

MFSK/TDM Processing Transponder System

The Ku band spread spectrum multiple access system presented in Chapter 3 is limited by the downlink carrier to noise ratio. To improve this ratio, which is influenced significantly by the co-channel interference that the users present to one another, an appropriate non-spread spectrum multiplexing scheme must be chosen. Any type of frequency division multiplexing would require that the satellite's transmitted power be backed-off to reduce intermodulation interference. Since the satellite demodulates all of the users' signals, the synchronization required in TDM systems can be done at the satellite. Since no synchronization between different transmitters is needed, a TDM downlink signal should give the best system performance.

Figure 25 shows the operation of the on-board processing system described. N parallel receivers demodulate the N MFSK/DS spread spectrum signals each with a data rate of R_b . Each synchronizes to one of the transmitted signals. A baseband digital multiplexer accepts the data from each of the receivers and forms a single data stream at a rate $N \times R_b$. This TDM data stream is then transmitted at the downlink frequency using BPSK modulation. The earth stations then demodulate the BPSK signal. At this point, all of the data signals from each transmitter are available at every receiver.

The analysis of the performance of this system is done separately for the uplink and downlink (Table 5.1). The link bit error rate is given by equation 5.2.

Table 5.1. Ku Band MFSK/DS - TDM System :110 users

Satellite Parameters

EIRP	=	41.0 dBW
G/T	=	2 dB/K
Bandwidth	=	54 MHz

Earth Station Parameters

Antenna diameter	=	2.0 m
Aperture Efficiency	=	65
EIRP	=	46.6 dB
G/T	=	18.8 dB/K

Uplink Parameters

Propagation and Pointing Loss	=	208.5 dB
Uplink E_s/N_s	=	21.2 dB

Downlink Parameters

Propagation and pointing loss	=	206.8 dB
TDM bit rate	=	6.16 Mbps
Downlink E_s/N_s	=	13.7 dB

The link analysis confirms that this system can accommodate 110 users at 56 kbps versus 57 users for the same system which uses a classical transponder. The throughput has been increased by 93% from .059 bps/Hz to .114 bps/Hz. The system is now limited by the uplink to 110 users assuming that $M=16$ and the MFSK/DS/FDM multiple access system (Figure 11) is used. The downlink E_b/N_0 is 13.7 dB which gives a downlink BER of less than 10^{-6} . The MFSK/DS/FDM multiple access system can handle 110 users for $M=16$ at an E_b/N_0 of 18 dB. Since the uplink E_b/N_0 is 21.2 dB, its BER will also be much less than 10^{-6} , assuring that the system BER is less than 10^{-6} .

The throughput of the system is nearly doubled. The price for this increase in performance is an extremely complex and expensive satellite, more complicated than probably any in current commercial use.

VI. VSAT Networks – An Overview

This section examines the technology and constraints of very small aperture terminal (VSAT) networks, a special type of wide-area thin-route satellite network that represents a recent innovation in the field of satellite communications. VSAT network architectures suitable for both data and voice communications are studied in this chapter. Several issues concerning the frequency of operations that is, C-band versus Ku-band are examined, and trade-offs between non-spread spectrum and spread spectrum techniques, as well as modulation and multiple access schemes, are considered in detail. Link design examples are given to illustrate the performance of various types of VSAT networks.

Introduction

The very small aperture terminal (VSAT) (or micro earth terminal) is a low-cost satellite earth station with a small dish antenna and low power transmitter that is already playing a major role in data communication networking. VSAT networks provide viable alternatives to bypass terrestrial telephone systems by bringing a number of inherent advantages to the data communication problem,

such as distance insensitivity, higher data rate (in the range of 1.2 kbps to 128 kbps) and good reliability. In this section, we look at this important bypass technology from the system point of view.

Satellite communications offers unique advantages for networks which have a very large number of remote terminals which occasionally communicate with a hub station. Additional remote terminals can share the communications medium at little additional cost. However, to make such networks viable, the VSAT used at each remote location must have a low capital and operational cost - typically a few thousand dollars per unit compared to the millions of dollars required to purchase and operate a large earth station. In VSAT networks, the capital cost of the earth station dominates the economics of the system.

The next four sections discuss various VSAT architectures, the critical differences between 8/4 - GHz (C-band) and 14/12 - GHz (Ku-band) operation, the power-limited nature of VSAT networks and link analysis for non-spread spectrum VSAT networks that are compared to spread spectrum VSAT networks, and a look into the future of VSAT technology.

Architectures

VSAT networks are wide-area, thin-route satellite networks. They may have a variety of architectures depending on the applications: single-hop, double-hop, a mixture of both single-hop and double-hop (hybrid), and full mesh. The single-hop architecture (Fig.25) connects many remote VSATs to a hub station at a central site or headquarters. The communication links are the remote-to-hub link and the hub-to-remote link. The hub station may be connected to the terrestrial telephone or data network via a circuit switch or a packet-switched network via a packet switch. Both data and voice communications are possible via a single-hop link. Several data terminals or personal computers may be connected to a remote VSAT which may also be able to handle one or two digital voice channels at 32 kbps (using adaptive delta modulation or adaptive differential PCM). A VSAT network like this one may have hundreds or even thousands of widely distributed data terminals, each

generating a low duty cycle (bursty) data traffic communicating with a host computer connected to the hub station.

In the double-hop architecture, the remote VSAT communicates indirectly through the hub station which is capable of switching calls originating from one remote VSAT to a second remote VSAT. Because a link experiences a double-hop delay, this architecture is suitable for data traffic but not for voice traffic (unless it is recorded voice traffic).

A mixture of both single-hop and double-hop architectures (Fig.26) provides a general and attractive configuration for many applications. In this hybrid architecture, connectivity between the hub station and the remote VSAT is possible (voice, data) as well as the connectivity between remote VSAT (data and recorded voice messages). In the full mesh architecture (Fig.27), any remote VSAT may communicate directly with any other remote VSAT. A master control station must be used to control the network activity and assign channels on demand.

The selection of a VSAT architecture depends on the type of networking. The single-hop architecture in Fig.25 is the simplest and perhaps the most widely used network for this start-up technology. The full mesh architecture in Fig.27 is perhaps the most complex but offers full connectivity and may use the satellite capacity more efficiently in a demand assignment mode.

Ku-Band versus C-Band

VSAT networks are now available at both the 6/4-GHz and 14/12-GHz bands. The first commercial VSAT system operating in the 6/4-GHz band was introduced by Equatorial Communication Company in 1981 [33,35]. This system uses spread spectrum technology to greatly reduce the power flux density of the transmitted signal and thus avoid interference to adjacent 6/4-GHz satellites and 6/4-GHz terrestrial microwave systems. The spread spectrum signal is spread by a pseudo-noise (PN) code (or sequence) over a satellite bandwidth that is much wider than the data bandwidth. The receiving equipment correlates the received signal with the same PN code to extract the transmitted

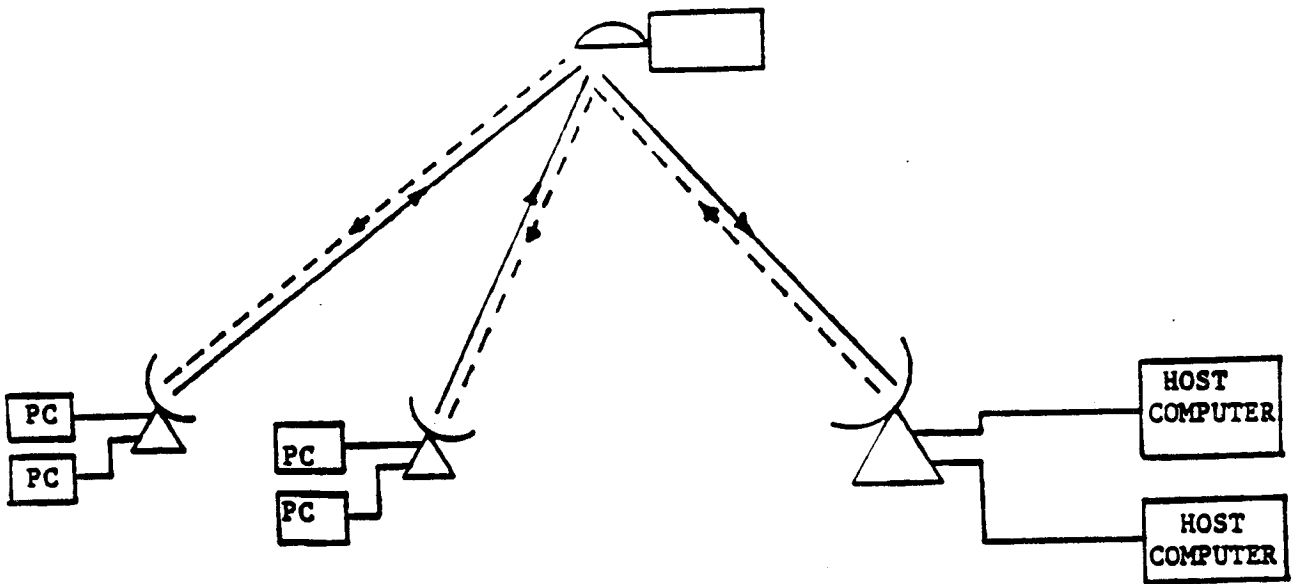


Figure 25. Single-Hop Architecture

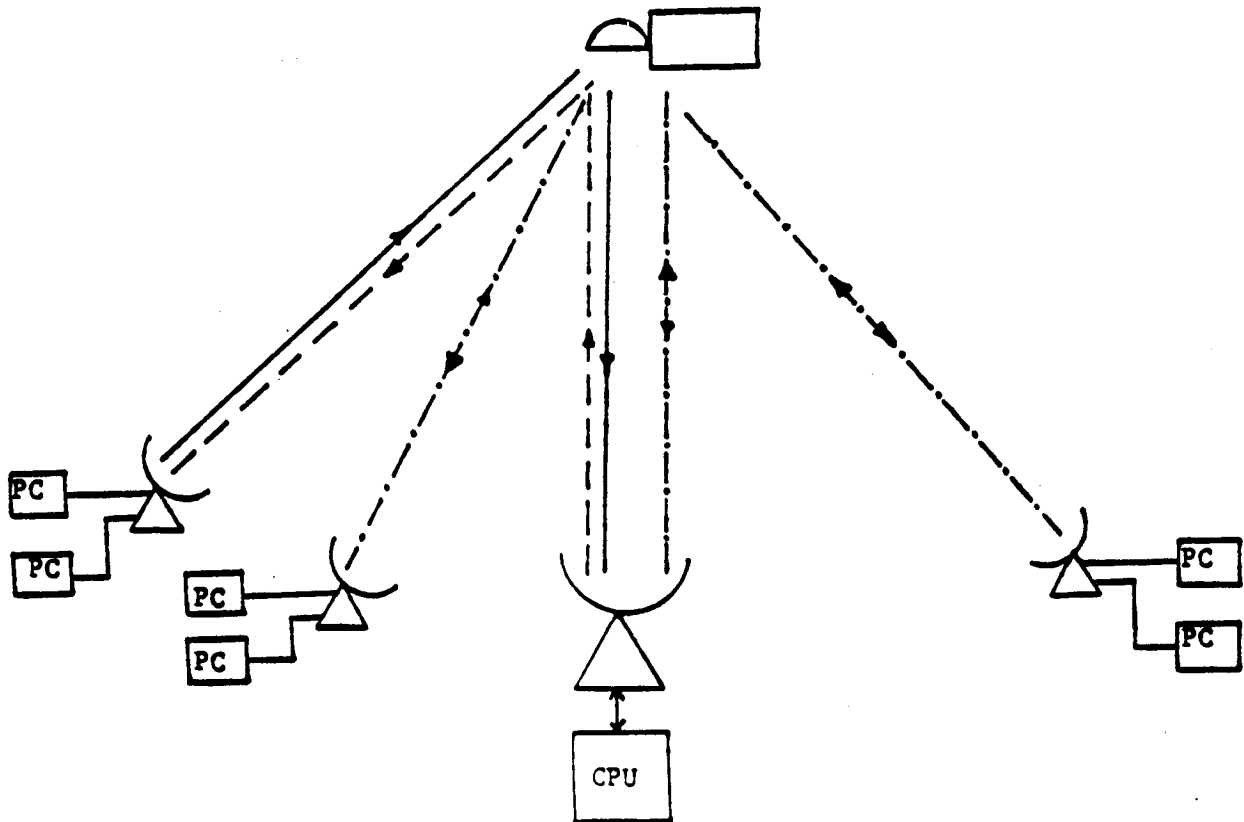


Figure 26. Hybrid Architecture(Mixture of Single-hop and double-Hop)

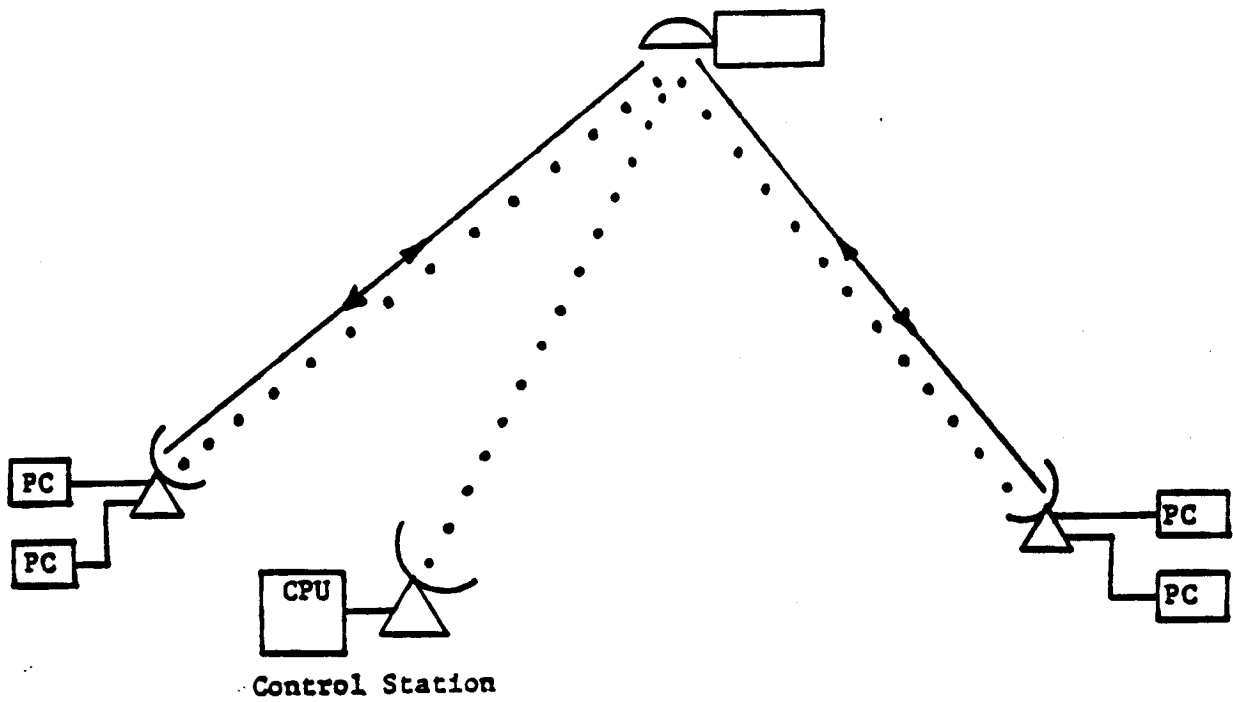


Figure 27. Full Mesh Architecture

**ORIGINAL PAGE IS
OF POOR QUALITY**

data. The Equatorial VSAT network uses the single-hop architecture. Even with spread spectrum technology, the severe interference limitations at the 6/4-GHz band can cause any spread spectrum VSAT network to use the satellite capacity inefficiently, and consequently the link data rate is low. The average efficiency for a 6/4-GHz VSAT network is estimated to be less than 0.03 bps/Hz and the average data rate is less than 9.6 kbps. The inefficiency of spread spectrum VSAT networks at the 6/4-GHz band has prompted unfavorable criticism [36]. Undoubtedly, spread spectrum systems use transponder bandwidth inefficiently. But without the use of spread spectrum signals, there could be no 6/4-GHz VSATs with dish antennas as small as 0.6 meter in diameter, at a potential price of less than \$7,000 per terminal. It is likely that the market place will decide how the satellite bandwidth is going to be used.

The situation is very much different for VSAT networks operating in the 14/12-GHz band which is free of terrestrial microwave interference. In the United States, the Federal Communication Commission (FCC) has relaxed licensing requirements for relatively large VSAT networks (500 terminals) operating in the 14/12-GHz band. In this band, VSAT networks can be designed to take advantage of the higher power flux density allowed and the lack of terrestrial interference. They can provide data rates of 56 kbps or more using dish antennas with diameter in the range of 1.2-1.8 m. For the same antenna diameter, the antenna gains in the 14/12-GHz band are approximately 7.4 dB(transmit) and 9.5 dB (receive) higher than those in the 6/4-GHz band. On the other hand, the attenuation caused by heavy rain will be much greater at 14/12-GHz band than at 6/4-GHz band, and consequently the VSAT networks operating at the higher frequency band suffer more and longer outages. A study of the constraints for VSAT networks operating in the 14/12-GHz band has recently been discussed in [37].

Power-Limited Networks

Because of the use of very small antennas and low power transmitters, a VSAT network is inherently a power-limited network. Therefore, the satellite capacity usage is very inefficient whether spread spectrum or non-spread spectrum technology is employed. This is obvious from the analysis of three VSAT networks (Tables 6.1-6.4) using PSK/QPSK as the modulation scheme and TDM and/or SCPC as the multiple access technique. The analysis of these particular non spread spectrum VSAT networks shows that the throughput is only 4.48 Mbps with 54 MHz transponder bandwidth. Thus the transponder efficiency is $4.48 \text{ Mbps}/54 \text{ MHz} = 0.08 \text{ bps/Hz}$. Each of these networks can accommodate more than 40 VSATs in one transponder by assigning many VSATs to one SCPC carrier and operating the group in the random access Aloha mode. The number of VSATs per group is determined by the average duty cycle of their traffic. For each VSAT group the hub-to-remote link (Tables 2-3) can be arranged in a broadcast time-division-multiplex (TDM) mode; that is, each station in the group receives the same data stream from the hub station and then selects the data destined for it, either by searching for its own address or by selecting its own time slot in the TDM frame. The Aloha/TDM multiple access scheme can accommodate a very large number of bursty users but does not in anyway improve the transponder efficiency (defined by the maximum number of simultaneous users) which is very low. Furthermore, when the 14/12-GHz space segment becomes crowded, the interference into the adjacent satellites by remote VSATs and the interference into the remote VSAT by adjacent satellites would be a major problem for VSAT networks using non spread spectrum technology. However, at the present time, these networks are indeed attractive, especially for the single-hop architecture. For the full mesh network where one remote VSAT communicates directly with another remote VSAT, the non-spread spectrum technology using SCPC or Aloha as a multiple access scheme would require a frequency synthesizer that can operate over the entire transponder bandwidth for full connectivity. Because of the high cost of microwave frequency synthesizers, this type of remote VSAT would cost more than those used in the single-hop architecture.

Table 6.1. Network Parameters

Satellite	
Transponder EIRP with 3.5 dB Back-off G/T	36.5 dBW + 2 dB/K
Hub Station	
Antenna	
Diameter	5.5 m
Gain (14 GHz)	56.5 dB
Gain (12 GHz)	55 dB
System Noise Temperature	260 K
G/T	30.9 dB/K
HPA Output Power	8.5 dBW
Remote VSAT	
Antenna	
Diameter	1.8 m
Gain (14 GHz)	46.5 dB
Gain (12 GHz)	45 dB
System Noise Temperature	370 K
G/T	19.3 dB/K
HPA Output Power	2.3 dBW
FEC Coding Gain @ 10^{-7} BER(Rate 1/2)	4 dB
PSK Bit Rate per VSAT	56 kbps
Number of VSATs	
Tables 6.2-6.3	40
Table 6.4	80

Table 6.2. Link Analysis. Hub Station Transmits 40 Coded 112 kbps

	Hub-to-Remote	Remote-to-Hub
Uplink		
EIRP/Carrier (dBW)	49	48.8
Propagation and Pointing Loss (dB)	208.7	208.5
Satellite G/T (dB/K)	2	2
Boltzmann's Constant (dBW/K-Hz)	-228.6	-228.6
$(C/N)_e$ (dB-Hz)	70.9	70.9
Dowlink		
EIRP/Carrier	17.5	17.5
Propagation and Pointing Loss (dB)	206.8	207
Station G/T (dB/K)	19.3	30.9
Boltzmann's Constant (dBW/K-Hz)	-228.6	-228.6
$(C/N)_e$ (dB-Hz)	58.6	70
Intermodulation and Interference C/I_0 (dB-Hz)	70.6	70.6
C/N_0 (dB-Hz)	58.1	65.7
E_b/N_0 (dB)	10.6	18.2
Required E_b/N_0 @ 10^{-7} BER (dB)	8(FEC)	12
Margin for Rain and Implementation (dB)	2.6	6.2

Table 6.3. Link Analysis. Hub-Station Transmit One Coded 4.48 Mbps TDM Carrier

	Hub-to-Remote	Remote-to-Hub
Uplink		
EIRP/Carrier (dBW)	65	48.8
Propagation and Pointing Loss (dB)	208.7	208.5
Satellite G/T (dB/K)	2	2
Boltzmann's Constant (dBW/K-Hz)	-228.6	-228.6
$(C/N)_u$ (dB-Hz)	86.9	70.9
Downlink		
EIRP/Carrier (dBW)	35	15
Propagation and Pointing Loss (dB)	206.8	207
Station G/T (dB/K)	19.3	30.9
Boltzmann's Constant (dBW/K-Hz)	-228.6	-228.6
$(C/N)_d$ (dB-Hz)	76.1	67.5
Intermodulation and Interference C/I (dB-Hz)	83.5	68
C/N_o (dB-Hz)	75	62.9
E_b/N_o (dB)	11.6	15.4
Required E_b/N_o @ 10^{-7} BER (dB)	8(FEC)	12
Margin for Rain and Implementation (dB)	3.6	3.4

Table 6.4. Link Analysis of a Full Mesh Network of 80 VSATs.

Each VSAT transmits a Coded 112 kbps SCPC Carrier.

Uplink

EIRP/Carrier (dBW)	48.8
Propagation and Pointing Loss (dB)	208.5
Satellite G/T (dB/K)	2
Boltzmann's Constant (dBW/K-Hz)	-228.6
$(C/N)_u$ (dB-Hz)	70.9

Downlink

EIRP/Carrier (dBW)	17.5
Propagation and Pointing Loss (dB)	206.8
Station G/T (dB/K)	19.3
Boltzmann's Constant (dBW/K-Hz)	-228.6
$(C/N)_d$ (dB-Hz)	58.6

Intermodulation and Interference C/I_i (dB-Hz) 70.6

C/N_i (dB-Hz)	58.1
E_s/N_o (dB)	10.6

Required E_s/N_o @ 10^{-7} BER (dB)	8(FEC)
Margin for Rain and Implementation (dB)	2.6

Spread Spectrum VSAT Networks

The use of SCPC as a multiple access scheme, especially in the full mesh network, is constrained by frequency instability and phase noise. These constraints limit the data rate that can be handled by the network. At a data rate of 56 kbps, the required frequency stability and phase noise are 1 part in 10^7 per 6 months and -85 dBc/Hz @ 10 kHz, respectively. To alleviate the precise frequency assignment in SCPC, spread spectrum multiple access (SSMA) may be used.

The low power spectral density of spread spectrum signals allows the use of very small antennas without significant interference to adjacent satellites, while the processing gain allows the rejection of narrow band signals from adjacent satellites and terrestrial systems. In a SSMA satellite system, each uplink earth terminal has its own addressed pseudo-noise (PN) code, and unlike the situation in TDMA or FDMA where the carriers are separated by time and frequency, all active earth terminals transmit in the same allocated bandwidth and overlap in time. Carrier separation is achieved at the earth terminal by correlation of the received signal with the properly addressed PN code. Therefore, in a SSMA system each carrier in the group represents a low interference signal to the others. The block diagram of a SSMA system is shown in Fig.28. To keep the system as simple as possible, and to reduce equipment costs of the VSAT, all users transmit asynchronously.

Two main modulation techniques are considered: phase shift keying (PSK/QPSK) and wide band M-ary frequency shift keying (MFSK). The precise performance of an asynchronous PSK-SSMA system is difficult to compute because an evaluation of the partial cross-correlations between PN codes is required [3]. When the user population is large, and the PN codes have low mutual cross-correlations, the ensemble average performance is normally considered knowing that some combination of users may have worse performance than the ensemble average performance and some a better performance. The ensemble average performance may be derived as follows. Let us assume equal carrier power C for each VSAT. The inter-user interference power spectral density is $kC/R_c = kE_b R_b / R_c = kE_b / N$ where $k+1$ is the number of simultaneous users in the system, R_b is the bit rate, R_c is the PN chip rate, $N = R_c R_p$ is the PN code period, and E_b is the bit energy. Therefore the

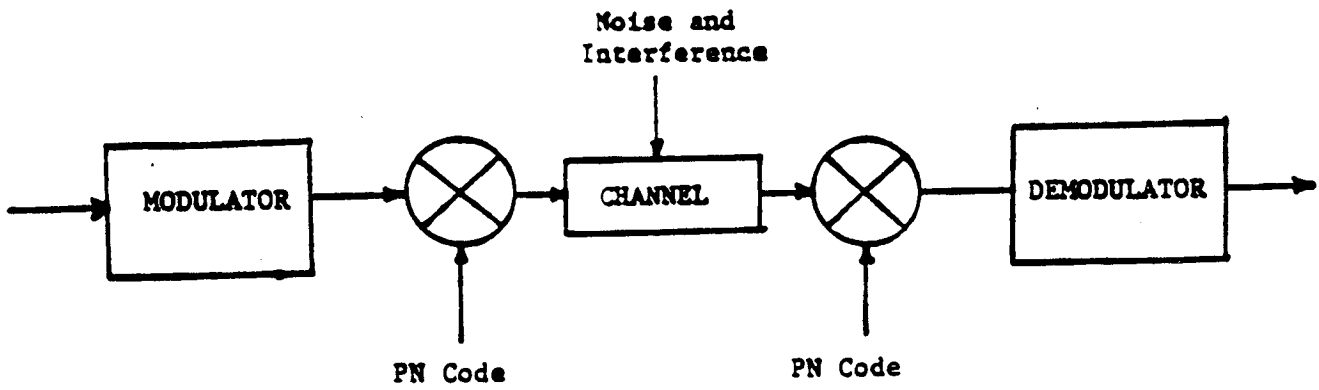


Figure 28. SSMA Modem

ORIGINAL PAGE IS
OF POOR QUALITY

total noise power spectral density is $kE_b/N + N_b$ where N_b is the thermal noise power spectral density. Consequently, the total energy per bit to noise density ratio is

$$\frac{E_b}{kE_b/N + N_b} = \frac{1}{k/N + (E_b/N_b)^{-1}} \quad (6.1)$$

and hence the PSK/QPSK-SSMA bit error probability is

$$P_b = Q(\sqrt{2[k/N + (E_b/N_b)^{-1}]}) \quad (6.2)$$

where $Q(x)$ is the Gaussian integral defined as

$$Q(x) = \frac{1}{\sqrt{2\pi}} \int_x^\infty e^{-y^2/2} dy \quad (6.3)$$

As an example, consider a single-hop QPSK-SSMA VSAT network with the same network parameters shown in Table 6.1. The hub-to remote link is a coded 3.92 Mbps TDM carrier, and there are 35 remote-to-hub links with QPSK-SSMA carriers, each with a data rate of 56 kbps. The PN code period is 1023 and the QPSK-SSMA signal is filtered to 54 MHz bandwidth ($T_c B = 0.8$). A link analysis similar to Table 6.3 shows that $E_b/N_b = 15.6$ dB in clear air. With $k = 34$, the link uncoded bit error probability is 10^{-7} with no margin for rain attenuation and implementation for remote-to-hub links. As a comparison, the SCPC-TDM system in Table 6.3 allows 40 carriers at 56 kbps carriers for the remote-to-hub links and a 3.4 dB margin. As a second example, we consider a full mesh QPSK-SSMA VSAT network with the same network parameter and a total of 80 QPSK-SSMA carriers. A link analysis similar to that in Table 6.4 shows that $E_b/N_b = 10.6$ dB in clear air. With $k = 79$ the link coded bit error probability is 10^{-7} with 1.4 dB margin.

In the above two examples the SCPC systems outperform the SSMA systems, but the difference is small. The advantage of the SSMA system is that no frequency synthesizer is required, which could significantly reduce the cost of the full mesh VSAT network. In addition the lower power spectral density and the interference rejection capability of SSMA systems make it attractive for 6/4-GHz

operation. It is doubtful that the interference levels generated by VSATs using SCPC transmission could be tolerated with 2° satellite spacing unless a large antenna (5 m or more) is used.

When wideband MFSK is used as the modulation scheme, the performance of VSAT networks can be improved. The performance of an MFSK-SSMA system is shown in Table 6.5. It is seen that MFSK-SSMA can provide a much larger number of simultaneous users than PSK/QPSK-SSMA. For example, at 10^{-7} BER and link $E_b/N_0 = 15$ dB, MFSK-SSMA can accommodate 70 users for $M=16$ while QPSK-SSMA can accommodate only 46 users. A single hop MFSK-SSMA ($M=16$) VSAT network with the same network parameters in Table 6.1 would require a link $E_b/N_0 = 12$ dB to achieve a 10^{-7} BER with 40 remote VSATs. This would yield a margin of 3.4 dB. A full mesh MFSK-SSMA ($M=16$) VSAT network with the same network parameters and a total of 80 MFSK-SSMA carriers achieves a coded bit error probability of 10^{-7} with a margin of 2 dB. A summary of the performance of these multiple access systems is given in Table 6.8.

Table 6.5. Performance of MFSK-SSMA @ 10^{-7} BER

$R_b = 56$ kbps, $B = 54$ MHz, Code Length = 511.

E_b/N_0 (dB)	M	Δf (MHz)	Users (k + 1)
16	16	2.6	80
15	16	2.6	70
14	16	2.6	60

Table 6.6. Summary of VSAT Systems

	Architecture	Users	System Margin Throughput	
SCPC/SCPC	single hop	40	6.2/2.6	8
SCPC/TDM	single hop	40	3.4/3.6	8
SCPC	full mesh	80	2.6	8
MFSK/DS	full mesh	80	2.0	8
MFSK/DS	single hop	40	3.4/3.6	8
QPSK/DS	single hop	35	0.0/3.6	7.2
QPSK/DS	full mesh	80	1.4	8

Epilogue

We have presented an overview of VSAT networks, a new bypass technology. Twenty-five percent of the large corporations in the United States bypass the local and long-distance telephone systems and the trend has been accelerating since the breakup of the Bell System in 1984 under a court-supervised anti-trust agreement. Until the nation implements a wholly digital transmission network called the Integrated Services Digital Network, (ISDN), bypass systems will continue to grow, and this undoubtedly will favor development of more low-cost VSAT networks.

The technology for VSAT networks is here. It is just a matter of selecting the right architecture and the right multiple access scheme for the intended service. Because VSAT networks are severely power-limited, it makes little difference to link performance whether non-spread spectrum or spread spectrum technology is used. However, the interference received at adjacent satellites is much lower when a VSAT uses spread spectrum modulation. Interference control in VSAT networks can also be improved by using rectangular antenna reflectors. By orienting the longer of the antenna dimensions in the plane of the geostationary arc, the adjacent satellite interference can be reduced while keeping the overall antenna dimensions reasonably compact. Non-spread spectrum systems such as SCPC-TDM are favorable for the single-hop architecture operating at 14/12-GHz band, while in this band QPSK-SSMA or MFSK-SSMA may be preferable for the full mesh architecture. The average transponder efficiency in the 14/12-GHz operation is expected to be around 0.08 bps/Hz for either technology. For 6/4-GHz operation, the low power spectral density and the interference rejection capability of spread spectrum systems make them preferable for VSAT networks. The transponder efficiency in the 6/4-GHz operation is dependent not only on the power constraints of VSAT networks but also on the adjacent satellite interference and terrestrial microwave interference. The estimated efficiency in this band is about 0.03 bps/Hz.

The future of VSAT technology ~~was~~ promising, at least for another decade before ISDN becomes available at all locations. ~~It never does~~. Most VSAT networks will be implemented in the 14/12-GHz band to take advantage of the higher antenna gain and the relatively free interference

environment. Thus they can provide higher data rate services for both data and voice communications for a larger number of widely distributed users at much lower cost than that of terrestrial telephone systems. For VSAT networks to use the satellite resources (i.e. bandwidth) efficiently, a new generation of VSAT satellites must be designed to take into account the severe power constraints imposed on VSAT networks. Recall from the link design shown in Tables 6.2- 6.4 that a typical 14/12-GHz VSAT network transmits only 4.48 Mbps in a 54 MHz transponder. For a non-spread spectrum system, a 10 MHz transponder would suffice. This represents a bandwidth saving factor of 5.4. A typical domestic 14/12-GHz satellite with dual polarizations has 16 54 MHz-transponders spanning a total bandwidth of 500 MHz. A satellite designed for VSAT operation could have 16 10 MHz-transponders spanning a total bandwidth of only 93 MHz (or 80 10 MHz transponders spanning 500 MHz). If growth in VSAT networks proves to be as explosive as it is at present, there may be a demand for more 14/12-GHz satellites in the geostationary arc. By designing VSAT satellites especially for small terminals, the geostationary arc would be able to accommodate more satellites to meet business demand, and the capital cost of the networks could be lowered.

VII. Conclusions

The analysis in the previous chapters demonstrates that spread spectrum multiple access is feasible, though still inefficient relative to non spread spectrum systems. The MFSK/DS systems proposed can achieve bandwidth efficiencies up to 11% for the Ku band example (56 kbps) and for the C band example (1200 bps). When the power and interference constraints of practical satellite systems are considered, the throughput is reduced to approximately 6% for the Ku band example and 3% for the C band example. The advantage of spread spectrum systems is that they make VSAT networks possible when operated at C band and when the angular satellite spacing is small, situations which make VSAT networks infeasible for other modulations. The construction of SSMA VSAT networks, because of their inefficient use of satellite bandwidth, is mainly a question of economics. If transponder leasing costs remain low, SSMA VSAT networks may proliferate. Presently, networks exist which are far less bandwidth efficient than the systems presented here but are still commercially successful [33].

Spread spectrum overlay will probably be implemented by a small number of satellite users that need an extra low data rate channel. The results of Chapter 4 predict that DS overlay signals with data rates of approximately 3000 bps can be superimposed on general satellite traffic. When convolutional coding is used, the data rate may be increased to 10 to 20 kbps. While these data rates are generally insufficient to accommodate even a single voice channel, they can accommodate several low rate

terminals. Because of the overlay systems' limited performance, their commercial appeal will probably be limited.

On-board processing has the ability to dramatically increase the throughput of SSMA systems, as seen in the near doubling of the throughput in our example. The Ku band MFSK/DS multiple access system considered in Chapter 3 could accommodate 57 simultaneous users. The addition of a processing transponder which converts the MFSK/DS uplink to a TDM downlink increases the number of simultaneous users to 110. The future of on-board processing in the commercial market, however, is probably not bright. The complex on-board electronics required would make the satellite very expensive, and would probably decrease its reliability. More importantly, the transponder becomes dedicated to a certain type of service. The ability of the classical transponder to handle general signals allows it to be leased to many different users at different times. This makes its commercial success independent of the success of an individual company or specific system, an advantage that the dedicated processing transponders do not enjoy.

IIX. References

- [1] Timothy Pratt and Charles W. Bostian, *Satellite Communications*, New York: Wiley, 1986 p. 225.
- [2] S. Joseph Campanella, and John V. Harrington, "Satellite Communications Networks", *Proceedings of the IEEE*, November 1984, p. 1507.
- [3] T.T. Ha, *Digital Satellite Communications*. New York: Macmillan, 1988. pp. 206-213.
- [4] Pratt and Bostian, p. 235.
- [5] Campanella and Harrington, p 1510.
- [6] Robert C. Dixon, *Spread Spectrum Systems* , New York: Wiley, 1984, pp. 15-28.
- [7] Dixon, pp. 28-42.
- [8] Robert M. Gagliardi, *Satellite Communications* , Belmont, California: Lifetime Learning Publications, 1984, pp. 267-268.
- [9] T.T. Ha, pp. 538-539.
- [10] T.T. Ha, pp. 539-544.
- [11] T.T. Ha, p. 543.
- [12] T.T. Ha, pp. 544-548.
- [13] M.B. Pursley and D.V. Sarwate, "Performance Evaluation for Phase-Coded Spread Spectrum Multiple Access Communication II. Code Sequence Analysis," *IEEE Transactions on Communications*, Vol. COM-25, No. 8, August 1977, pp. 800-803.
- [14] Gagliardi, pp. 282-288.
- [15] Rodger E. Ziemer and Roger L. Peterson, *Digital Communications and Spread Spectrum Systems*, New York: Macmillan 1985, pp. 569,581,585.

- [16] Y. Yamauchi, M. Sato, N. Morinaga, and T. Namekawa, "Improvement in Multiple Access Capability in M-ary-FSK/Direct Sequence SSMA," *Electronics and Communications in Japan, Part 1*, Vol. 69, No. 3, pp. 86-91, 1986.
- [17] Pratt and Bostian, p. 274.
- [18] Andrew J. Viterbi, "A Processing Satellite Transponder for Multiple Access by Low-Rate Mobile Users," *Proceedings of the Fourth International Conference on Digital Satellite Communications*, Montreal, Canada, October, 1978, pp. 166-174.
- [19] T.T. Ha, pp. 560-561.
- [20] Pratt and Bostian, p. 250.
- [21] H.J. Kochevar, "Spread Spectrum Multiple Access Communications Experiment Through a Satellite," *IEEE Transactions on Communications*, Vol. COM-25, No. 8, August 1977, p. 855.
- [22] Yamauchi, pp. 88-91.
- [23] T.T. Ha, pp 544-546.
- [24] K. Yao, "Error Probability of Asynchronous Spread Spectrum Multiple Access Communication Systems," *IEEE Transactions on Communications*, Vol. COM-25, No. 8, pp. 803-809, August 1977.
- [25] George C. Clark, and J. Bibb Cain, *Error Correction Coding for Digital Communication*, New York: Plenum Press, 1982, p. 369.
- [26] A. Papoulis, "Narrow Band Systems and Gaussianity", *IEEE Transactions on Information Theory*, January, 1972.
- [27] V.K. Prabhu, "Error Rate Considerations for Coherent Phase-Shift Keyed Systems with Co-Channel Interference," *The Bell System Technical Journal*, March 1969, pp.743-767.
- [28] T.T. Ha, p 202.
- [29] T.T. Ha, p. 538.
- [30] T.T. Ha, pp. 150.
- [31] T.T. Ha, pp. 561.
- [32] Pratt and Bostian, p. 273.
- [33] E.B. Parker, "Micro Earth Stations as Personal Computer Accessories," *Proceedings of the IEEE*, vol. 72, November 1984, pp. 1526-1531
- [34] T.T. Ha, pp. 428-433.
- [35] E. B. Parker, "Cost-effective Data Communications for Personal Computer Applications using Micro Earth Stations," *IEEE Journal on Selected Areas in Communications*, vol. SAC-3, No. 3, pp. 449-456, May 1985.
- [36] A. Viterbi, "When Not to Spread Spectrum-A Sequel", *IEEE Communications Magazine*, vol. 23, pp. 12-17, Apr. 1985.

- [37] D. Chakrabortz, "Constraints in Ku-band Continental Satellite Network Design", IEEE Communications Magazine, vol. 24, no. 8, pp. 33-43, August 1986.

Appendix A. Performance of Noncoherent MFSK in Colored Noise

An MFSK modulator transmits M distinct symbols

$$s_1, s_2, \dots, s_M$$

A noncoherent MFSK detector is composed of M parallel channels each containing a matched filter for one of the M symbols (Figure 5). The sampled outputs of these filters define a set of observation random variables

$$r_1, r_2, \dots, r_M$$

The probability that symbol q is chosen in the receiver given symbol p was transmitted is denoted by

$$\Pr(r_q > r_p | s_p)$$

In the usual case where the interference is additive white Gaussian noise and the spacing between symbols satisfies the orthogonality condition, the output of a channel whose symbol has been transmitted is the envelope of a signal plus noise, and is described by a Rician probability density function. The outputs of the other channels are the envelopes of Gaussian noise, and are described by Rayleigh probability density functions.

For the case where the noise is Gaussian but colored and has a PSD described by the function $\Phi(f)$ the appropriate probability density functions are [34]

$$p(r_p | s_p) = \frac{2r_p}{E_r N_p} \exp\left[-\frac{r_p^2 + E_s^2}{E_r N_p}\right] I_0\left[\frac{2r_p E_s}{N_p}\right] \quad (\text{Rician}) \quad (\text{A1})$$

$$p(r_q | s_p) = \frac{2r_q}{E_r N_q} \exp\left[-\frac{r_q^2}{E_r N_q}\right] \quad (\text{Rayleigh}) \quad (\text{A2})$$

where $N_p = \Phi(\zeta)$, $N_q = \Phi(\zeta)$, I_0 is the modified Bessel function of order zero, and E_s is the energy per symbol.

$$\begin{aligned} \Pr(r_q > r_p | s_p) &= \\ &= \int_0^\infty p(r_p | s_p) \int_0^\infty p(r_q | s_p) dr_q dr_p \\ &= \int_0^\infty p(r_p | s_p) \exp\left[-\frac{r_p^2}{E_r N_q}\right] dr_p \end{aligned}$$

$$= \frac{2}{E_s N_b} \int_0^{\infty} r_p \exp \left[-\frac{r_p^2 + E_s^2 \frac{N_b}{N_b + N_g}}{\frac{E_s N_b N_g}{N_b + N_g}} \right] I_0 \left[\frac{2r_p}{N_b} \right] dr_p$$

Now making the substitution

$$z^2 = \frac{r_p^2 N_b}{N_b + N_g}$$

$$= \frac{N_g}{N_b + N_g} \int_0^{\infty} \frac{2z}{E_s N_b} \exp \left[-\frac{z^2 + E_s^2}{E_s N_b} \right] I_0 \left[\frac{2z \frac{\sqrt{N_b}}{\sqrt{N_b + N_g}}}{N_b} \right] dz$$

Multiplying by

$$\exp \left[\frac{E_s}{N_b + N_g} \right]$$

inside the integral and compensating outside the integral gives:

$$= \frac{N_g}{N_b + N_g} \exp \left[-\frac{E_s}{N_b + N_g} \right] \int_0^{\infty} \frac{2z}{E_s N_b} \exp \left[-\frac{z^2 + E_s^2 \frac{N_b}{N_b + N_g}}{E_s N_b} \right] I_0 \left[\frac{2z \frac{\sqrt{N_b}}{\sqrt{N_b + N_g}}}{N_b} \right] dz$$

now let

$$A^2 = \frac{E_s N_s}{N_b - N_s}$$

and

$$\sigma^2 = \frac{E_s N_b}{2}$$

and the expression becomes

$$\frac{N_b}{N_b + N_s} \exp\left[-\frac{E_s}{N_b + N_s}\right] \int_0^\infty \frac{z}{\sigma^2} \exp\left[-\frac{z^2 + A^2}{2\sigma^2}\right] I_0\left[\frac{Az}{\sigma^2}\right] dz$$

Since the function inside the integral is a Rician pdf, the integral = 1, giving the final result:

$$\Pr(r_s > r_s) = \frac{N_b}{N_b + N_s} \exp\left[-\frac{E_s}{N_b + N_s}\right] \quad (A3)$$

When the noise power spectral density is flat, $N_s = N_b$ and this equation is identical to that for the probability of error for noncoherent binary FSK in white noise.

Appendix B. Derivation of Interference PSD

The power spectral density (PSD) of a pseudo-noise (PN) sequence is of the form

$$\left[\frac{\sin(af)}{af} \right]^2 \quad (B1)$$

The envelope of this function can be approximated by

$$\frac{1}{1 + a^2 f^2} \quad (B2)$$

The power spectral density $I(f)$ of an FSK tone spread twice by being multiplied by two uncorrelated PN codes can therefore be approximated by a convolution of the approximating function above with itself

$$\frac{1}{1 + a^2 f^2} \cdot \frac{1}{1 + a^2 f^2} \quad (B3)$$

$$\begin{aligned}
I(f) &= \int_{-\infty}^{\infty} \frac{1}{1+a^2k^2} \times \frac{1}{1+a^2(f-k)^2} dk \\
&= \int_{-\infty}^{\infty} \frac{1}{1+a^2k^2} \times \frac{1}{k^2a^2 - 2a^2fk + f^2a^2 + 1} dk \quad (B4) \\
&= \int_{-\infty}^{\infty} \frac{lk+n}{1+a^2k^2} dk + \int_{-\infty}^{\infty} \frac{mk+p}{k^2a^2 - 2a^2kf + f^2a^2 + 1} dk
\end{aligned}$$

where l , n , m , and p are partial fraction expansion coefficients which satisfy

$$(lk+n)(k^2a^2 - 2a^2kf + f^2a^2 + 1) + (mk+p)(1+a^2k^2) = 1 \quad (B5)$$

Equating like coefficients of powers of k and solving gives

$$p = \frac{3}{4+a^2f^2}$$

$$m = \frac{-2}{x(4+a^2f^2)}$$

$$l = \frac{2}{x(4+a^2f^2)}$$

$$n = \frac{1}{4+a^2f^2}$$

EVALUATE INTEGRALS:

$$\begin{aligned}\int_{-\infty}^{\infty} \frac{lk+n}{1+a^2k^2} dk &= \int_{-\infty}^{\infty} \frac{lk}{1+a^2k^2} dk + \int_{-\infty}^{\infty} \frac{n}{1+a^2k^2} dk \\ &= 0 + \frac{n}{a} \left[\tan^{-1}(ak) \right]_{-\infty}^{\infty} \\ &= \frac{n\pi}{a}\end{aligned}$$

$$\int_{-\infty}^{\infty} \frac{mk}{k^2a^2 - 2a^2kf + f^2a^2 + 1} dk =$$

$$\begin{aligned}
&= \int_{-\infty}^{\infty} \frac{mk}{k^2a^2 - 2a^2kf + f^2a^2 + 1} dk + \int_{-\infty}^{\infty} \frac{p}{k^2a^2 - 2a^2kf + f^2a^2 + 1} dk \\
&= \frac{m}{2a^2} \ln(a^2k^2 - 2a^2kf + a^2f^2 + 1) \Big|_{-\infty}^{\infty} + mx \int_{-\infty}^{\infty} \frac{dk}{a^2k^2 - 2a^2kf + f^2a^2 + 1} \\
&\quad + \int_{-\infty}^{\infty} \frac{p}{a^2k^2 - 2a^2kf + f^2a^2 + 1} dk \\
&= 0 + \frac{m\pi x}{a} + \frac{p\pi}{a}
\end{aligned}$$

Combining terms gives

$$I(f) = \frac{n\pi}{a} + \frac{m\pi f}{a} + \frac{p\pi}{a} \quad (B6)$$

Substituting the values for n, m, and p gives

$$I(f) = \frac{2\pi}{4 + a^2f^2} \quad (B7)$$

Normalizing the function to have an area of 1 by multiplying by a constant c

$$c \frac{2\pi}{a} \int_{-\infty}^{\infty} \frac{df}{4 + a^2 f^2} = c \frac{\pi}{2a} \frac{2\pi}{a} \equiv 1$$

$$c = \frac{a^2}{\pi^2}$$

which gives a normalized interference PSD function of

$$I(f) = \frac{2a}{\pi(4 + a^2 f^2)} \quad (\text{B8})$$

For a PN code with a code rate of R_c , $a = \frac{\pi}{R_c}$

Substituting this into equation (B8) above gives a normalized interference PSD function of

$$I(f) = \frac{2R_c}{4R_c^2 + \pi^2 f^2} \quad (\text{B9})$$

ORIGINAL PAGE IS
OF POOR QUALITY

Appendix C. MFSK/DS/FDM Performance Analysis

Program

```
C THIS PROGRAM EVALUATES THE BER FOR A DS/MFSK MULTIPLE ACCESS
C SYSTEM. THE PROGRAM CALCULATES THE ALLOWABLE NUMBER OF USERS
C IN A MFSK/DS SSMA SYSTEM FOR A GIVEN SYSTEM BIT ERROR RATE AND
C VALUES OF EB/NO FROM 10 TO 18 DB.
C
C INPUT PARAMETERS:
C RC - THE CODE (OR CHIP RATE) OF THE SPREADING CODE
C IN BPS
C DELF - THE FREQUENCY SPACING BETWEEN MFSK FREQUENCIES
C IN HZ
C M - THE NUMBER OF MFSK FREQUENCIES
C K - LOG BASE TWO OF M
C TB - THE BIT DURATION OF THE DATA SIGNAL = 1/RB
C BER - THE DESIRED SYSTEM BIT ERROR RATE
C NO - THE NOISE POWER SPECTRAL DENSITY (ALWAYS NORMALIZED
C TO 1)
C
C OUTPUT PARAMETERS:
C N - THE NUMBER OF USERS
C
C PROGRAM OPERATION:
C A VALUE OF EB/NO (= 10) IS SELECTED. THE BER IS CALCULATED
C FOR INCREASING VALUES OF N UNTIL THE BER IS GREATER THAN OR
C EQUAL TO THE DESIRED SYSTEM BER. THIS VALUE OF N IS THEN
C OUTPUT AND THE PROCESS IS REPEATED FOR THE NEXT EB/NO.
C
C APPLICATION TO MFSK/DS/FDM SYSTEM PERFORMANCE
C THIS PROGRAM IS USED TO CALCULATE THE NUMBER OF USERS THAT
```

C
C
C
C
C
C
C

CAN BE ACCOMODATED IN AN FDM SLOT. TO FIND THE TOTAL NUMBER OF SYSTEM USERS, THIS PROGRAM'S OUTPUT MUST BE MULTIPLIED BY Z, THE NUMBER OF FDM SLOTS.

COMMON RC,C,DELF,N,M,K,TB,NO

RC = 210000.00

DELF = 308000.00

M = 18

K = 4

TB = 1/58000.0

BER = 1.E-08

NO = 1

DO 200 J = 6,10

C = 10.**((J-1)/5.)/TB

DO 100 N = 1,500

Y = E(N)

IF (Y.GE.BER) THEN

WRITE(6,*) C,N

GO TO 200

ENDIF

100 CONTINUE

200 CONTINUE

STOP

END

C
C
C
C
C

FUNCTION PHI(I)

FUNCTION TO EVALUATE THE INTERFERENCE POWER FUCTION
EVALUATES EQUATION NUMBER 2.12 IN CHAPTER 2

C
C
C
C
C
C

COMMON RC,C,DELF,N,M,K,TB,NO

PI = 3.141592654

PHI = 0.0

DO 100 J = 1,M

PHI = PHI + 1.0/(4.*RC**2 + (PI*(I-J)*DELF)**2)

100 CONTINUE

C

PHI = 2.*RC*C*(N-1)/M*PHI + NO

RETURN

END

C
C
C
C
C
C

FUNCTION E(N)

EVALUATES THE BER OF THE SSMA SYSTEM AS A FUNCTION OF THE
NUMBER OF USERS IN THE SYSTEM USING EQUATION 2.9

C
C
C

```

C
C
REAL*16 V1,V2,PROD,SUM,ONE
FUNCTION EVALUATES THE PROB OF BIT ERROR FOR DS/MFSK
C
C
INTEGER P,Q
COMMON RC,C,DELF,N1,M,K,TB,N0
SUM=0.0
C
DO 200 P=1,M
  PROD=1.0
  TP=PHI(P)
  ONE=1.0
  DO 100 Q=1,M
    IF(Q.EQ.P) GOTO 100
    TQ=PHI(Q)
    V0=-C*TB*K/(TP+TQ)
    V1=EXP(V0)
    V2=ONE-TQ/(TQ+TP)*V1
    PROD=PROD*V2
100  CONTINUE
    SUM=SUM+(1.D0-PROD)
200  CONTINUE
C
E=SUM/(2.*(M-1))
RETURN
END

```

Appendix D. MFSK/DS/FH Performance Analysis

Program

```
C THIS PROGRAM EVALUATES THE BER FOR A FH/DS/MFSK MULTIPLE ACCESS
C SYSTEM.
C
C THE INPUT PARAMETERS ARE IDENTICAL TO THOSE OF THE MFSK/DS
C PROGRAM AND ARE READ FROM UNIT NUMBER 4.
C
C Z IS THE NUMBER OF FH SLOTS IN THE SYSTEM BANDWIDTH
C NMIN - THE START VALUE OF THE NUMBER OF USERS IN THE ITERATIVE
C CALCULATION OF THE NUMBER OF USERS
C INC - THE INCREMENT APPLIED TO THE NUMBER OF USERS
C
C PROGRAM OPERATION:
C THE PROGRAM STARTS WITH THE NUMBER OF USERS N=NMIN.
C IT THEN COMPUTES THE BER FOR THIS N. IF THE BER IS LESS
C THAN THE DESIRED SYSTEM BER THEN N IS INCREMENTED BY INC
C AND THE CALCULATION IS PERFORMED AGAIN, UNTIL THE BER IS
C GREATER THAN OR EQUAL TO THE DESIRED BER. THIS VALUE OF N
C IS OUTPUT AND THE PROCESS IS REPEATED FOR A NEW EB/NO.
C
C
C REAL NO
C COMMON RC,C,DELF,M,K,TB,NO
C READ(4,10) RC,C,DELF,M,K,RB,NO,BER,Z
10  FORMAT(F20.5/,F20.5/,F20.5, 20 20, F20.5/,F20.5,
C $ /,F20.5/,F20.5)
C
C BER = 1.E-08
C WRITE(7,12) RC,DELF,M,K,RB,NO,BER,Z
```



```

C
C
REAL*16 PROD
INTEGER DENOM

C
IF(N-K.GT.K) THEN
  JMIN=N-K+1
  DENOM=K+1
ELSE
  JMIN=K+1
  DENOM=N-K+1
ENDIF

C
PROD=1.0
DO 100 J=JMIN,N
  DENOM=DENOM-1
  PROD=PROD*J/DENOM
100 CONTINUE

C
COMB=PROD
RETURN
END

C
C
C
C
FUNCTION W(N,K,Z)
  EVALUATES THE BERNOULLI TRIALS FORMULA
  COMB(N,K)*P**K*Q**(N-K) WHERE P AND Q ARE DEFINED BELOW
  USES LOGARITHMS IF THE VALUES OF THIS FUNCTION ARE
  SUFFICIENTLY SMALL TO CAUSE UNDERFLOW IN THE COMPUTER

  P=1./Z
  Q=1.-1./Z
  IF (N.LE.200) THEN
    R=ALOG10(COMB(N,K))
  ELSE
    D0=FACLOG(N)
    IF(K.LE.50) THEN
      D1=ALOG10(FACT(K))
    ELSE
      D1=FACLOG(K)
    ENDIF
    IF(N-K.LE.50) THEN
      D2=ALOG10(FACT(N-K))
    ELSE
      D2=FACLOG(N-K)
    ENDIF
    R=D0-D1-D2
  ENDIF
  X=E(K)
  IF(X.LE.0.0) THEN
    U=-50
  ELSE
    U=ALOG10(X)
  ENDIF

```

```

                ENDIF
W=U+K*ALOG10(P)+(N-K)*ALOG10(Q)+R
IF(W.LT.-60.) THEN
    W=0.0
    RETURN
ELSE
    W=10.**W
    RETURN
ENDIF
END

C
C
C
FUNCTION FACT(K)
    COMPUTES K FACTORIAL
    FACT=1.
    DO 10 J=2,K
        FACT=FACT*J
    10 CONTINUE
    RETURN
END

C
C
C
FUNCTION FACLOG(K)
    THIS FUNCTION COMPUTES THE COMMON LOG OF
    STIRLING'S APPROXIMATION TO K
    PI=3.1415926538
    E=2.7182818284
    FACLOG=K*ALOG10(K/E)+0.5*ALOG10(2.*PI*K)
    RETURN
END

```

***Part B. Chirp Spread Spectrum System and
Overlay Service***

1. Introduction

The pulsed FM or chirp modulation technique, invented by B. M. Oliver at Bell Labs in 1951 and formulated by C. E. Cook in 1958, has been widely used in radar systems as a solution for the conflicting requirements of simultaneous long-range measurements and high range resolution. [1]. The range resolution is obtained by transmitting a long frequency modulated pulse that is time compressed in the receiver into a much narrower pulse. The energy distributed in the long pulse is coherently processed in a matched filter receiver to yield a short pulse of enhanced amplitude. [1], [2] A detailed account of the chirp concept and the relevant mathematics has since been given by many authors. [1], [2], [3], [4], [5]

The physical constraint of building delay lines that have dispersion characteristics which provide the required high Time-Bandwidth product have been overcome recently by using surface acoustic wave (SAW) devices and other types of dispersive delay lines (DDL). Chirp has now become an effective tool for producing small, low cost, lightweight spread spectrum systems for communication and ranging systems, as well as for radar. [1]

Spread spectrum techniques have made the use of small earth terminal satellite networks commercially valuable for low data rate users. The low power spectral density of spread spectrum signals allows the use of very small antennas without significant interference to adjacent satellites when transmitting, while the processing gain allows the rejection of

ORIGINAL PAGE IS OF POOR QUALITY

signals received from adjacent satellite when receiving. Among the four basic types of spread spectrum techniques, chirp spread spectrum systems have been proven to have advantages over other techniques like Direct Sequence (DS), Frequency Hopping (FH), Time Hopping (TH), and various hybrids. No coding is necessary, in principle, and thus no code synchronization is necessary either. In addition, multiple access can be achieved with simple sweep rate changes rather than by using different pseudo random sequence codes. [6], [7]. The low vulnerability of chirp systems to deliberate jamming has been the major obstacle to their application for military use. Thus, the technique has received little attention.

In a chirp system, all non-chirp type interfering signals and noise at the input of the pulse compression filter appear at the output either with the same mean power or with decreased power. However, the desired chirp signal gets enhanced by the processing gain, resulting in the rejection of the interference and noise. The possibility of relatively simple equipment implementation makes the chirp spread spectrum system attractive for low data rate, bursty commercial communication systems.

The feature which makes chirp attractive for low data rate satellite communications is the absence of a synchronization loop in the receiver. In all other spread spectrum systems, the receiver must synchronize to the PN sequence used to spread the original data. If data rates are low and the messages are short, the receiver may take many seconds to synchronize to the received signal, in order to receive a message less than a second in length. The lower the data rate and the longer the PN sequence, the more pronounced this problem becomes, and very low throughput is achieved. A bursty system, in which messages are transmitted infrequently to a given receiver, makes the problem even worse, because receiver synchronization cannot be maintained between transmissions. It is in this application that the chirp system has the best performance, since no receiver synchronization is needed, and throughput can be maintained at 100%.

In this report, several chirp spread spectrum systems are studied, using different modulation techniques. These include within chirp, and multiple chirp, where single or multiple chirps modulate the carrier amplitude, frequency or phase. Based on the preliminary

study, the proposed Coded Multiple Chirp Spread Spectrum System is described in detail, together with a performance analysis. This forms the major part of the work in Task 2. In addition, the possibility of Multiple Access (SSMA) using the proposed system is also evaluated as the final step in Task 2.

For Task 3, the overlay system study, interference analyses were performed when the proposed chirp spread spectrum system is overlaid on an existing FM-TV satellite link in C-band and Ku-band. In this study, various models of FM-TV signals are used to find a general expression for interference which can be used to find the error signal in an FM-TV discriminator. Finally, typical FM-TV signals are modeled with a linear multi-step function and a random step function, and are then overlaid with the chirp signal. By reviewing the spectral and time domain analysis, an optimum overlay method is proposed based on the carrier to interference ratio. The best offset frequency for the chirp signal and some performance evaluation data which support this method are presented.

ORIGINAL PAGE IS
OF POOR QUALITY

2. Review of Chirp Spread Spectrum Systems

Because of the inherent capability of interference rejection, the chirp modulation technique is a strong candidate for use in spread spectrum communication systems. A number of authors have proposed chirp signals for the representation of binary digital communication by assigning an increasing frequency expanded pulse known as 'up-chirp' to a binary '1' and decreasing frequency expanded pulse known as 'down-chirp' to a binary '0' (or vice-versa). [2], [7], [8] The degree of orthogonality between these two signals determines the possibility of overlapping time-frequency regions, and thus the efficiency of bandwidth utilization. Berni and Greg [9] compared BPSK, chirp and FSK and found that chirp signalling performance is between the performance of BPSK and FSK from the power and bandwidth utilization viewpoints [2]. Hirt and Pasupathy [10] investigated the effect of designing chirp signals with continuous phase at bit transitions, but the use of these techniques increases the receiver complexity.

The use of up and down chirp signal for the spread spectrum system was suggested in 1962 by Winkler [7]. Dayton [11] found that these signals gave excellent performance in multipath situations due to the narrow compressed pulse width. In addition, various applications such as high-frequency data transmission [12] and air-ground satellite communication [13] have been reported [14]. Recently Baier et al. [15] had suggested the

so call 'PN chirp' technique in 1981, which is the combination of chirp modulation with pseudonoise (PN) phase shift keying (PSK) using a fixed tap matched-filter. A similar suggestion was also proposed independently by M. Kowatsch et al. [16]. The advanced version of their proposal in 1983 [16] proposed a PN-chirp spread spectrum system which combines standard linear FM surface acoustic wave (SAW) devices, DDL, and an external code modulator. But this proposed system [15] still has the disadvantage of some hardware complexity and a need for synchronization, even though it offers high flexibility by avoiding the use of a programmable matched filter. [15]

In the foregoing paragraphs, we have discussed the application of the chirp (or linear FM modulation) technique in binary digital data communication systems and in various spread spectrum communication systems. Of the abundant applications of chirp, though, none are directly applicable for the purposes of our study, because of the complexity in practical implementation in a satellite link or the nature of the purely theoretical analysis in those proposals. Because of these difficulties, we have investigated some possible techniques using chirp modulation and PN coding, in an attempt to find the most feasible scheme. The desired features were selective addressing of a large number of potential users operating in a common band-limited channel, and good system performance measured by low probability of errors in data transmission.

We have reviewed several ways in which chirp can be used to provide spread spectrum coding of a communication link. We classified the systems under consideration at large as class I: 'Within-chirp Modulation' and class-II: 'Multiple Chirp Modulation', as illustrated in Fig. 1 and Fig. 2a. The term 'Within Chirp Modulation' comes from the fact that a single chirp is modulated by a finite length PN code within a chirp period, whereas the term 'Multiple Chirp Modulation' comes from the fact that multiple chirps are generated within the finite length of a PN code.

Also we can further classify the Within chirp Modulation (class I) as the Amplitude (I-1), Frequency (I-2), and Phase (I-3) versions that are depicted in Fig. 1. Note that all three systems need synchronization in the receiver and the anticipated complexity of this synchronization

ORIGINAL PAGE IS OF POOR QUALITY

(which was already mentioned in M. Kowatsch's proposal [14]) make these systems less desirable for our purpose of a relatively simple configuration. The other category, 'Multiple Chirp Modulation', can also be classified as the Multi-chirp (II-1), Time Delay (II-2), and Frequency Hop (II-3) as shown in Fig. 2

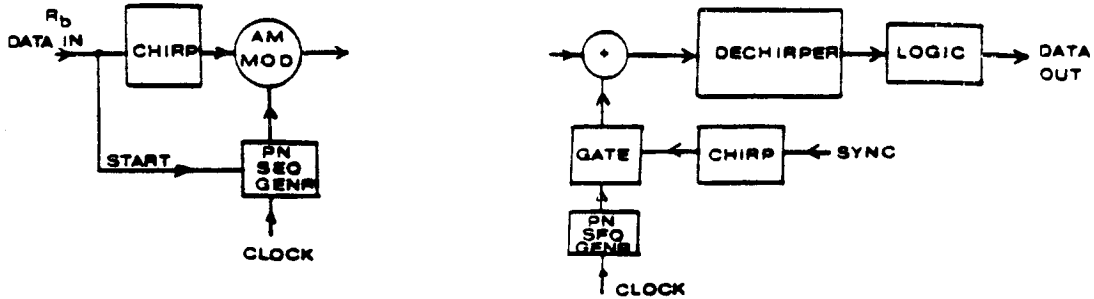
The proposed system II-1 Multi-chirp, is basically similar to the ordinary binary chirp system because it uses up and down chirps according to the input digital data. This system does not need synchronization in its receiver. Instead, a code correlator which looks for a specific code word can detect the desired code asynchronously. For multiple access, the easiest way is to assign different chirp slopes to the various users. Another system, II-2, Time delay, uses a variable time delay to generate a sequence of chirps with time delays set by a PN code, within each input data bit duration. This system needs a complementary PN sequence in the receiver for synchronization, and a window with the proper time delay in order to find the pulses at the dechirper output at the correct times. Therefore synchronization, and thus the windowing procedure may be the major difficulties in practical implementation because of their complexity. The proposed system II-3, Frequency Hop, uses the method of frequency hopping. The transmitter generates the sequence of chirps with shifted center frequencies and this frequency shift in a chirp signal produces a time delay at the output of the dechirper. If the idea of hopping is applied for the phase, it is also possible to design a similar system to the frequency hopping case, but this does not appear to be feasible. Unless the compression filter has excellent phase coherence, comparison of phase at the compressor output from pulse to pulse will be difficult. Fig.2b. shows some typical waveforms for the multiple chirp schemes illustrated in Fig.2a

Until now, we have proposed six kinds of spread spectrum chirp systems and studied the possibilities of practical implementation for our purpose in Task 2. If we set the design goal as a simple structured, low cost earth station, systems which need complex synchronization can be excluded from consideration. Therefore five of the systems with the exception of Multi-chirp system II-1 are considered non-starters. Once it can be proven that the 'Multi-chirp System' exhibits the proper performance, this system seems to be the most

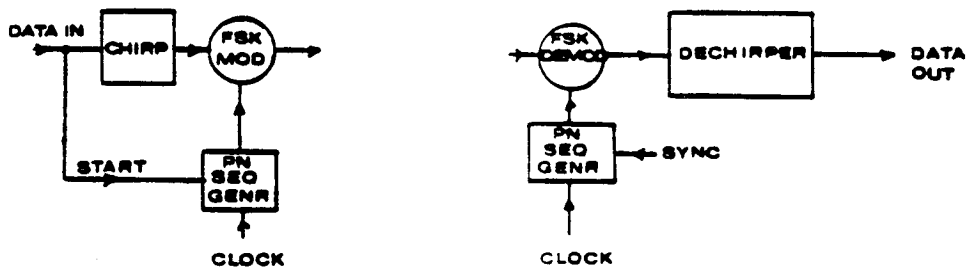
SPREAD SPECTUM CHIRP SYSTEM

class I: within chirp modulation

I-1. AM



I-2. FM



I-3. PM

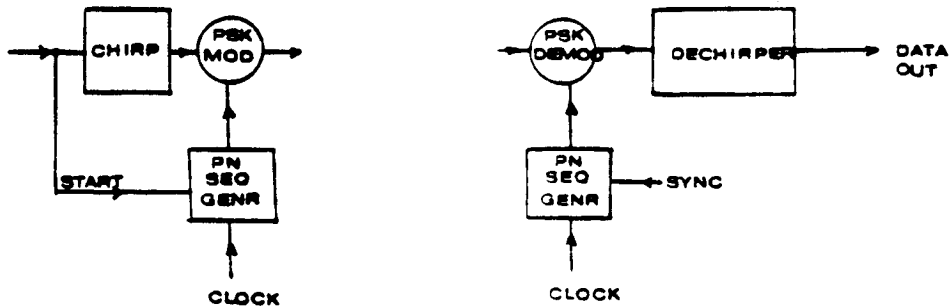
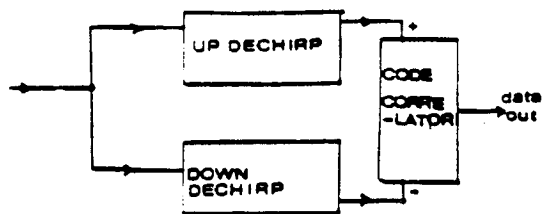
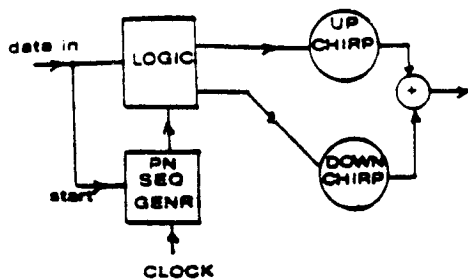


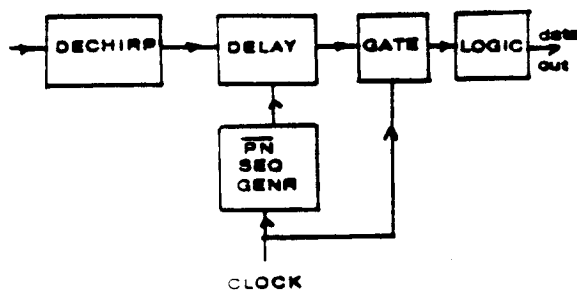
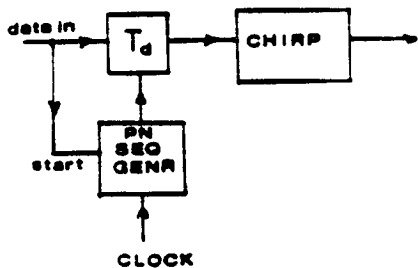
Figure 1. Within Chirp Modulations

Class II : multiple chirp modulation

II-1. Multi-chirp



II-2. Time delay



II-3. Frequency hop

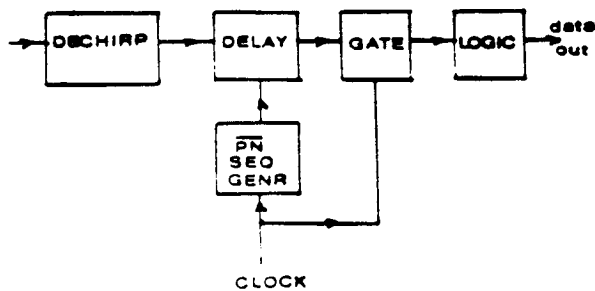
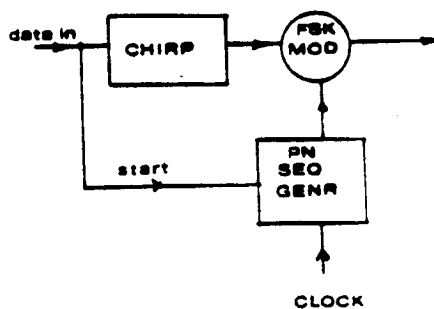


Figure 2a. Multiple Chirp Modulations

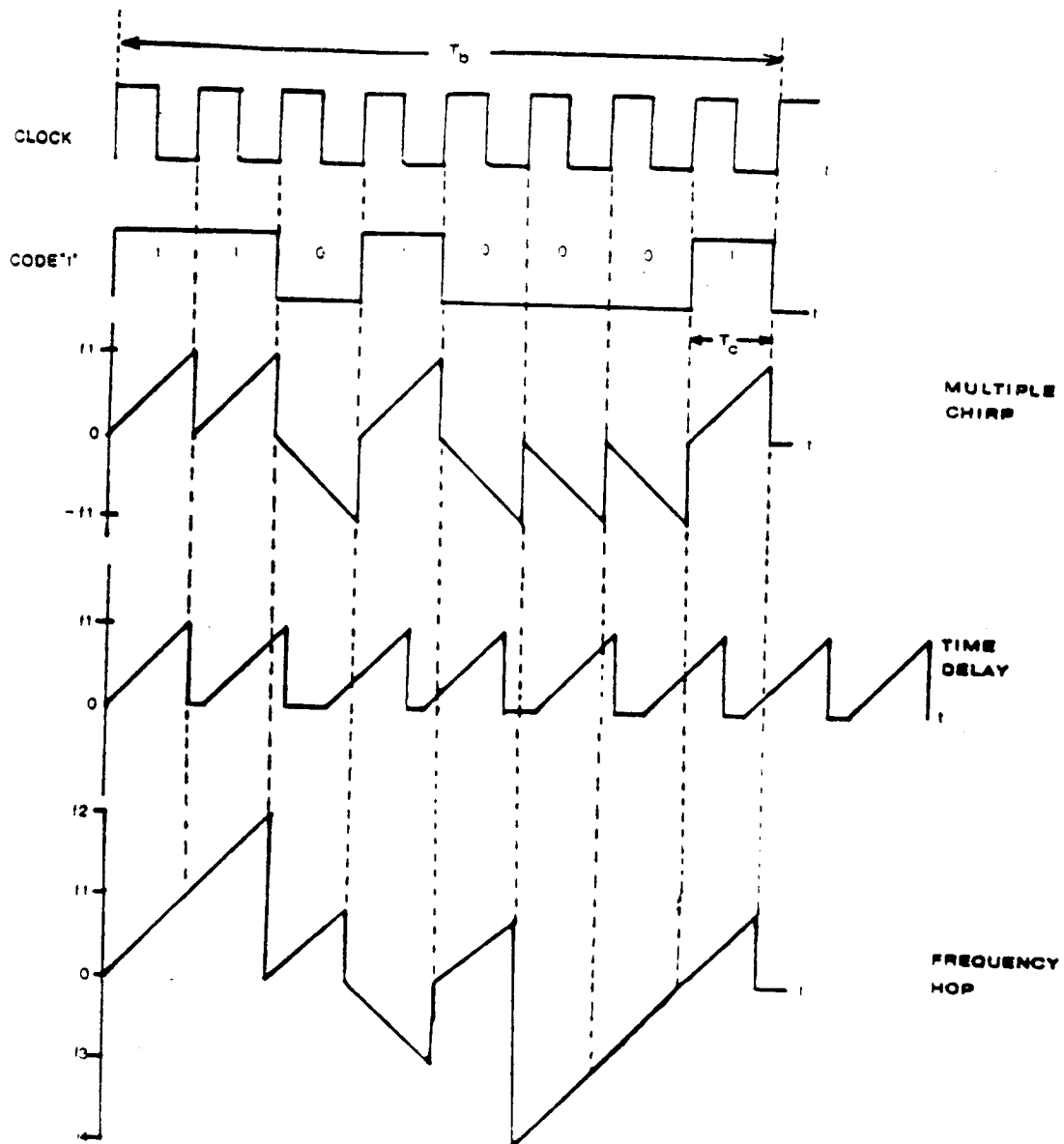


Figure 2b. Typical Waveforms of Multiple Chirp Modulations

feasible because it doesn't require additional synchronization in its receiver and it uses the proven binary chirp modulation scheme which was proposed by Winkler. [7]

This preferred system is depicted in Fig. 2a (II-1), with multiple chirps for signalling. The signal consists of a sequence of chirp pulses, typically using two slopes, one up and one down. The sequence is chosen for good cross-correlation and autocorrelation properties, so that other sequences entering the decoder produce minimal output. Because this system uses the typical binary chirp system configuration in its modem, the anticipated performance will be between that of BPSK and FSK, as was pointed out by Berni and Greg [9]. Strictly speaking, because no synchronization is required, this system is very similar to a non-coherent FSK system using codewords. However, whereas a FSK system would have a single frequency narrow band filter to detect a wanted tone, the chirp system uses a 'Dechirp' filter (a pulse compressor) to detect the presence of a wanted chirp.

Let's call this system a 'Coded Multiple Chirp Spread Spectrum System', because the transmission of a single data bit is achieved by sending a sequence of chirp pulses. The sequence could be made up of any combination of chirp slopes, but the use of a single slope with up and down chirps permits all receivers in a network to use the same pulse compression filter, with notable cost savings when many receivers are built. Detailed description of the system is left for the next section for convenience.

3. Coded Multiple Chirp Spread Spectrum System

3.1. Basic System Concept

The block diagram of the proposed system called 'Coded Multiple Chirp Spread Spectrum' is shown in Fig. 3a. In the transmitting section, the input binary data stream with a relatively slow data rate (compared with the chip rate of a PN code) is sorted into logical ones and zeros by the 1/0 selector at the data input, and encoded with a finite length PN code (16 or 32 chips) with given chip rate. After encoding, a sequence of up-chirps or down-chirps is generated by impulsing an up or down chirp generator (a SAW dispersive delay line (DDL)). These encoded data are summed, amplified and transmitted. Because each data bit is now represented by a sequence of chirp slopes, the bandwidth of the data has been spread. In this scheme, a single data bit duration is equal to the total number of chip durations of the PN code word. Typical waveforms and spectra for this system are shown in Fig. 3b. By using multiple chirps to constitute a code word, it is possible to use different slopes for each user. However the use of single slope with up and down chirp enables the selection of single dechirper filter (SAW DDL), and thus reduces the cost of device. If all the users in the network use the same sloped chirp, the multiple access can be accomplished by assigning different code words

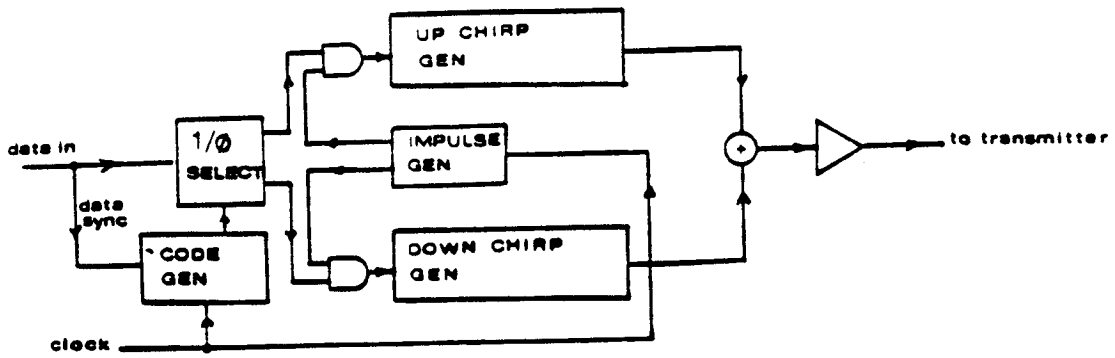
which promise good autocorrelation and cross-correlation, for example, Kasami or Gold codes with medium length. [17] [18]

We have modeled the receiving system in two steps: the Dechirper and the Digital Code Word Correlator. In the dechirper, the received multiple-chirp word entering the receiver passes through the RF and IF stages and is converted to polar binary data using a pair of dechirpers and a pair of threshold (Envelope) detectors. In the dechirping process, the wanted input signal corresponding to one chip duration is compressed with a predetermined compression gain and thus has enhanced amplitude. These compressed outputs from a pair of dechirpers, each assigned to detect a particular up- and down-chirp, are summed (in reality, one channel output is inverted then summed) to be processed by a sample and hold (S/H) circuit before code recognition by the digital code word correlator. Because only one of the two dechirpers produces a large output at the end of a given chip duration, even in an interfering situation, the summer gives a positive or negative polarized output to the sample and hold circuit. The sample and hold circuit acts as a threshold detector and passes stable binary data corresponding to the chip state (one or zero) to the word correlator.

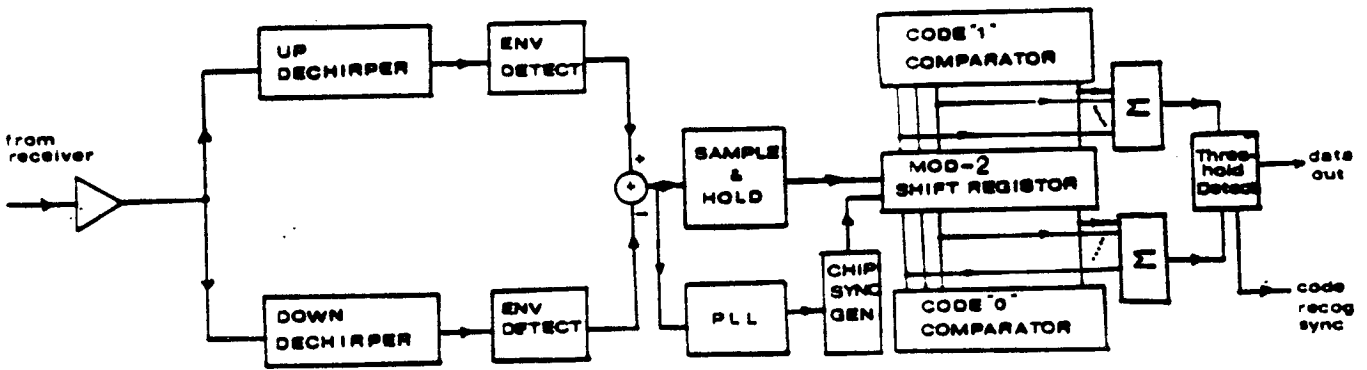
The sample-hold circuit output is in the form of polar binary pulses, each of one chip duration, corresponding exactly to the data driving the chirp generators in the transmitter. The chips have been recovered from the spread spectrum signal without any form of synchronization, and are always present whenever the receiver picks up a chirp signal with the correct slope.

The second step is a code word correlator followed by an analog threshold decision circuit, which determines whether a word is present in the correlator. The dechirper (or chirp compression filter) and detector behave like a non-coherent FSK system. The digital word correlator behaves like a unique word detector used in TDMA systems. Synchronization at the bit and word level are required for correct sampling and read-in of the binary word, as in any other binary data transmission system. The input binary data from the S/H output and the self-generated chip synchronization clock driven by a Phased Locked Loop (PLL) are simultaneously given to the digital word correlator. The digital word correlator consists of a

Coded Multiple Chirp.S.S System



< Modulator >



< Demodulator >

Figure 3a. Coded Multiple Chirp S.S. system (proposed)

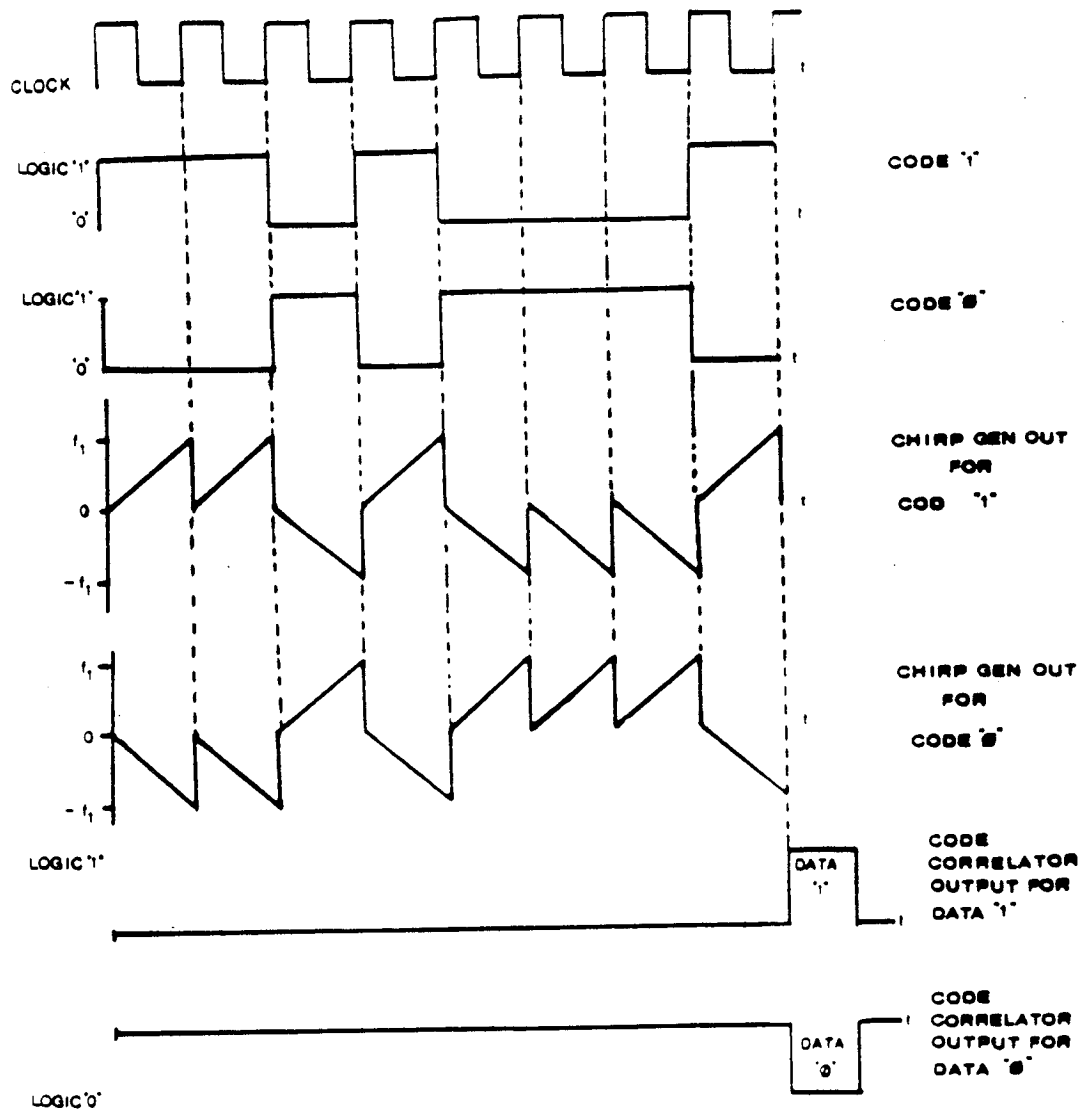


Figure 3b. Typical waveforms of Coded Multiple Chirp S.S. System

**ORIGINAL PAGE IS
OF POOR QUALITY**

pair of word comparators and Modulo-2 shift registers with the same length as the code word. After the n th (where n is the length of the shift register) shift, the register contents are compared, and the results are summed and detected by an analog threshold detector. If a code word is present in the shift register, the output will be $\pm n$. If the spread spectrum is operated with many simultaneous users in the channel, interference from other users will be the limiting factor in causing degradation of system performance expressed in bit errors in the detected data stream. If we use the same chirp slope for all users, the signals must be separated by the differences between their code words.

3.2. Performance Analysis

The performance analysis is organized as follows. Section one introduces the system parameters and waveform definitions for the proposed system. Section two briefly describes the correlation aspects of up and down chirps; in addition, the cross-correlation of desirable codes are studied. Gold or Kasami [17] [18] codes are strong candidates for the code in our system. Finally, as a general error criteria, chip error probability at the dechirper output is investigated. Then the probability of word (or code) error and corresponding word (code) miss probability is also described under the constraint of a finite length of code.

3.2.1. System Parameters and Waveform Definitions.

The following are the system parameters necessary to define general expressions for the waveform of a Coded Multiple Chirp S S. Signal.

- R_b : input (binary) data bit rate
- T_b : input (binary) data duration ($= 1/R_b$)
- R_c : Chirp rate of the word (or code sequence)

T_c ;	Chip duration
μ ;	Chirp slope (or dispersive slope)
G_p ;	Processing gain (or pulse compression ratio)
$d(t)$;	input data signal (binary NRZ)
$G(t)$;	word (or code) sequence with period $N = 2^n - 1$ (n : shift register length)
$R_{aa}(k)$;	autocorrelation of sequence $a(k)$
$R_{ab}(k)$;	Crosscorrelation of sequence $a(k)$ and $b(k)$
$R_{f_a f_b}(t)$;	Crosscorrelation of two time function $f_a(t)$ and $f_b(t)$
$R_{S_a S_b}(t)$;	Crosscorrelation of code symbol S_a and S_b (up and down chirp)
P ;	Transmitted power of signal
Δf ;	Chirp frequency sweep range

Then the general expression of the wave form for a single chirp duration is given by

$$S_c(t) = \sqrt{2P} d(t)G(t) \cos(\omega_c t + \frac{1}{2}\mu t^2 + \theta_0)$$

where ω_c : carrier radian frequency

θ_0 : Initial phase in radians

3.2.2. Crosscorrelation of Up Chirp and Down Chirp

Because the proposed system uses the chirp technique along with a code sequence to spread the spectrum, it is necessary to find the correlation between up and down chirps at first, even though the relationship between a series of chirps coded by finite length sequences is needed finally. The autocorrelation and the typical spectrum of chirp are well defined in the relevant papers by Cook [19] or by Klauder et al. [1]. So it is not described here.

Assuming only one chirp slope (but negative for down-chirp, if positive slope is assigned to up-chirp) is used, the up-chirp signal is given by

$$U(t) = \begin{cases} e^{j(\omega_c t + \frac{1}{2}\mu t^2)} & -\frac{T}{2} \leq t \leq \frac{T}{2} \\ 0 & \text{elsewhere} \end{cases}$$

and the down-chirp signal is given by

$$D(t) = \begin{cases} e^{j(\omega_c t + \frac{1}{2}\mu t^2)} & -\frac{T}{2} \leq t \leq \frac{T}{2} \\ 0 & |t| > \frac{T}{2} \end{cases}$$

The cross-correlation $C(\tau)$ between $U(t)$ and $D(t)$ is defined as [20]

$$C(\tau) \triangleq \langle U(t)D(t - \tau) \rangle$$

for $t > 0$, and under the assumption the $U(t)$ and $D(t)$ are periodic over T , the cross-correlation $C(\tau)$ is given by

$$C(\tau) = \frac{1}{T} \int_{-T/2+\tau}^{T/2} e^{j(\omega_c t + \frac{1}{2}\mu t^2)} e^{-j(\omega_c(t-\tau) + \frac{1}{2}\mu(t-\tau)^2)} dt$$

$$= \frac{1}{T} e^{j(\omega_c \tau + \frac{1}{2}\mu \tau^2)} \int_{-T/2+\tau}^{T/2} e^{j(\mu t^2 - \mu \tau t)} dt$$

$$= \frac{1}{T} e^{j(\omega_c \tau + \frac{1}{4}\mu \tau^2)} \int_{-T/2+\tau}^{T/2} e^{j(\sqrt{\mu t} - \frac{\sqrt{\mu}}{2}\tau)^2} dt$$

$$\text{(By setting } \sqrt{\mu t} - \frac{1}{2}\sqrt{\mu}\tau = \sqrt{\frac{\pi}{2}}x \text{)}$$

$$= \sqrt{\frac{\pi}{2\mu T^2}} e^{j(\omega_c \tau + \frac{1}{4}\mu \tau^2)} \int_{-x_1}^{x_2} e^{-\frac{\pi}{2}x^2} dx$$

$$\text{where } x_1 = \sqrt{\Delta FT} \left[1 + \frac{\tau}{T} \right]$$

$$x_2 = \sqrt{\Delta FT} \left[1 - \frac{\tau}{T} \right]$$

then

$$C(\tau) = \frac{1}{\sqrt{4\Delta FT}} e^{j(\omega_c \tau + \frac{1}{4}\mu \tau^2)} \{C(X_2) + C(X_1)\} + j\{S(X_2) + S(X_1)\}$$

and

$$|C(\tau)| = \frac{1}{\sqrt{4\Delta FT}} \{ [C(X_2) + C(X_1)]^2 + [S(X_2) + S(X_1)]^2 \}^{\frac{1}{2}}$$

where $C(X)$ and $S(X)$ are Fresnel cosine and sine integrals respectively. It is also possible to find identical expression to $C(\tau)$ as above for the $t < 0$ case.

For large values of ΔFT , $C(X)$ and $S(X)$ are approximately 0.5. Then

$$|C(\tau)| = \frac{1}{\sqrt{2\Delta FT}} \quad -T \leq \tau \leq T$$

therefore, the cross-correlation approaches 0 for large processing gain (or compression gain) G_p . This also implies that the quasi-orthogonality of up and down chirp signals during one chip duration approaches orthogonality if the processing gain G_p is sufficiently large. Under this condition, the performance of a chirp system is almost identical to the noncoherent orthogonal binary FSK system. [2] Fig. 4 shows an example of autocorrelation and cross-correlation of a chirp signal.

3.2.3. Cross-Correlation Between Code (Word) Sequence

For effective Spread Spectrum Multiple Access (SSMA), the following methods can be considered for the proposed chirp system:

- Using N different codes for N users as in CDMA.
- Using multiple chirp slopes with frequency dispersion variation or time dispersion variation.
- A mixture of multiple slope and multi-code.

Because the single slope chirp is regarded as the only economical way for simple and practical implementation, the most desirable method of achieving multiple access is by varying the code sequences of the network users. Under this condition, the selection of the codes plays an important role in deciding the performance of the system. The Gold Code [17] or Kasami Code [18] are strong candidates for our purposes, in that they show low cross-correlation between any pair of codes. Besides, both of them meet the general requirement of the code sequence that interference due to a different code be far less than the code's autocorrelation, and any two codes having the same period must satisfy a lower bound in cross-correlation [21]. For a detailed description of these codes, see D. Sarwate and B. Pursley. [22]

For an asynchronous system using code sequences for multiple access, such as the proposed coded multiple chirp spread spectrum system, the cross-correlation of sequences is a key parameter. The aperiodic cross-correlation function of two sequences X and Y is generally given by [22]

$$C_{X,Y}(\ell) = \begin{cases} \sum_{j=0}^{N-1-\ell} X_j Y_{j+\ell} & 0 \leq \ell \leq N-1 \\ \sum_{j=0}^{N-1-\ell} X_{j-\ell} Y_j & 1-N \leq \ell \leq 0 \\ 0 & |\ell| \geq N \end{cases}$$

where

X, Y; Code sequence having same period N
N; Code length $N = 2^n - 1$

n; Shift register length
 ℓ ; Relative time delay between sequences X and Y

and the lower bound of the aperiodic cross-correlation function is

$$|C_{X,Y}(\ell)| \leq [C_X(0)C_Y(0)]^{1/2}$$

Also, the peak aperiodic cross-correlation magnitude for two sequences is

$$C_C = \max\{|C_{X,Y}(\ell)|; 0 \leq \ell \leq N - 1, X \neq Y\}$$

whereas the aperiodic autocorrelation magnitude is written as

$$C_a = \max\{|C_X(\ell)|; 0 \leq \ell \leq N - 1\}$$

From the result [23], if there are K users in a multiple access system, with K unique sequences with the same period $N = 2^n - 1$. (the Gold or Kasami Codes have period $N = 2^n - 1$), the following condition must be satisfied to ensure the effective multiple access.

$$\frac{(2N - 1)}{N} \left(\frac{C_C^2}{N}\right) + \frac{2(N - 1)}{N(K - 1)} \left(\frac{C_a^2}{N}\right) \geq 1$$

3.2.4. Chip Error Probability (Dechirper BER)

The performance of the proposed coded multiple chirp S.S. system can be expressed in terms of two probability measures. chip error probability for the dechirper and word (code) miss probability for the digital code correlator. False alarms, in which a data bit is produced in the absence of a received codeword also contribute to errors in system performance. In this section, the probability of error of the chips in the dechirper will be found and discussed.

For the derivation of probability of chip error, the following justifications are necessary.

1. The performance of binary chirp signaling is identical to that of orthogonal non-coherent binary FSK because the cross-correlation of up and down chirps is negligible, assuming large compression gain G_c .
2. If the justification above is reasonable, multiple chirps, which are derived from a series of up and down chirps, give a code sequence which can be viewed as a binary FSK signal waveform.
3. By assuming the noise is AWGN and that interference from other chirp signals behaves as a Gaussian Random Variable, the generally accepted analysis of non-coherent binary FSK can be used to find the probability of chip error in the proposed chirp system. [2], [24], [25]

Under the assumption that the above three justifications are admissible, the system performance, as measured by probability of chip error rate, (denoted by P_e , or Bit error Rate (BER)) can be found by either of the following two methods.

- (1) Method 1; Direct use of the P_e of non-coherent binary FSK
- (2) Method 2; Derivation of the expression for the P_e in binary non-coherent FSK in the presence of interfering signals

Method 1 gives a simple expression for P_e , even though it is valid only when the compression gain is sufficiently large. Method 2 gives a more accurate expression without any restrictions. Here, in this report, only the results are written for convenience. For more detailed procedures, see Couch [26] for method 1 and Appendix A of Ramanan [2] for method 2.

By method 1, the P_e of the dechirper is given by [26]

$$P_e = \frac{1}{2} e^{-\rho}$$

where

$$\rho = E_b/2N_o$$

E_b : average energy per bit
 N_o : two sided noise power spectral density

By method 2, P_e is given by [2]

$$P_e = Q[\sqrt{\rho(1 - \sqrt{1 - \alpha^2})} + \sqrt{\rho(1 + \sqrt{1 - \alpha^2})}] - \frac{1}{2} e^{-\rho} I_0(\rho\alpha)$$

3. Coded Multiple Chirp Spread Spectrum System

where $Q(X, Y)$; standard Q function

$$\rho = E_p/2N_0$$

$$\alpha = 1/G_p$$

$I_0(X)$; modified Bessel function of 1st kind.

G_p ; processing gain

Note that the P_e of the dechirper derived in both methods above assumes that the signal power as well as the noise power is the same for each case of up chirp and down chirp. In addition, noise is assumed to be AWGN and interference used in method 2 is assumed to be a Gaussian Random Variable.

Fig.5a shows the P_e of the dechirper when it is calculated by method 1 assuming AWGN in the channel, and that the dechirper is identical to a non-coherent binary FSK system. Fig.5b [2] shows a comparison of the calculated P_e curves by method 1 and method 2 for several compression ratios. From Fig. 5b, it can be seen that for large Time-Bandwidth products, hence for large compression ratios, non-coherent FSK (orthogonal) and chirp signals (quasi-orthogonal) have nearly identical performance.

ORIGINAL PAGE IS
OF POOR QUALITY

PROB. OF BIT ERROR (for chip)

$$P_b = \frac{1}{2} e^{-x}$$

where $x = \frac{1}{2} \frac{E_b}{N_0}$

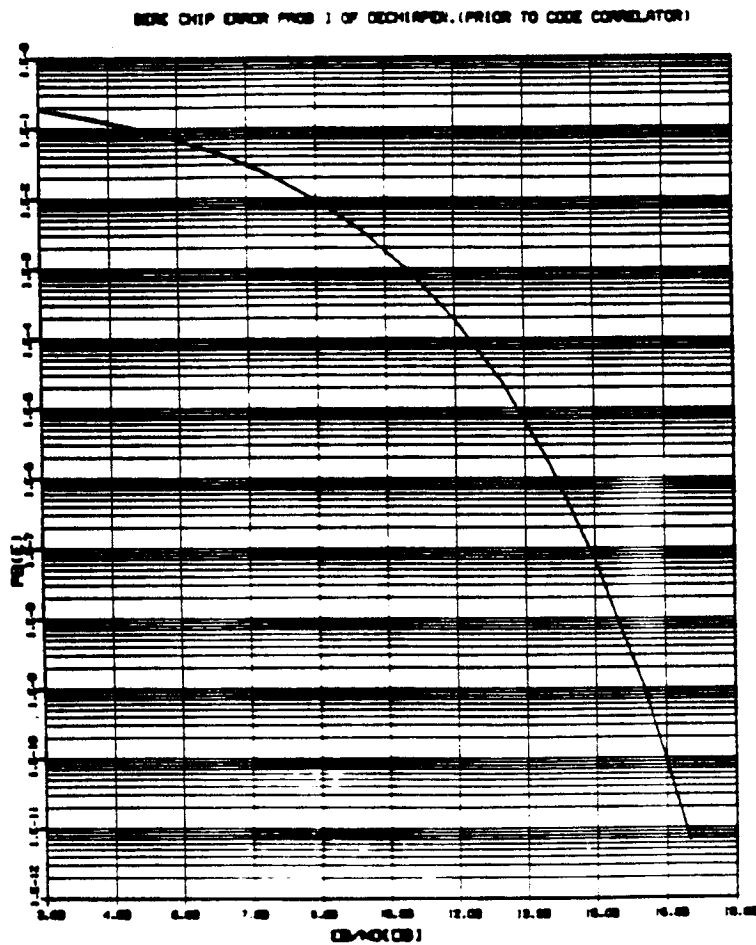


Figure 5a. BER [Chip Error Prob.] of Dechirper. [Prior to Code Correlator]

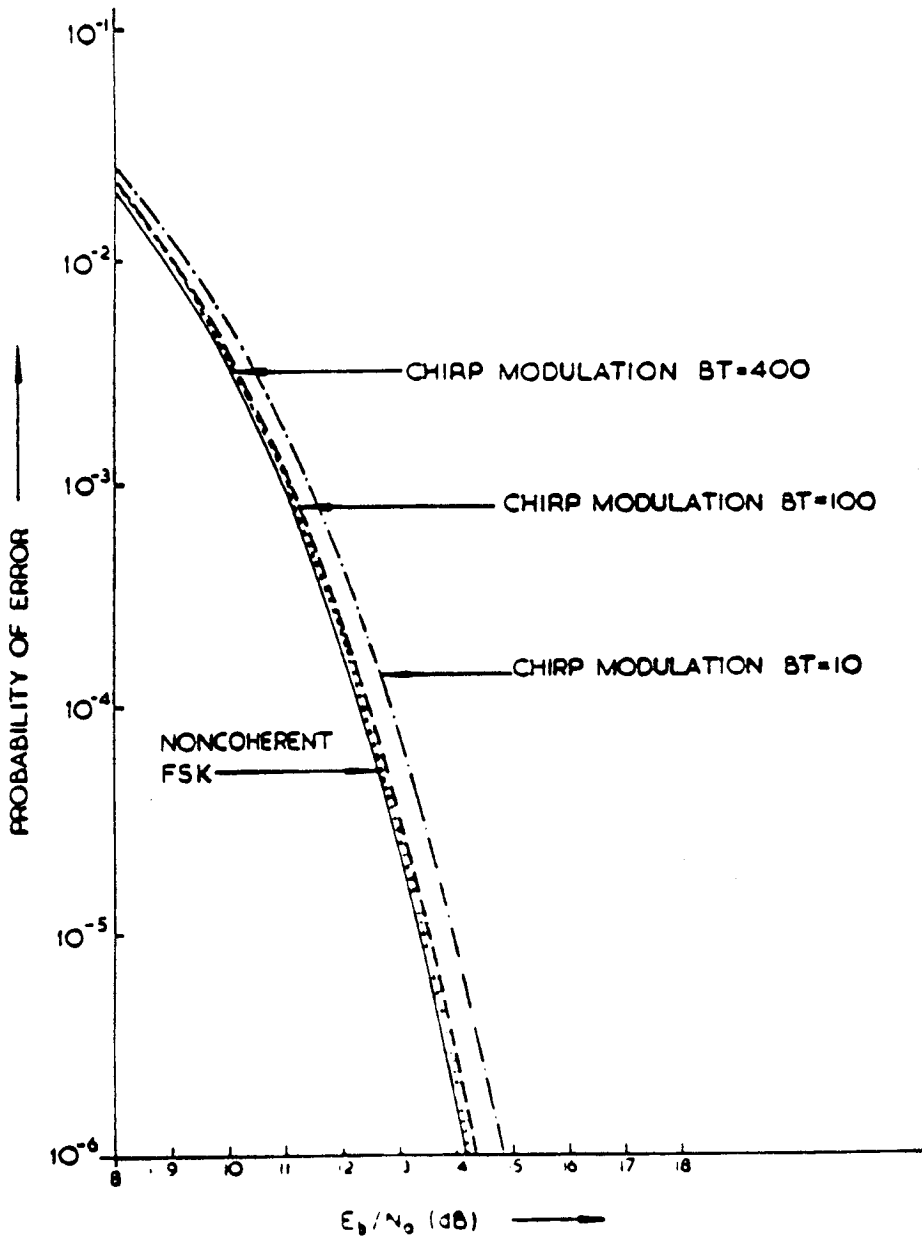


Figure 5b. Probability of error versus E_b/N_0 for noncoherent FSK and chirp signals of different time-bandwidth products.

3.2.5. Performance of Digital Code Correlator

A digital code correlator is used to determine whether the received code (word) sequence is matched with the unique word stored in the comparator. Because the proposed digital code correlator uses the same idea as a unique word (UW) detector used in TDMA systems [27], the performance of our correlator can be directly formulated from that of a UW detector (correlator) used in the INTELSAT system [28]. Because two identical code correlators are used to detect a binary '0' and binary '1', the probability of a word (code) error for an individual code (word) correlator is found initially, and then the joint probability of error can be determined.

Let's find the probability of word error P_e for a single code correlator by the result of Feher [29]. The probability that an N bit (chip) word is received correctly is given by [29]

$$P = \sum_{l=0}^E \binom{N}{l} p^l (1-p)^{N-l}$$

where N is the word length, E is the number of errors to reach the code correlator threshold, ' p ' is the bit (chip) error probability which was previously defined as the P_e of dechirper in section 3.2.4. In addition ' l ' is the number of possible error bits received from the dechirper, under the constraint that $l < E$

Because the probability of correct word detection is given by P , the probability of word miss Q , for a given threshold E is given by

$$Q = 1 - P = \sum_{l=E+1}^N \binom{N}{l} p^l (1-p)^{N-l}$$

The above probability of word miss Q is a function of code length N and dechirper bit (chip) error rate, so there can be plenty of cases to calculate. In Fig. 8, the probability of word miss Q as a function of dechirper BER p is illustrated for $N = 16, 32, 64,$ and 128 , with $E =$

ORIGINAL PAGE IS
OF POOR QUALITY

0, 1, 2, and 3. It is seen that code miss rates can be made quite low, even for fairly high bit-error rates of the dechirper, especially for large value of N [29]. However medium length codes like N = 16 or 32 are recommended because of shift register size restriction.

Another measure of system performance is word false alarm rate F. A word false alarm occurs when bit patterns due to random noise are allowed to enter the code correlator. There exists a small but finite probability that random patterns will accidentally correspond to the unique code and cause the erroneous production of a correlation detection. The probability of a false alarm F is given by the probability of accidental occurrence of the unique code in the wrong location within the number of errors E established by the unique code threshold and expressed by [27]

$$F = 2^{-N} \sum_{l=0}^E \binom{N}{l}$$

Fig. 7 illustrates the dependence of F on code length and bit (chip) error probability of the dechirper. In this figure, unique code false alarm probability, F, and unique code miss probability, Q, are drawn as a function of selected bit (chip) error rate and code matching ratio M/N, where M is the number of bits in the received sequence of a code that must match the unique code stored in the correlator [27]. (M is the threshold of the word presence detector which follows the correlator and is triggered by the correlation between an incoming bit pattern and the stored code sequence)

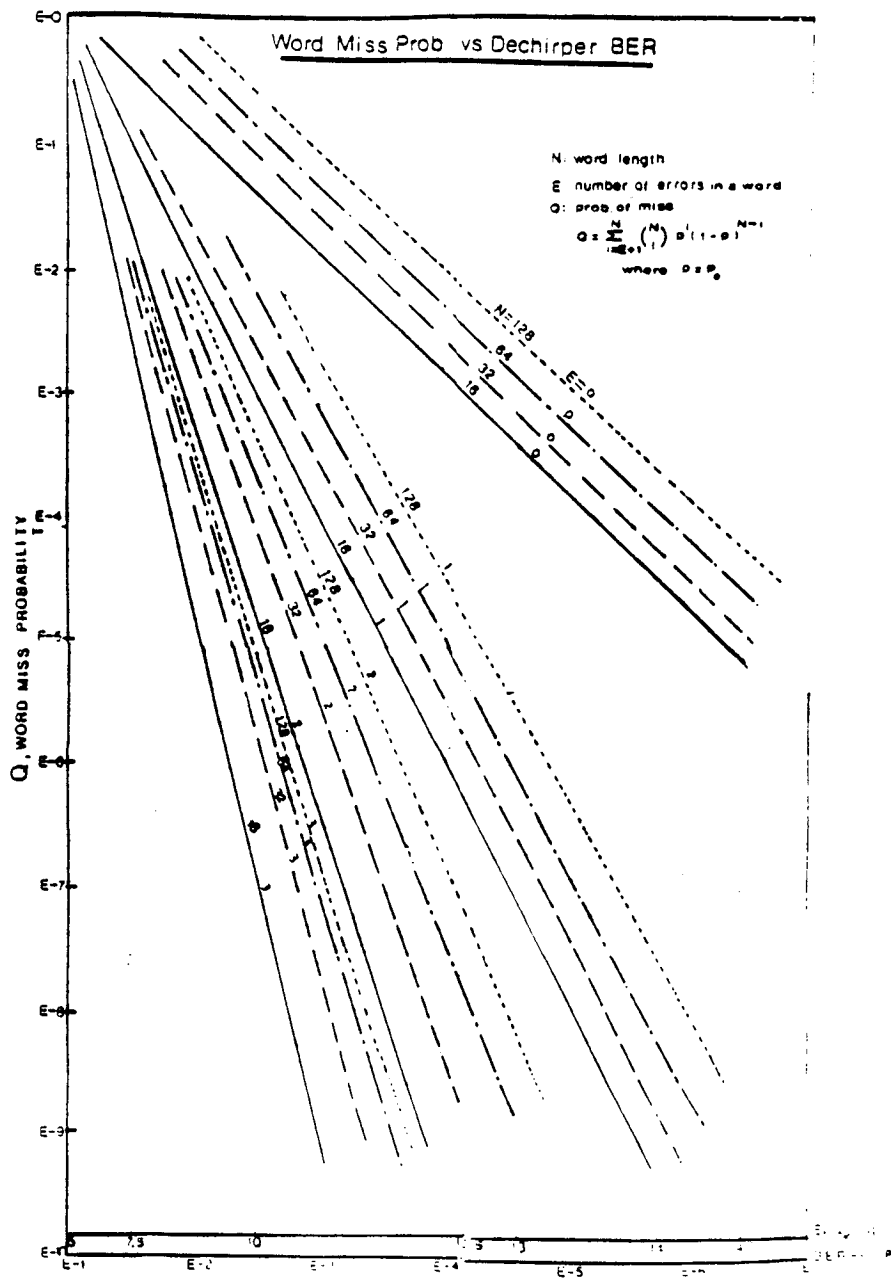


Figure 6. Word Miss Probability vs Dechirper BER.

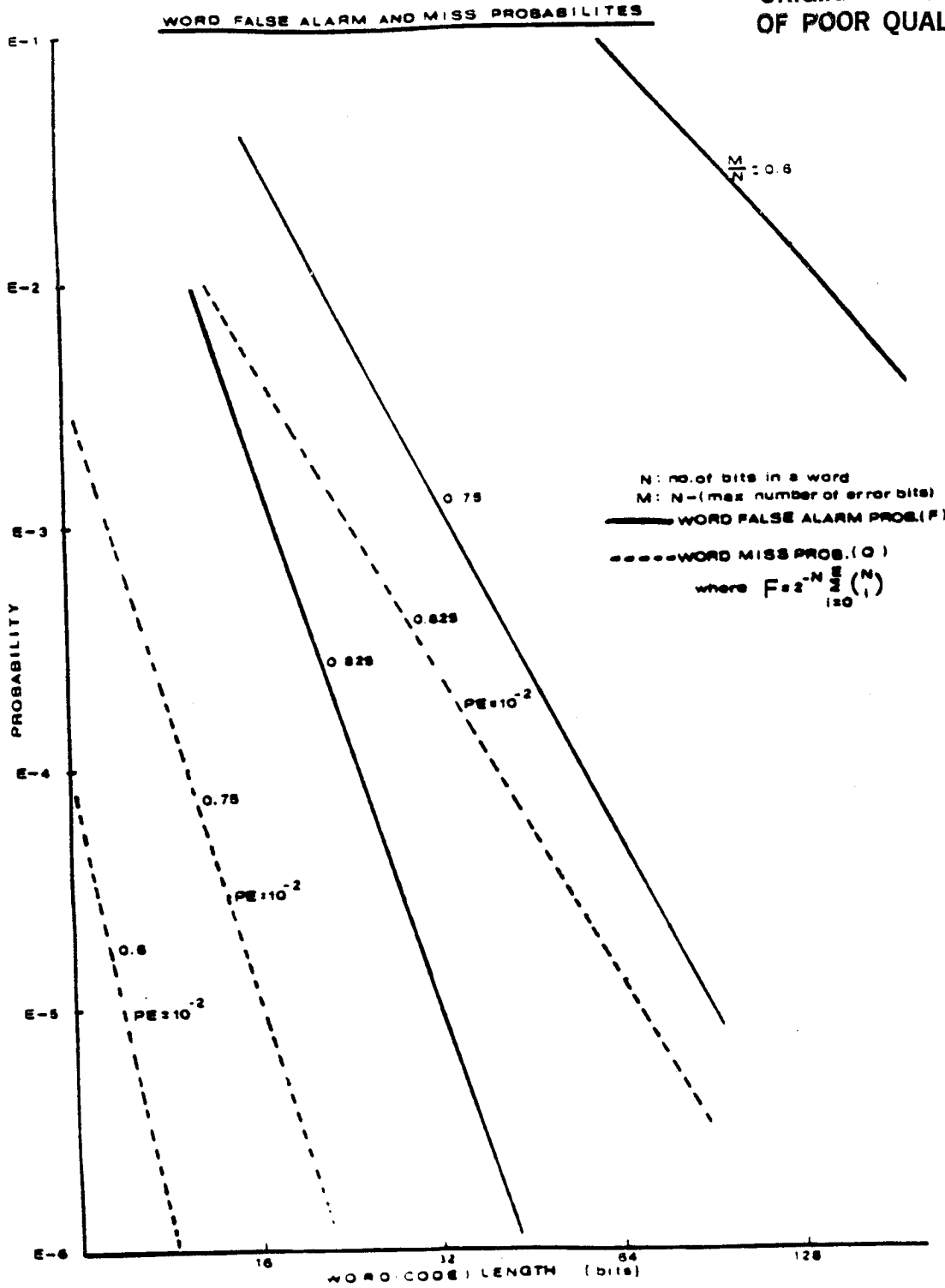


Figure 7. Word False Alarm Probability vs Miss Probability

3.2.6. Chirp Spread Spectrum Multiple Access

As was briefly mentioned earlier in section 3.2.3, the method of varying the chirp slope either by time dispersion or by frequency dispersion, or using a unique pseudo-random code can be employed for multiple access with chirp spread spectrum. In addition, hybrid versions of those methods can be considered. In other spread spectrum methods like Direct Sequence (DS) and Frequency Hopping (FH), the number of users who can access the transponder simultaneously is limited by the cross-correlation achievable between the codes used. If the method of slope variation is used, the major decision factor for the number of simultaneous users (n) will be the cross-correlations of different sloped chirp waveforms.

The signal selection to keep low cross-correlation between the multiple simultaneously chirps must involve taking signals with differing time-bandwidth products, because the actual difference between the products determines the degree of orthogonality. Overall system performance depends on the influence of all the interfering signals on any one channel. From this point of view, the number of simultaneous users is dictated by the following three factors, regardless of slope varying method:

1. The time-bandwidth product of individual signals
2. The minimum difference in the time-bandwidth products used
3. The summation of $n-1$ distorted outputs has to be below a certain desired level for any given user for satisfactory operation.

The analysis of cross-correlation [2] between a desired chirp slope and an unwanted slope confirms the dependence of cross-correlation on the above mentioned time bandwidth product. Therefore, proper adjustments between slopes may allow multiple access to a certain degree. However, this scheme using differently sloped chirps is not considered a good choice

for practical applications, because varying time-bandwidth products result in a different data rate for multiple users if the time dispersion is varied, and different bandwidth utilization in the limited transponder bandwidth. In addition, different SAW devices are needed for all the multiple users. From this point of view, spread spectrum multiple access using chirp with varying chirp slopes seems to be a bad choice. This conclusion is in agreement with reference [2], where it was shown that only 5 users could share a typical transponder using multiple slope chirp.

If we use the method of assigning unique codes for multiple users, while keeping the same chirp slope for all users, multiple access is possible. The performance of this scheme is no different from other conventional spread spectrum techniques, and the merit of a relatively simple implementation in the chirp system will be retained. The alternative choice of combining slope variation and a unique code also seems undesirable because the system gets complicated. In conclusion, spread spectrum multiple access using many slopes in a chirp system is not considered desirable, even though it is possible, compared with other spread spectrum techniques. In this situation, spread spectrum overlay on an existing service seems to be the proper alternative to keep the inherent advantages of chirp.

ORIGINAL PAGE IS
OF POOR QUALITY

4. Overlay Service --An Overview

Spread spectrum overlay is a kind of practical implementation of "frequency reuse" by adding a comparatively low data rate signal to an existing high traffic channel. This service can increase the capacity of an existing satellite transponder, hence can provide additional service and function to existing users in the satellite network. Because the primary concern is the effective reuse of the existing system without causing any harmful interference to the users already occupying the transponder, minimizing the possible occurrence of mutual interference between the existing signal and the overlay signal is the key factor in this service.

The performance degradation of existing signals caused by overlay can be kept to a minimum by reducing the transmitted power of the overlay signal. The data rate of overlay signals then must also be reduced to maintain the desired bit energy to noise density ratio. In this situation it is obvious that the overlay signal experiences relatively high level interference from the existing signal, and spread spectrum techniques are a proper choice to reject this interference, thereby achieving effective frequency reuse or overlay.

In the study of this task, spread spectrum overlay, the existing signal being sent through the transponder is confined to analog FM-TV. Other possible choices such as FDM telephone and data signal were not studied. FM-TV is probably the most susceptible signal for interference from a chirp

overlay, because both signals are frequency modulated, so the FM-TV demodulator is capable of demodulating the chirp signal directly.

This report is organized as follows. Chapter 5 introduces the fundamental analysis of interference between analog FM-TV signals and chirp signals by modeling the FM-TV signal in various forms. Chapter 6 describes the procedures of modeling the FM-TV signal in practical form by using multi-level step functions, or random multi-level step functions. In these procedures, some results of computer simulations are illustrated and analyzed both in the time and frequency domains. Then, based on our interference analysis between television and chirp s.s. signals, a satellite link analysis for C band is performed to find the proper C/I ratio in a practical situation. A comparative study of C/I ratio and optimum overlay position within the analog FM-TV bandwidth, and a performance analysis of an analog FM-TV system with chirp overlay concludes this report.

5. Interference Analysis I (General Approach)

For effective overlay service between existing analog FM television and spread spectrum chirp systems, mutual interference between the two signals must be studied. It is first necessary to define the type of signals used and the receivers for these two systems. What is needed is a good description, in the frequency domain, of a FM-TV signal. Unfortunately, there exists no finite description or definition of this form that we could find in the literature. Therefore, modeling the TV signal appears to be a major difficulty in our study.

In this chapter, the demodulation process in analog FM television (TV) and the proposed spread spectrum chirp system are briefly reviewed as a preliminary stage. Then, for a defined chirp signal and frequency discriminator in the TV receiver, various case studies of interference into the analog FM-TV channel were conducted using an analytical approach. As another phase of the interference study, the interference caused by FM-TV signals into the chirp channel was also investigated. In this analysis, because we had no definition of the FM-TV signal and its corresponding spectra, computer simulations as well as analytic expressions were used to support the analysis.

5.1. Analog FM-TV demodulation

The process of FM-TV demodulation recovers the baseband signal as a TV video signal. A frequency discriminator or PLL demodulator, which follows the receiver IF stage, is used for this purpose. Only the frequency discriminator is considered for our purpose. The received FM-TV signal is converted into baseband form after RF amplification and IF amplification. The FM discriminator is usually followed by a deemphasis filter and a video amplifier. In the situation when there is interference added to the FM-TV signal, an error voltage will appear at the discriminator output according to the intensity and phase relation of the interference signal to the FM-TV signal. This phenomena will be explicitly dealt with in the next section.

While interference to the FM-TV signal reception can be analyzed through the FM-discriminator output, the other aspect of interference in an overlay service is analog FM-TV interference into the chirp signal channel of the proposed coded multiple chirp spread spectrum system. Because the interference power from the FM-TV signal is generally at a much higher level than the received chirp system, the performance of the chirp compression filter and the receiver IF filter preceding the dechirper input play an important role in this interference analysis. Obviously, the output of the dechirper filter (compressor) must spread the input interference signal into a wider duration of time for effective detection of the compressed chirp pulse.

5.2. Chirp interference to analog FM-TV signals

In section 5.1, the principle of the demodulation process of an analog FM-TV signal was briefly reviewed. Because the FM-discriminator output is expressed as a voltage, the response of the discriminator of an FM-TV receiver for various inputs must be studied before practical modeling of

analog FM-TV signal can begin. In this preliminary analysis, we found a generalized formula for FM-discriminator output with a general message signal which frequency modulates the carrier. This formula can be applied to any kind of message information, video or audio, that is used in an FM system. Fig. 8 and Fig. 9 illustrate examples of the time waveform of FM-discriminator output error voltage for an unmodulated TV carrier and a modulated carrier with chirp interference, under various input signal to interference ratios.

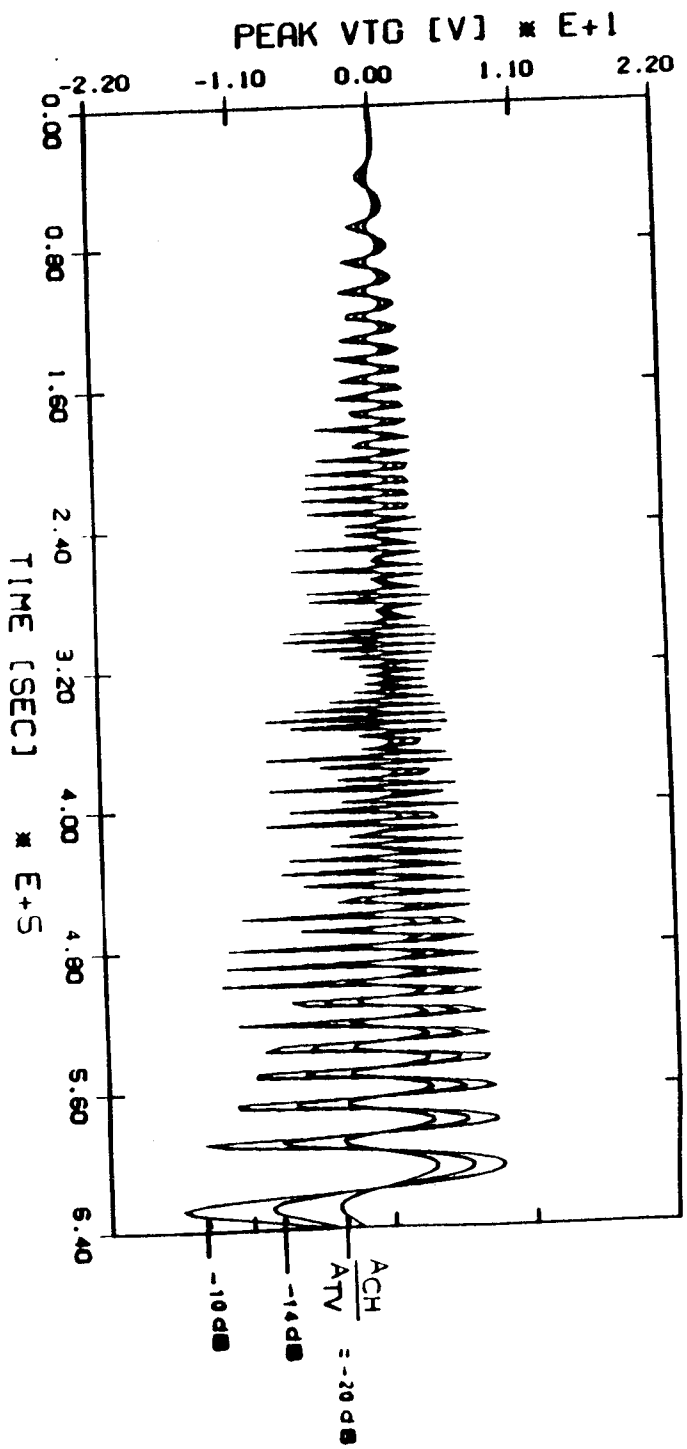


Figure 8. Time waveform of FM-discriminator output error voltage for unmodulated FM-TV carrier plus chirp interference

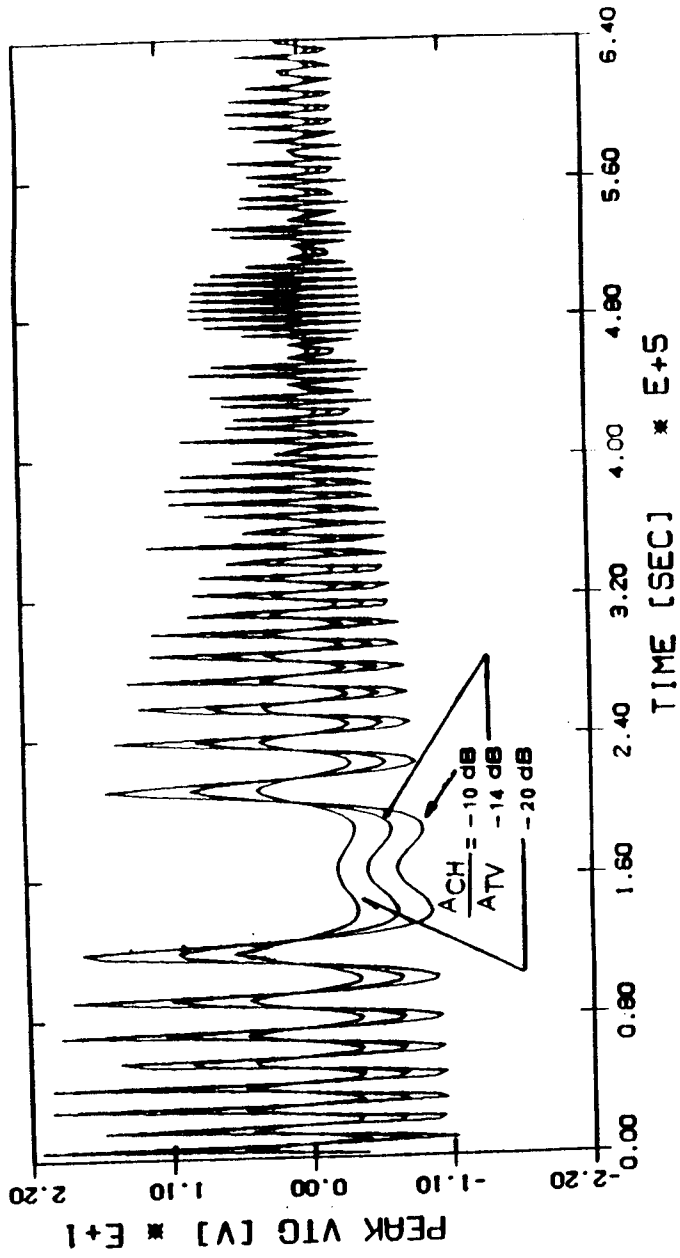


Figure 9. Time waveform of FM-discriminator output error voltage for FM-TV carrier($m(t) = 0.5V \text{ dc}$) plus chirp interference

<1> General Expression of FM-discriminator Output Under Interference.

To see the effect of interference to the FM signal, we need to find general expressions for error phase, instantaneous frequency deviation and corresponding error voltage at the FM-discriminator output caused by the interference.

If the desired FM signal is expressed as:

$$w(t) = A \cos[\omega_1 t + \phi(t)] \quad (1)$$

where A : FM carrier amplitude
 ω_1 : FM carrier radian frequency
 $\phi(t)$: FM carrier phase

and interference is expressed as

$$i(t) = R \cos[\omega_2 t + \psi(t) + \hat{\mu}] \quad (2)$$

where R : interference carrier amplitude
 ω_2 : interference carrier radian frequency
 $\psi(t)$: interference carrier phase
 $\hat{\mu}$: initial phase

then, the input signal to the FM-discriminator is the sum of the above two signals, written as

$$\begin{aligned} s(t) &= w(t) + i(t) \\ &= A(t) \cos[\omega_1 t + \Phi(t) + \beta(t)] \end{aligned} \quad (3)$$

where $A^2(t) = (A + R \cos[\Phi(t)])^2 + (R \sin[\Phi(t)])^2$

$$\Phi(t) = \omega_d t + \psi(t) - \varphi(t) + \hat{\mu}$$

$\omega_d = \omega_2 - \omega_1$; carrier frequency difference

$\beta(t)$: error phase

In detail, the Error phase caused by interference will be

$$\beta(t) = \tan^{-1} \left[\frac{R \sin[\omega_d t + \psi(t) - \varphi(t) + \hat{\mu}]}{A + R \cos[\omega_d t + \psi(t) - \varphi(t) + \hat{\mu}]} \right] \quad (4)$$

and the corresponding instantaneous frequency deviation is

$$\Delta f = \frac{d}{dt} \beta(t) = \left(\frac{R}{A} \right) \frac{\Phi'(t) \left[\frac{R}{A} + \cos \Phi(t) \right]}{\left[1 + \left(\frac{R}{A} \right)^2 + 2 \left(\frac{R}{A} \right) \cos \Phi(t) \right]} \quad (5)$$

therefore, the error output voltage for the FM-discriminator with slope k_D is

$$S_o(t) = \frac{1}{2\pi} k_D \left(\frac{R}{A} \right) \frac{\Phi'(t) \left[\frac{R}{A} + \cos \Phi(t) \right]}{\left[1 + \left(\frac{R}{A} \right)^2 + 2 \left(\frac{R}{A} \right) \cos \Phi(t) \right]} \quad (6)$$

<2> Complete formula of FM-discriminator Error Output

Based on the general expression in Eq. (6) above, the general case FM-discriminator output error voltage for any FM-TV carrier and energy dispersal signal and linear chirp interference can be written as:

$S_O(t) =$

$$\frac{1}{2\pi} K_D \left(\frac{A_{CH}}{A_{TV}} \right) \frac{[\omega_d + \mu t - 2\pi f_d m(t) + d'_2(t) - d'_1(t)] \left[\frac{A_{CH}}{A_{TV}} + \cos\left(\frac{1}{2}\mu t^2 + d_2(t) - 2\pi f_d \int^t m(\alpha) d\alpha - d_1(t) + \omega_d t - \hat{\mu}\right) \right]}{\left[1 + \left(\frac{A_{CH}}{A_{TV}}\right)^2 + 2\left(\frac{A_{CH}}{A_{TV}}\right) \cos\left(\frac{1}{2}\mu t^2 + d_2(t) - 2\pi f_d \int^t m(\alpha) d\alpha - d_1(t) + \omega_d t + \hat{\mu}\right) \right]}$$

where

A_{TV} ; TV-carrier amplitude (cf. $W(t) = A_{TV} \cos[\omega_1 t + \phi(t)]$)

A_{CH} ; chirp interference amplitude (cf. $i(t) = A_{CH} \cos[\omega_2 t + \frac{1}{2}\mu t^2]$)

ω_1 ; TV carrier radian frequency

ω_2 ; chirp carrier radian frequency

$\omega_d = \omega_2 - \omega_1$; carrier frequency difference (radian)

K_D ; FM-discriminator slope [Volt/Hz]

μ ; chirp slope [Hz/sec]

f_d ; TV signal peak frequency deviation [Hz]

$m(t)$; active TV video signal (message signal)

$d_1(t)$; Energy dispersal signal used in TV signal

$d_2(t)$; Energy dispersal signal used in interference (chirp)

$\phi(t) = 2\pi f_d \int^t m(\alpha) d\alpha$; TV carrier phase

$\hat{\mu}$; initial phase offset of interference.

NOTE: This expression is the same as the $S_O(t)$ of case 4 described in detail in a later page, except for the existence of initial phase $\hat{\mu}$ in chirp interference term.

<3> Case Study of Interference Effect

With the formula previously derived, the effect of chirp interference on a TV signal in various cases was studied as follow:

1. Case 1. [No interference, used as a reference case]

When there exists no interference, there will be no phase error, thus no frequency deviation and no error output voltage from the AM-discriminator.

input to FM-disc: $X_r(t) = A_{TV} \cos[\omega_1 t + \varphi(t)]$

where $\varphi(t) = 2\pi f_d \int^t m(\alpha) d\alpha$

phase error ; 0

instantaneous frequency deviation: 0

FM-disc output error voltage ; 0

2. Case 2. [unmodulated carrier plus chirp interference]

a. input to FM-DISC;

$$X_r(t) = A_{TV} \cos \omega_1 t + A_{CH} \cos \left[\omega_2 t + \frac{1}{2} \mu t^2 \right]$$

b. phase error;

$$\beta(t) = \tan^{-1} \left[\frac{A_{CH} \sin \left(\omega_d t + \frac{1}{2} \mu t^2 \right)}{A_{TV} + A_{CH} \cos \left(\omega_d t + \frac{1}{2} \mu t^2 \right)} \right]$$

c. instantaneous frequency deviation

$$\Delta f = \frac{A_{CH}(\omega_d + \mu t) \left[\frac{A_{CH}}{A_{TV}} + \cos \left(\frac{1}{2} \mu t^2 + \omega_d t \right) \right]}{A_{TV} \left[1 + \left(\frac{A_{CH}}{A_{TV}} \right)^2 + 2 \left(\frac{A_{CH}}{A_{TV}} \right) \cos \left(\frac{1}{2} \mu t^2 + \omega_d t \right) \right]}$$

d. FM-disc error output voltage:

$$S_o(t) = \frac{1}{2\pi} K_D \left(\frac{A_{CH}}{A_{TV}} \right) \frac{(\omega_d + \mu t) \left[\frac{A_{CH}}{A_{TV}} + \cos \left(\frac{1}{2} \mu t^2 + \omega_d t \right) \right]}{\left[1 + \left(\frac{A_{CH}}{A_{TV}} \right)^2 + 2 \left(\frac{A_{CH}}{A_{TV}} \right) \cos \left(\frac{1}{2} \mu t^2 + \omega_d t \right) \right]}$$

NOTE: 1. As a first approximation, assuming $A_{CH} \ll A_{TV}$ then,

$$S_o(t)_{\text{approx}} = \frac{1}{2\pi} K_D \left(\frac{A_{CH}}{A_{TV}} \right) (\omega_d + \mu t) \cos \left(\frac{1}{2} \mu t^2 + \omega_d t \right)$$

3. Case 3. [Frequency Modulated TV Carrier plus chirp interference]

a. input signal to FM-DISC:

$$X_r(t) = A_{TV} \cos[\omega_1 t + 2\pi f_d \int^t m(\alpha) d\alpha] + A_{CH} \cos[\omega_2 t + \frac{1}{2} \mu t^2]$$

where $2\pi f_d \int^t m(\alpha) d\alpha = \phi(t)$

$m(t)$: active TV message signal

b. phase error:

$$\beta(t) = \tan^{-1} \left[\frac{A_{CH} \sin[\gamma(t)]}{A_{TV} + A_{CH} \cos[\gamma(t)]} \right]$$

where $\gamma(t) = \omega_{CH} - \omega_{TV} + \omega_d t$

$$= \frac{1}{2}\mu t^2 - 2\pi f_d \int^t m(\alpha) d\alpha + \omega_d t$$

$$\Psi_{CH} = \frac{1}{2}\mu t^2; \text{ chirp interference phase}$$

c. instantaneous frequency deviation:

$$\Delta f = \left(\frac{A_{CH}}{A_{TV}}\right) \frac{[\omega_d + \mu t - 2\pi f_d m(t)] \left[\frac{A_{CH}}{A_{TV}} + \cos\{\gamma(t)\}\right]}{\left[1 + \left(\frac{A_{CH}}{A_{TV}}\right)^2 + 2\left(\frac{A_{CH}}{A_{TV}}\right) \cos\{\gamma(t)\}\right]}$$

d. FM-Disc output error voltage:

$$S_o(t) = \frac{1}{2\pi} K_D \left(\frac{A_{CH}}{A_{TV}}\right) [\omega_d + \mu t - 2\pi f_d m(t)] \frac{\left[\frac{A_{CH}}{A_{TV}} + \cos\{\gamma(t)\}\right]}{\left[1 + \left(\frac{A_{CH}}{A_{TV}}\right)^2 + 2\left(\frac{A_{CH}}{A_{TV}}\right) \cos\{\gamma(t)\}\right]}$$

Note: For approximation of $S_o(t)$ assuming $A_{CH} \ll A_{TV}$, use the following formula:

$$S_o(t)_{\text{approx}} = \frac{1}{2\pi} K_D \left(\frac{A_{CH}}{A_{TV}}\right) [\omega_d + \mu t - 2\pi f_d m(t)] \cos\{\gamma(t)\}$$

where $\gamma(t) = \frac{1}{2}\mu t^2 - 2\pi f_d \int^t m(\alpha) d\alpha + \omega_d t$.

4. Case 4. [Case 3 with an added energy dispersal signal]

a. input signal to FM-DISC:

$$X_r(t) = A_{TV} \cos \left[\omega_1 t + 2\pi f_d \int^t m(\alpha) d\alpha + d_1(t) \right] + A_{CH} \cos \left[\omega_2 t + \frac{1}{2}\mu t^2 + d_2(t) \right]$$

b. Phase Error;

$$\beta(t) = \tan^{-1} \left[\frac{A_{CH} \sin [Z(t)]}{A_{TV} + \cos [Z(t)]} \right]$$

where

$$Z(t) = \varphi_{CH_d} - \varphi_{TV_d}$$

$$= \frac{1}{2} \mu t^2 + d_2(t) - 2\pi f_d \int^t m(\alpha) d\alpha - d_1(t) + \omega_d t$$

$$\psi_{CH_d} = \psi_{CH} + d_2(t)$$

$$\varphi_{TV_d} = \varphi(t) + d_1(t)$$

$d_1(t), d_2(t)$: Energy dispersal signals

c. Instantaneous frequency deviation:

$$\Delta f = \left(\frac{A_{CH}}{A_{TV}} \right) \frac{\left[\omega_d + \mu t - 2\pi f_d m(t) + d'_2(t) - d'_1(t) \right] \left[\frac{A_{CH}}{A_{TV}} + \cos [z(t)] \right]}{\left[1 + \left(\frac{A_{CH}}{A_{TV}} \right)^2 + 2 \left(\frac{A_{CH}}{A_{TV}} \right) \cos [Z(t)] \right]}$$

where

$$d'_1(t) = \frac{d}{dt} d_1(t) \quad d'_2(t) = \frac{d}{dt} d_2(t)$$

d. FM-DISC output error voltage:

$$S_o(t) = \frac{1}{2\pi} K_D \left(\frac{A_{CH}}{A_{TV}} \right) \frac{\left[\omega_d + \mu t - 2\pi f_d m(t) + d'_2(t) - d'_1(t) \right] \left[\frac{A_{CH}}{A_{TV}} + \cos [Z(t)] \right]}{\left[1 + \left(\frac{A_{CH}}{A_{TV}} \right)^2 + 2 \left(\frac{A_{CH}}{A_{TV}} \right) \cos [Z(t)] \right]}$$

NOTE: For approximation of $S_o(t)$ assuming $A_{CH} \ll A_{TV}$, use the following formula:

$$S_o(t) = \frac{1}{2\pi} K_D \left(\frac{A_{CH}}{A_{TV}} \right) \left[\omega_d + \mu t - 2\pi f_d m(t) + d'_2(t) - d'_1(t) \right] \cos [z(t)]$$

where

$$z(t) = \frac{1}{2}\mu t^2 + d_2(t) - 2\pi f_d \int^t m(\alpha) d\alpha - d_1(t) + \omega_d t$$

5.3. Simulation of FM-discriminator output; chirp interference

case

In the previous section, some useful basic formula were found for the FM-discriminator output in the presence of chirp interference. In addition, illustrations Fig. 10 and Fig. 11 show the simple case of the error voltage output of an FM-discriminator when the FM-TV message signal has a simple form like an average dc voltage. In this section, a more complicated but more general form of the FM-TV message signal is used as the TV message signal, to determine a realistic result for the FM-discriminator output. Even though a more practical form of TV message signal with preemphasis filtering is simulated in a later part of this report, this section presents results for an interference analysis with a simpler form of signal.

In the simulation here, the reference TV video signal which we are using is a staircase voltage between 0.25 and 0.75 volts, with duration of 35 μ s. On a TV screen this video signal would produce a series of vertical bars of decreasing brightness, with a seven step gray scale. To test the accuracy of the simulation, a staircase signal was converted into the corresponding FM-wave, without any bandpass filtering, and then processed through the receiver simulation. The resulting video output was plotted, giving the result in Fig. 10 and Fig. 11. Fig. 10 shows the transmitted staircase function and Fig. 11 illustrates the video output after low pass filtering with 4.2 MHz cutoff frequency, the theoretical bandwidth for NTSC video signals. Note that in Fig. 11 the transients caused by the

**ORIGINAL PAGE IS
OF POOR QUALITY**

instantaneous step in the original signal in Fig. 10 cause the receiver filter to ring at the expected frequency. In the above simulation, the FFT routine used 2048 samples of the 64 μ s waveform. This sampling rate will theoretically reproduce all FM signal components up to 16 MHz.

The chirp signal was then overlaid on the FM-TV signal, and the error in the video staircase waveform at the receiver (FM-discriminator) was calculated and plotted. As mentioned earlier, when sampled at 2048 or 4096 samples in 64 μ s, aliasing does not appear and the resulting interference is small. Fig. 12 shows the error waveform for a 26 μ s chirp signal swept through 10 MHz. The chirp signal was set 26dB below the video signal, measured as a peak voltage ratio. The largest interference occurs at the end of the chirp signal, with a peak level of 0.005V, relative to a 1.0V nominal video signal. It is unlikely that this low level interference would be visible on a TV screen, and would appear as very small random dots if it could be seen. To check whether the chirp signal produced significant interference in the video signal spectrum between 3 and 4 M μ z, where the chrominance information is transmitted, additional simulations were performed. Fig. 13 shows the resulting spectrum of this interference component. For comparison purposes, Fig. 14 shows the calculated spectrum of the video staircase signal. The interference power level is well below that of the video signal, and has a very flat spectrum, indicating that chrominance interference should be very small.

From the above results, there appears to be very little interference at the video output of the TV system when a chirp signal is overlaid on an FM-TV signal, as carried by many satellite transponders. The interference peaks are more than 40dB below the FM-TV video signal when the chirp RF signal is 20dB below the FM-TV carrier, showing good interference suppression by the FM carrier. In the simulation procedure, the effect of deemphasis in the video receiver was ignored for convenience at this time. In general, deemphasis in the receiver will help to reduce the effect of interference peaks because of its low pass filter action. However, in a later part of this report, when a practical interference model is used, preemphasis in the transmitter was added to get more practical simulation results.

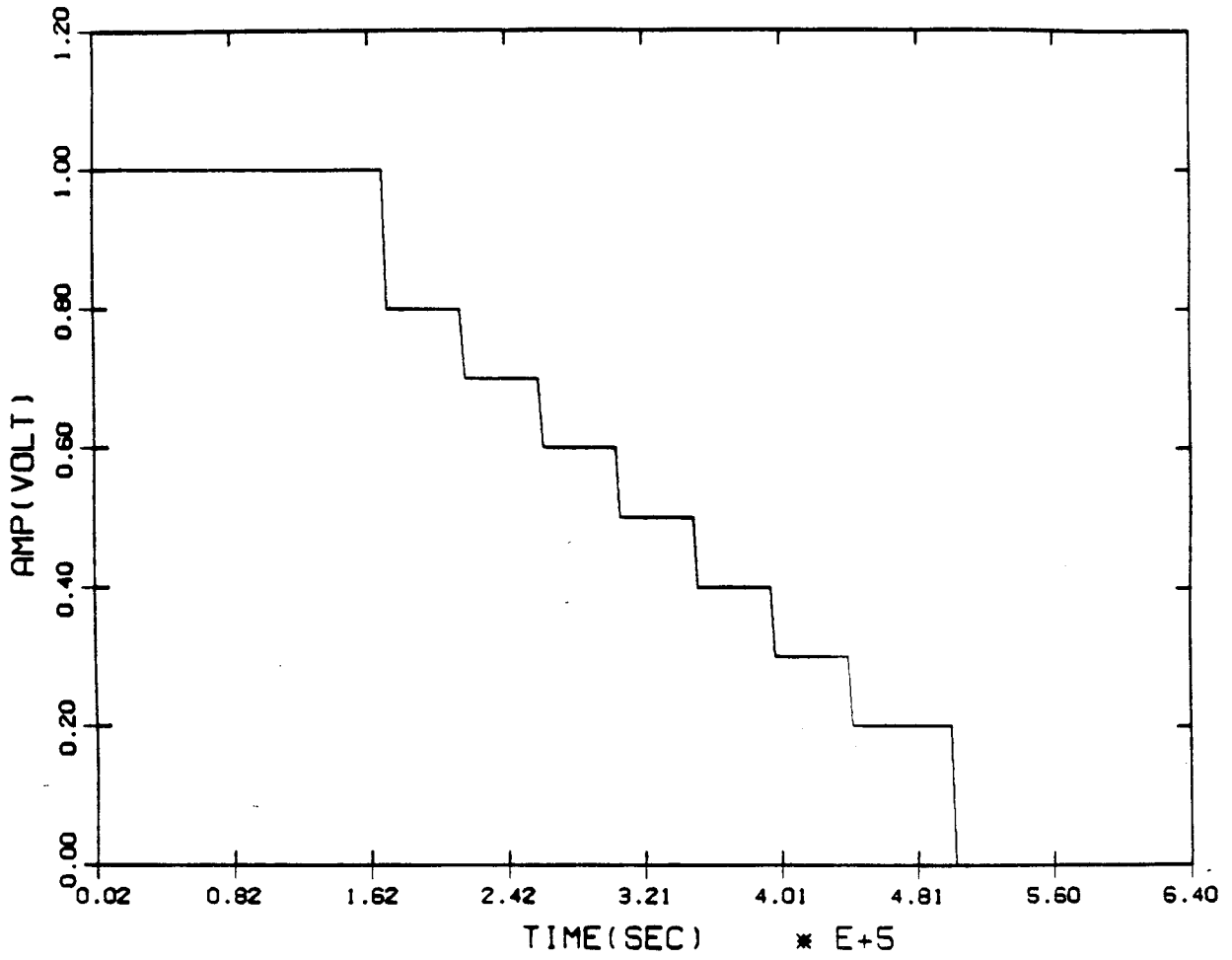


Figure 10. Simulated 9 step staircase function (time plot)

[N=2048,FC=4.2MHZ,UNIT GAIN]

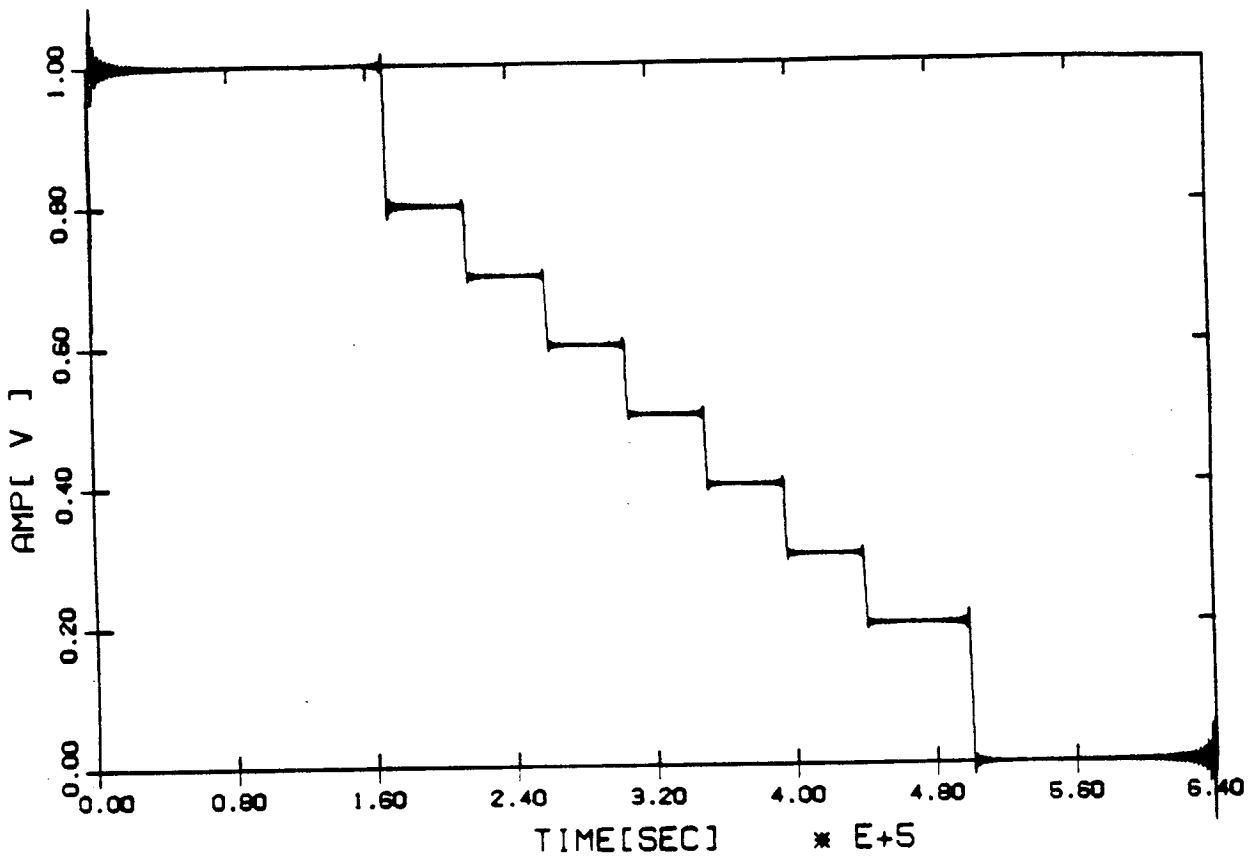


Figure 11. Received and lowpass filtered simulated 9 step staircase function

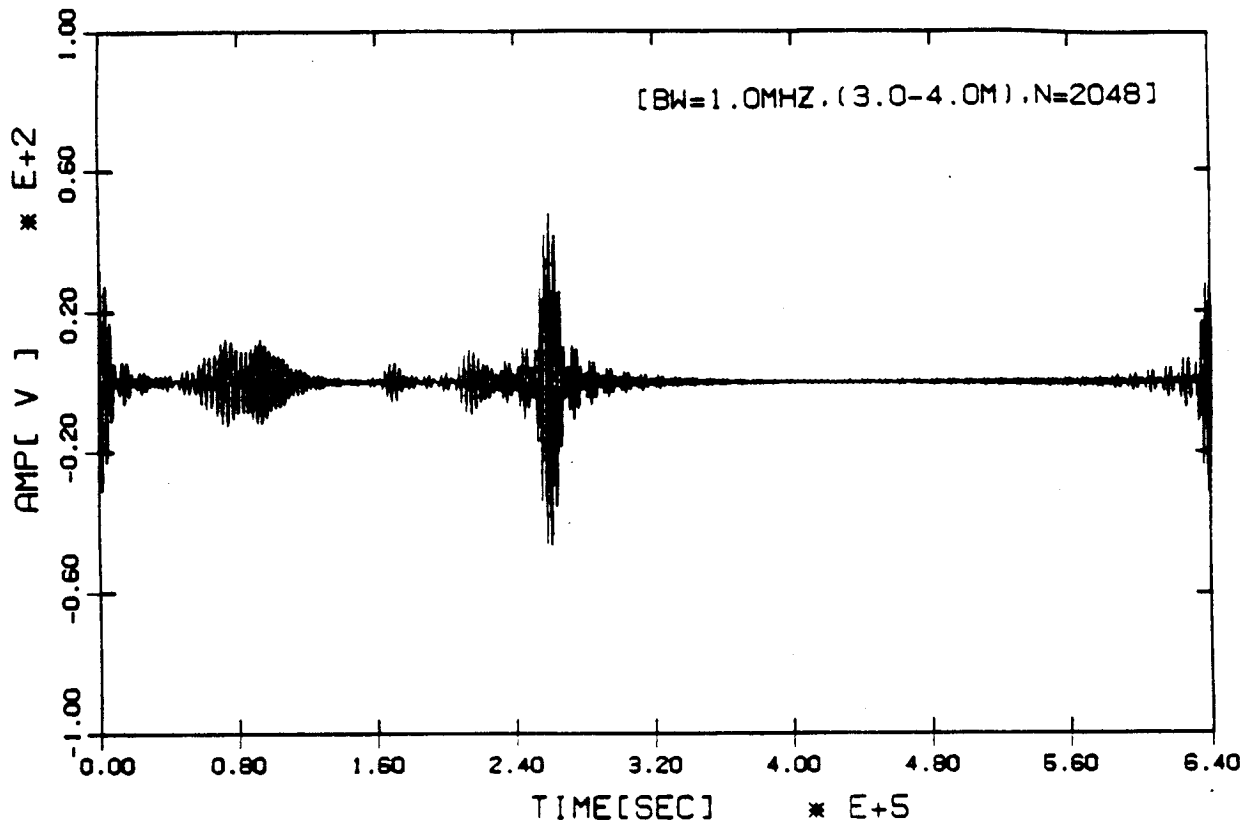


Figure 12. Error output voltage of FM-discriminator after bandpass filtering

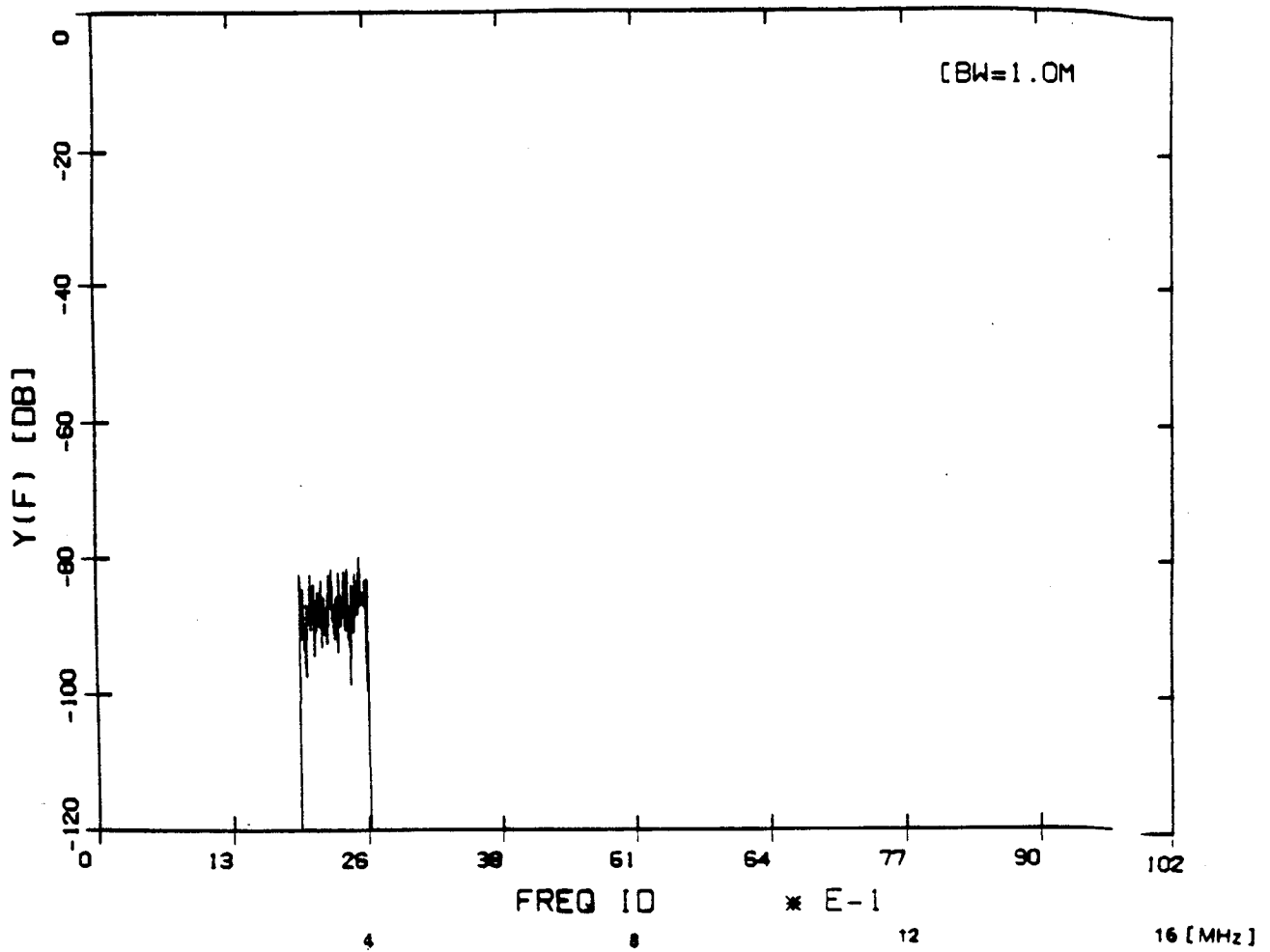


Figure 13. Spectrum of error output after bandpassing filtering (3-4 MHz)

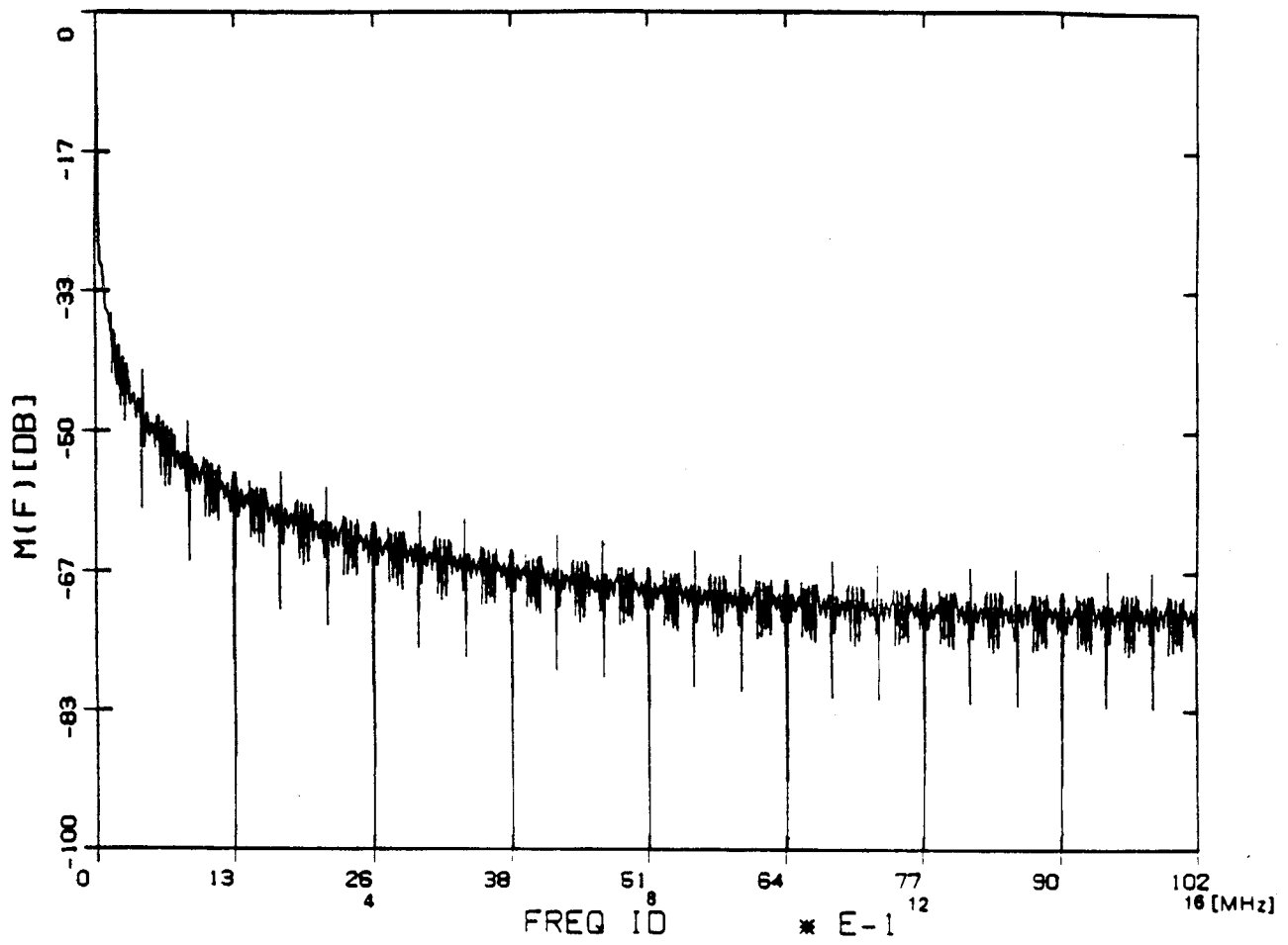


Figure 14. Spectrum of 9 step staircase function

5.4. Analog FM-TV signal interference on chirp demodulation

As another phase of the mutual interference study, the analog FM-TV signal can be modeled as interference in a chirp signal overlay service. To see the effect of such interference, we evaluated the output of a dechirper (compression filter) for the desired signal (chirp) and for the interference (FM-TV signal). For simplicity, detailed procedures are omitted, and only the results are described here.

Let the desired chirp signal be:

$$f(t) = \begin{cases} e^{j(\omega_c t + \frac{1}{2}\mu t^2)} & -T_0 < t < T_0 \\ 0 & |t| > T_0 \end{cases}$$

and the unwanted interference analog FM-TV signal be:

$$l(t) = \begin{cases} A_i e^{j[\omega_c t + \Phi(t)]} & -T_1 < t < T_1 \\ 0 & \text{elsewhere} \end{cases}$$

then the compressed output of the desired chirp signal is given by

$$g(t) = \sqrt{\frac{2\mu T_0^2}{\pi}} \frac{\sin \mu t T_0}{\mu t T_0} e^{j[\omega_c t - \frac{1}{2}\mu t^2 + \frac{\pi}{4}]}$$

and its real part is written as:

$$\text{Re}[g(t)] = \sqrt{\frac{2\mu T_0^2}{\pi}} \frac{\sin \mu t T_0}{\mu t T_0} \cos [\omega_c t - \frac{1}{2}\mu t^2 + \frac{\pi}{4}]$$

whereas the compressed output for analog FM-TV interference is

$$J(t) = A_i \sqrt{\frac{\mu}{2\pi}} e^{j(\omega_c t + \frac{\pi}{4})} \int_{-T_1}^{T_1} d\tau e^{j[\Phi(\tau) - \frac{\mu}{2}(t-\tau)^2]}$$

and its real part is written as

$$\text{Re}[J(t)] = t A_i \sqrt{\frac{\mu}{2\pi}} \int_{-T_1}^{T_1} \cos [(\omega_c t + \frac{\pi}{4}) - \frac{\mu}{2}(\tau - t)^2 + \Phi(\tau)] d\tau$$

In all the above equations, μ , ω_c , $\Phi(t)$ are the same as in the definitions in section 5.2. Based on the equation for the desired output $g(t)$ for chirp and unwanted outputs $J(t)$ for analog FM-TV interference, a computer simulation was performed under the following conditions:

chirp frequency dispersion	10.0 MHz
chirp time duration	26 μ s
chirp dispersion slope	10.0/26.0 MHz/ μ s
FM-TV message signal	0.5V dc
FM-TV signal duration	64 μ s
FM-TV signal max frequency deviation	10.0 MHz
Initial IF frequency	70.0 MHz
interference signal amplitude	0.1V, 0.2V, 0.5V.

For convenience of simulation, the message signal of the analog FM-TV was chosen as 0.5V dc, which is the average dc level of a video signal in a conventional analog FM-TV system. Fig. 15 and Fig. 16 show the outputs of the compression filter. Fig. 15 is the typical output of a compressor to the desired chirp signal. Fig. 16 illustrates the output of the compressor when simulated FM-TV signal interference with an amplitude 0.1V dc is applied. As can be expected from chirp theory, the mismatched (unwanted interference) signal is widely spread into a long time duration, while the matched signal (chirp) is compressed into a short time. From this result, it is possible to expect that

the interference from the TV signal can be effectively suppressed below a certain desired level if the proper conditions are provided in the overlay service.

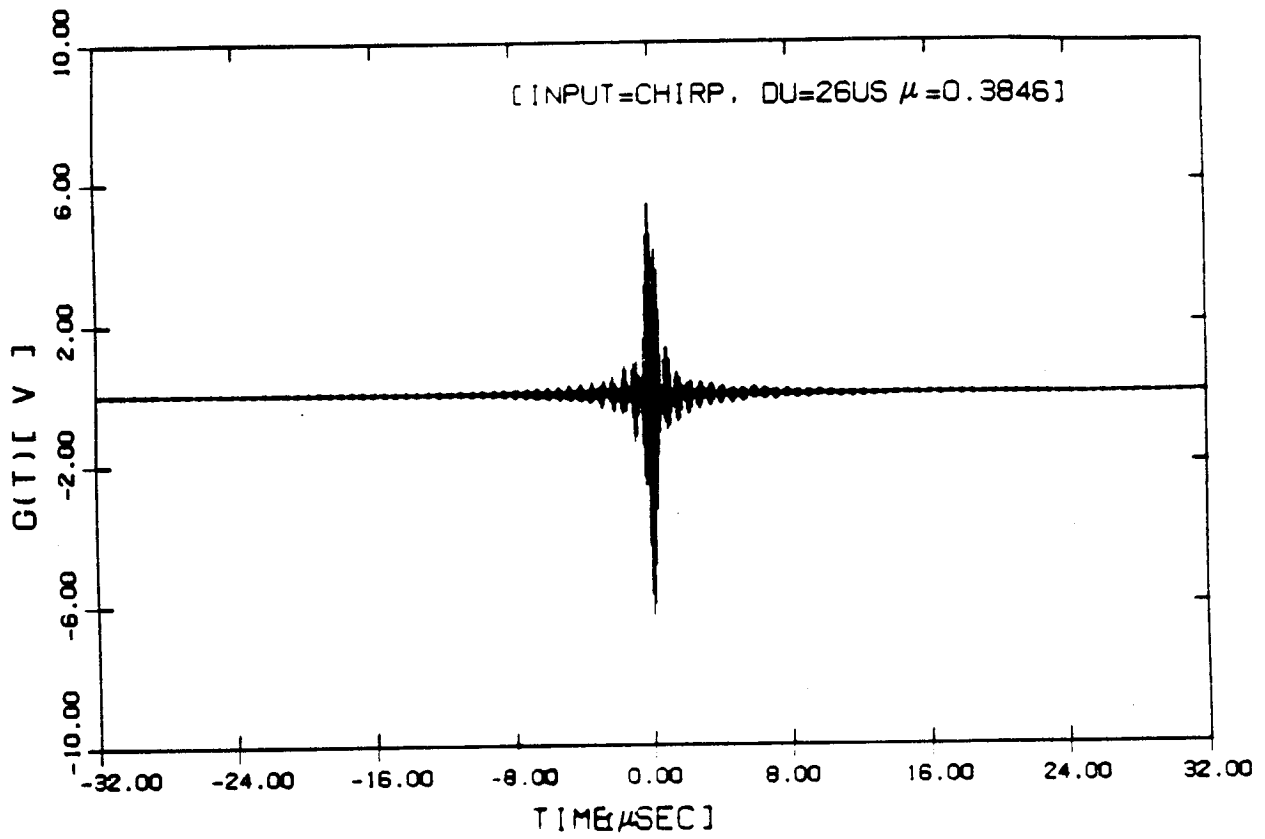


Figure 15. Typical compression filter output for chirp signal input

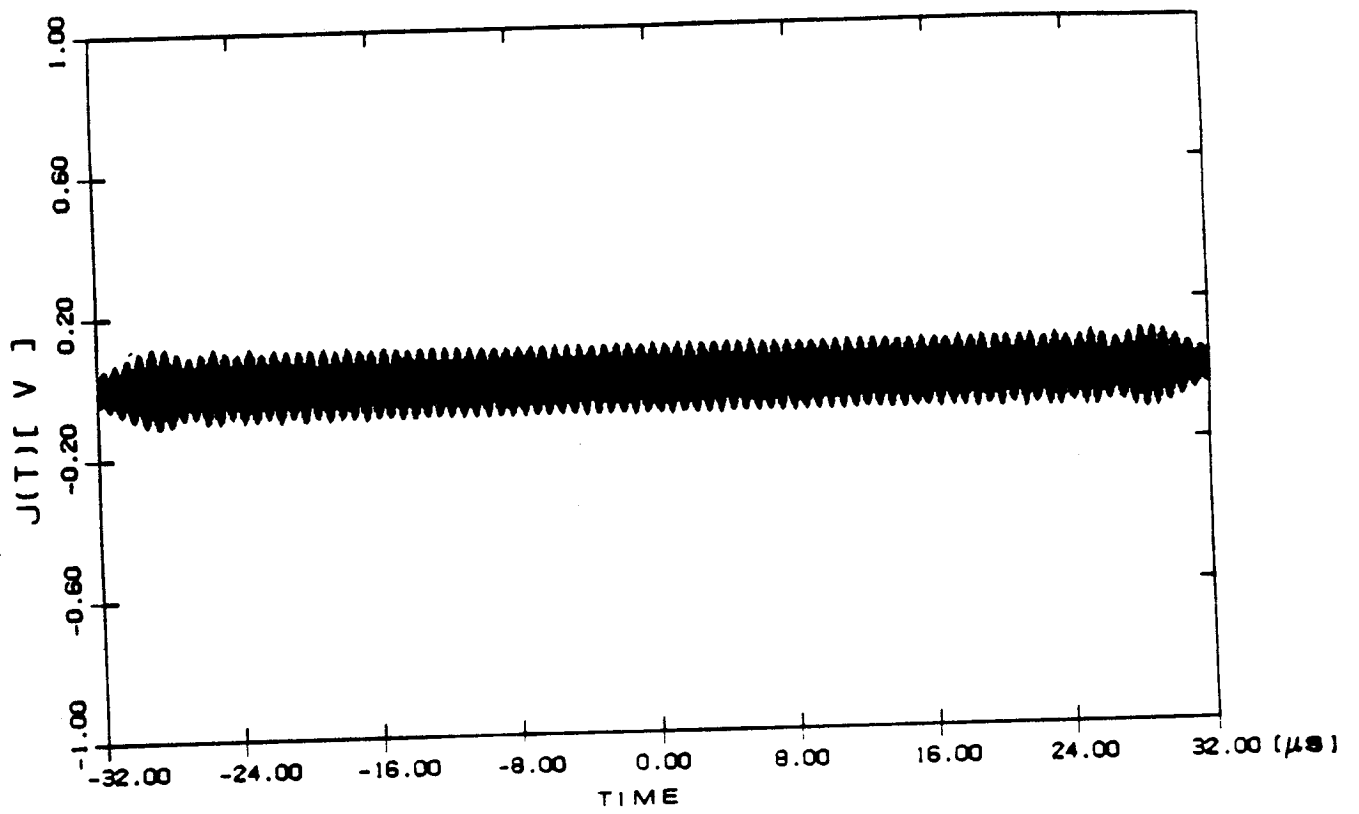


Figure 18. Compression filter output for FM-TV signal with amplitude of 0.1V

6. Interference Analysis II (Practical Modeling and Simulation)

So far, we have investigated the principle of an overlay service between analog FM-TV and a chirp spread spectrum system by finding the general expression of the FM-TV demodulator output error voltage when a chirp signal is interfering with the FM-TV signal, and vice versa. In those procedures, the message or information signal of the FM-TV has been simply modeled by a dc voltage or a pure sinusoidal wave, to investigate the general case of an interfering environment. However, it is essential to define a complete model of a TV video signal in the time and spectral domains, for the further analysis of an overlay service.

In this chapter, the modeling procedures of an analog FM-TV video signal without preemphasis, and corresponding computer simulation results are explained first. Then, the same procedures are repeated with a preemphasis filter. Finally, an overlay service link analysis for C band is done to permit a performance analysis in section 5.

Precise modeling of a general TV video signal is almost impossible because the spectrum of a general television signal is not known with any degree of certainty. The variety of images being shown gives a variety of spectral shapes. In addition, the FM television signal is a wideband signal; in practice the entire overlay signal (chirp) will be contained within the bandwidth of a television

receiver [31]. Nevertheless, a realistic model of a television video signal is required for analysis of the case of a TV signal overlaid with a chirp signal.

As a model for computer simulation, a typical television video signal with NTSC 525 line format was selected. The usual television signal contains synchronization pulses (vertical and horizontal), audio, color bars (in color television only) or chrominance patterns, as well as the luminance signals. In horizontal line scanning, about 64 μs duration (63.55 μs exactly) of a single horizontal scan duration contains all the necessary information. Of the 64 μs duration, the first 11 μs is devoted to synchronization and the last 13 μs is used for color burst in a color television. Therefore, the active video signal uses only 30 ~ 40 μs duration in a single horizontal scanning period of 64 μs . The maximum video signal is 1.0 volt peak to peak amplitude.

6.1. Analog FM-television signal modeling I -- Without preemphasis

A. Linear Step Staircase Function Model

Based on the typical model described above, a simple model in the time domain is illustrated in Fig. 10. The corresponding time domain expression can be written as a series of staircase functions as follows:

$$m(t) = A_1U(-t + \tau_1) + A_2U(-t + \tau_2) + \dots A_7U(-t + \tau_7) + A_8U(-t + \tau_8)$$

or, in general form, it also can be written:

$$m(t) = \sum_{i=1}^n A_i U(\mp t \pm \tau_i); n = 1, \dots, m$$

where

- $m(t)$; analog FM-TV video signal in a single horizontal scanning period ($64 \mu s$).
- A_i ; incremental magnitude of unit step function in voltage, $0 \leq A_i \leq 1$
- τ_i ; time increment of luminance signal corresponding to magnitude A_i
- m ; desired number of luminance level.

As an extension of this model, the step size was increased to 200 later, as in Fig. 17.

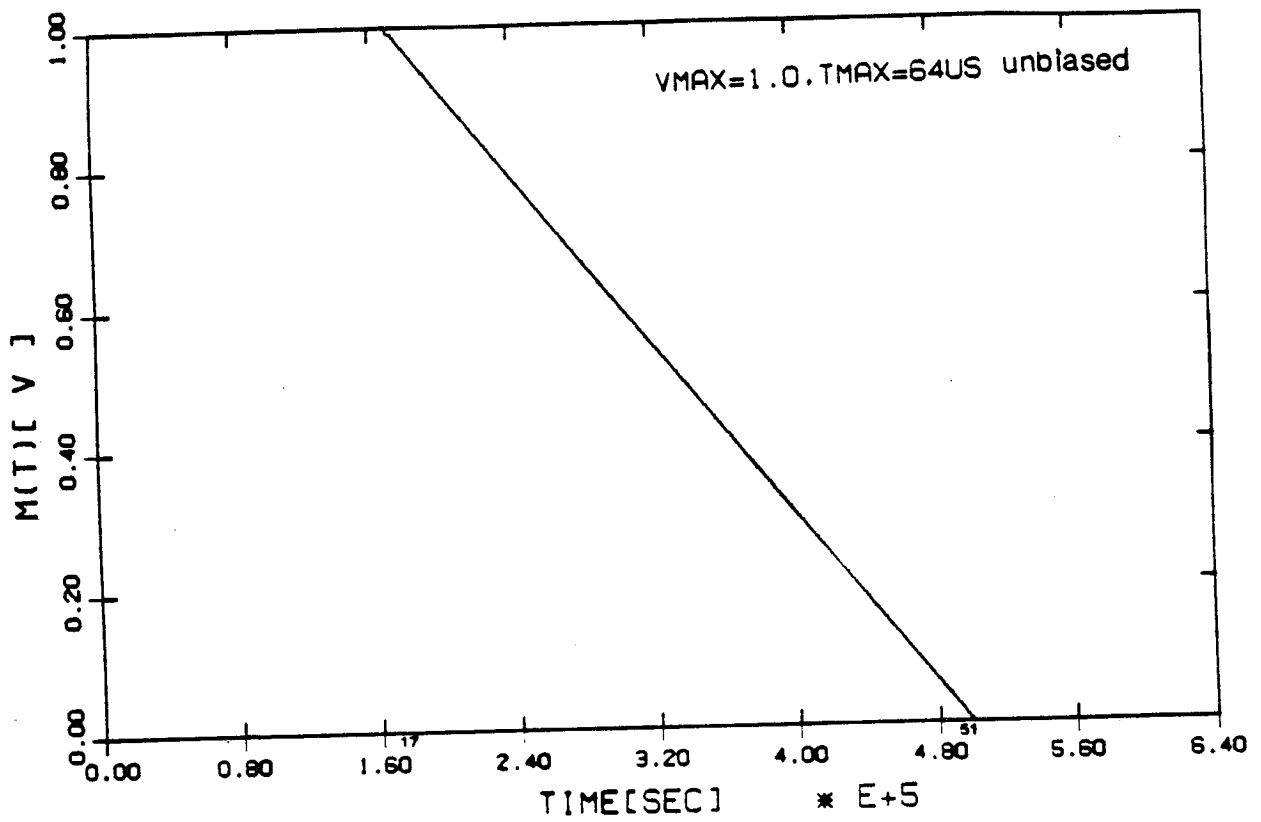


Figure 17. Time plot of simulated 200 step staircase function model for video signal

B. Random Step Staircase Function Model

The model of an analog television video signal with a linear, 9 step or 200 step staircase function can be used to represent a typical video signal, even though it is simple. But this cannot be the worst case model which can be encountered in a real system. So another model was made which consisted of 256 steps of random amplitude. A uniform random number was generated with an arbitrary seed, in the range of 1 to 256. Incremental times between 17 μ s to 50 μ s were given random amplitudes which were generated by the random number generator. This gave a random amplitude step function. Because of the uniform distribution of the random step amplitude, the mean value was 0.5 Volt, as with the linear staircase function. Fig.18 shows this function.

6.2 Simulation of Wideband FM-TV Signal and Chirp I--No

Preemphasis

As mentioned earlier, an analog FM television signal is a wideband signal. In domestic satellite television transmission, the baseband television signal, with its video information bandwidth of approximately 4.2 MHz, is FM modulated so that its RF bandwidth fills an entire 36 MHz bandwidth of a satellite transponder [2].

In the overlay service, when a chirp signal is overlaid on an existing television signal, the interference of the chirp signal into the television signal is an all pass function because the chirp RF bandwidth is usually much narrower than that of the FM television signal. But in the case when the chirp signal is interfered with by the television signal, only a specific 5.0 MHz bandwidth of television interference power is introduced in the chirp signal via the IF filter (if its bandwidth is set to 5.0 MHz).

For our study of mutual interference in an overlay system under the above conditions, the spectrum shape of the television signal is modeled by choosing a staircase or random video

waveform. Computer simulation is an effective alternative to the practical experiments, even though the final judgment on mutual interference is highly subjective and depends on the response of the human eye in the television case. Because of the complexity of modeling RF signals, all the simulations were done in baseband. By trial and error, we found that 2048 or more samples in the 64 μ s horizontal scanning period guaranteed no aliasing effects. So 2048 samples were used for overall simulation, both in the time and frequency domains. The chirp signal used in the simulation was the positive (up) frequency swept signal with 10.0 MHz/26.0 μ s sweep rate. By using 2048 samples, the maximum frequency span was -16 MHz to +16 MHz.

In spectral illustrations, the frequency i.d (or index) is the multiplier of incremental frequency (when $N = 2048$, $\Delta f = 0.015625$ MHz), so, for example, the index number 100 means 1.5625 MHz. The vertical axis of the graphs is the power density of the signal calculated with its minimum level set to -100dBW or -120dBW, assuming the maximum level of carrier amplitude is $\sqrt{2}$ for future convenience in power calculations.

For baseband simulation, the transmitted analog FM television signal and chirp signal are defined as follows:

$$w(t) = \sqrt{2} \cos[\omega_c t + 2\pi f_d \int^t m(\alpha) d\alpha]$$

where

$$\omega_c = 0 \text{ for baseband}$$

$$f_d = 10.0 \text{ MHz/volt}$$

$$m(\alpha) = 200 \text{ step linear staircase function or } 256 \text{ step random amplitude function}$$

The transmitted chirp signal is written as

$$i(t) = \sqrt{2} \cos[\omega_c t + \frac{1}{2} \mu t^2]$$

where

$$\omega_c = 0 \text{ for baseband simulation}$$

$$\mu = 10.0 \text{ MHz}/26 \mu\text{s}$$

**ORIGINAL PAGE IS
OF POOR QUALITY**

Simulation results in the time and frequency domains are illustrated in the following figures. Fig. 19 shows the transmitted analog FM-TV signal at baseband. The original message signal for television is the random function in Fig. 18 with 0.5 volt dc bias. Fig. 20 also illustrates the corresponding frequency spectrum (power spectral density) of the transmitted signal when the message signal is random. As another simulation model, the video is modeled by a 200 step linear staircase function; Fig. 21 shows the same form as Fig. 19 but with this linear step function as its message signal. Fig. 22 shows the corresponding spectrum. For the transmitted chirp signal, Fig. 23 shows the time waveform and Fig. 24 illustrates its spectrum.

The spectral plots, Fig. 20, Fig. 22, and Fig. 24 give the clues for an effective overlay service. Fig. 22 illustrates the transmitted FM-TV signal spectrum in baseband, with its message signal modeled as a 200 step linear decreasing staircase function, and Fig. 20 shows the same TV signal spectrum but with a 256 step random amplitude function as its video information. In both cases, the spectrum is nearly flat up to approximately 4.2 MHz. However, from 4.2 MHz to 16 MHz, the average level of the spectrum in the random video message case is much higher than that for the linear staircase function. Even though neither of these two cases is a real TV spectrum, they can be used as reference spectra for the design of a chirp overlay system. The spectrum depicted in Fig. 22 can be used as a general case of typical TV video spectrum, whereas that depicted in Fig. 20 can be considered a worst case spectrum. The fast decay of the energy in the spectrum in Fig. 22 (linear staircase message signal) above 4.2 MHz shows that this TV signal can be overlaid by a chirp signal if the relative power levels of the chirp and TV signals are set correctly in the transmission stage. The link analysis in the next section will provide the appropriate value of chirp signal suppression to prevent serious interference of the TV video reception, and also gives the specific value of compression gain required for chirp demodulation under the power limited situation of typical satellite links.

As mentioned before, the message signal (television video signal) used in the simulation up to this point has not been processed by a preemphasis filter. Preemphasis increases the energy at higher frequencies in the FM-TV spectrum which increases the interference into the chirp signal

channel. The simulation was repeated with a preemphasis filter in the video channel to get results both in the time and frequency domains and to see the effect of preemphasis filtering.

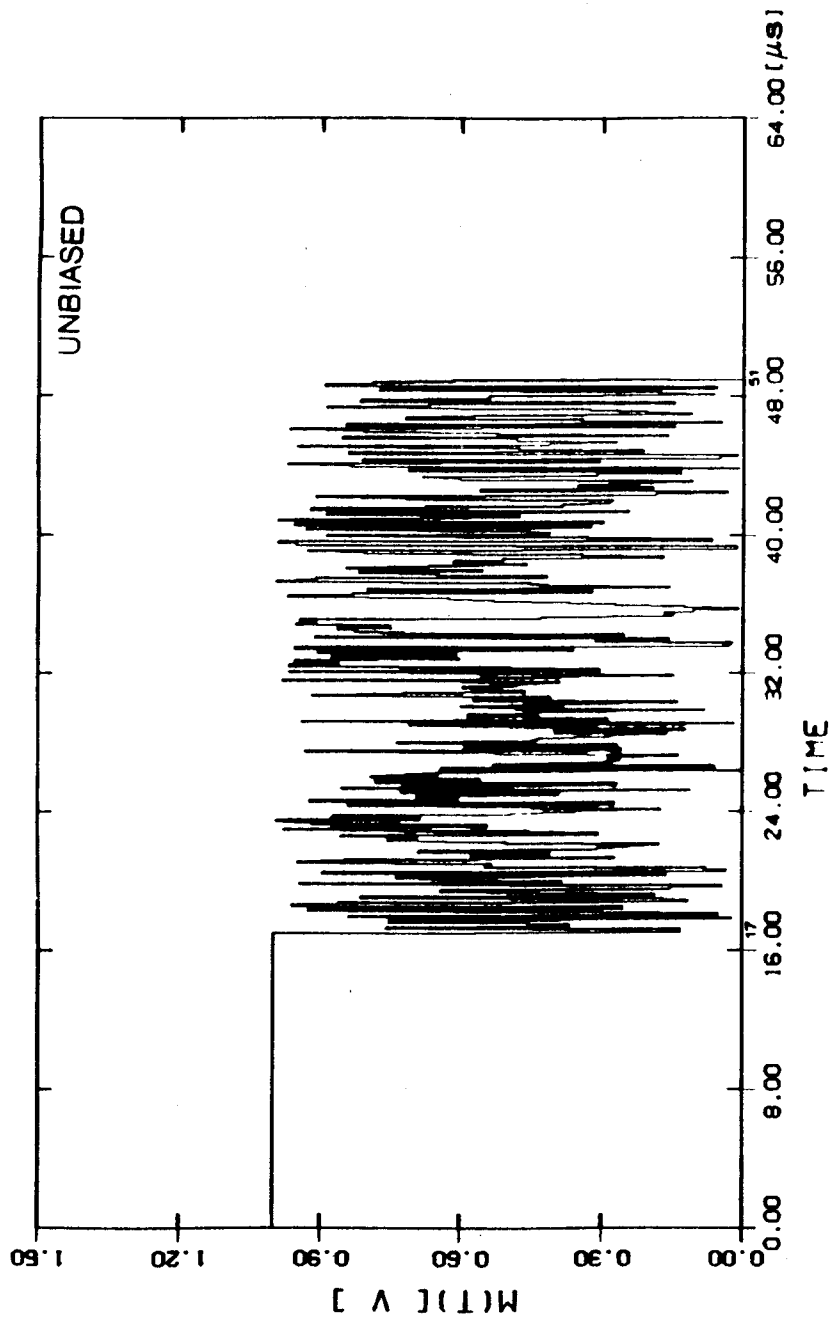


Figure 18. Time plot of simulated 256 step random amplitude model for video signal

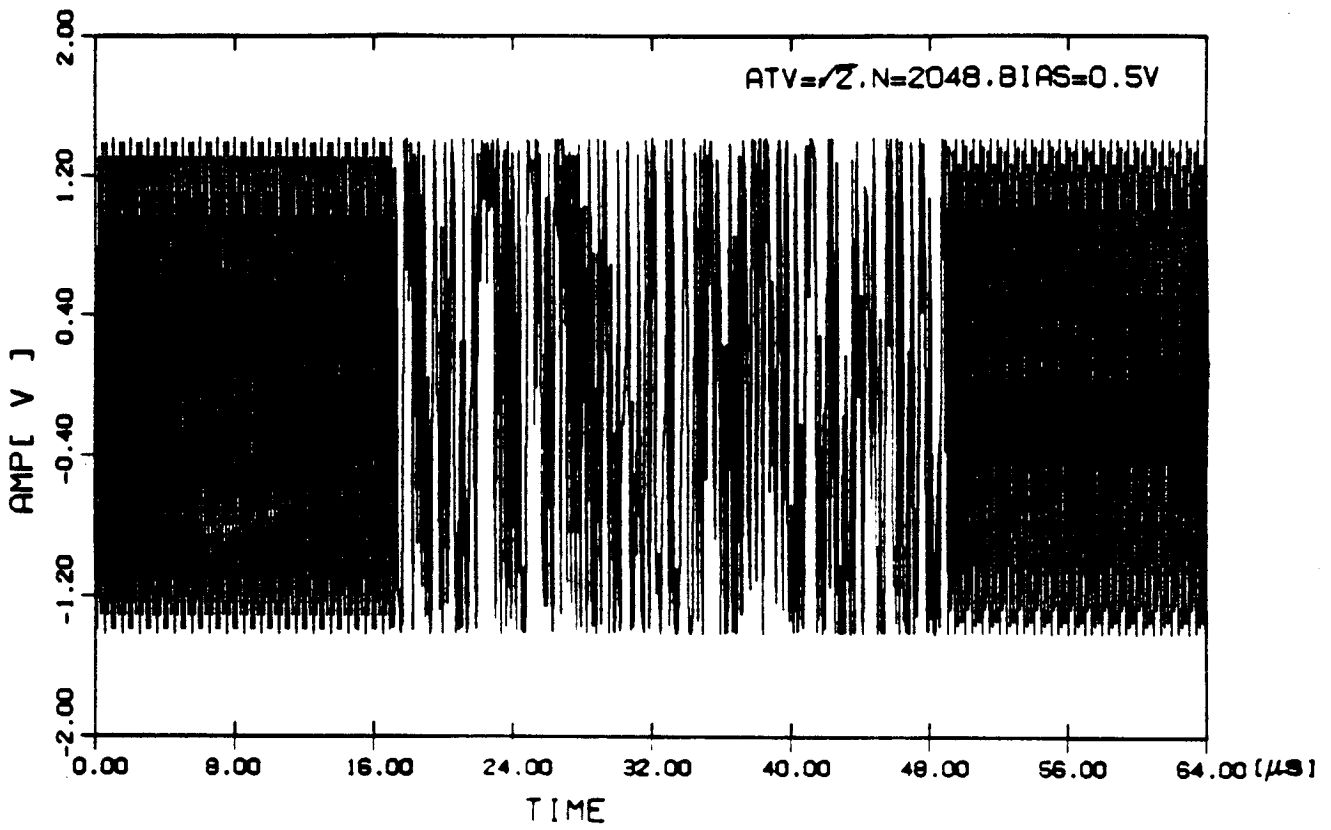


Figure 19. Transmitted FM-TV signal time plot (random)

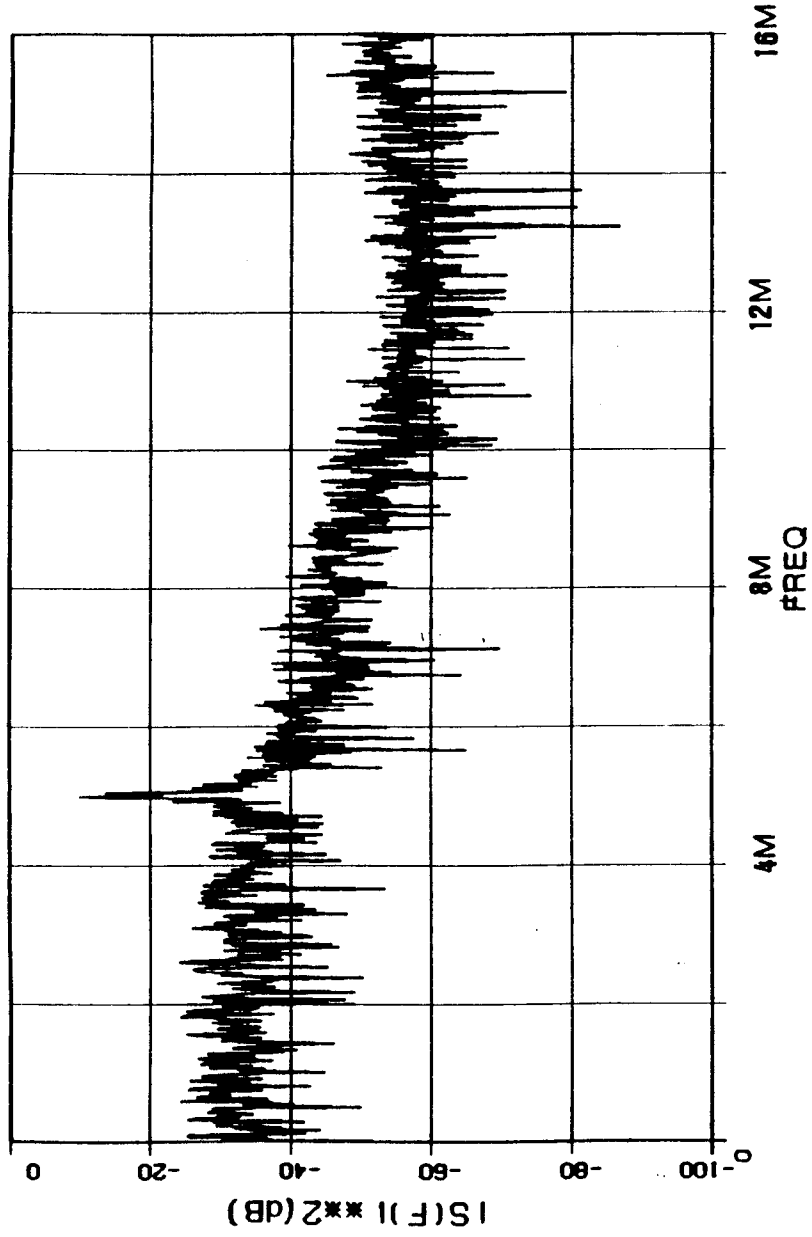


Figure 20. Frequency spectrum of Figure 19 (random)

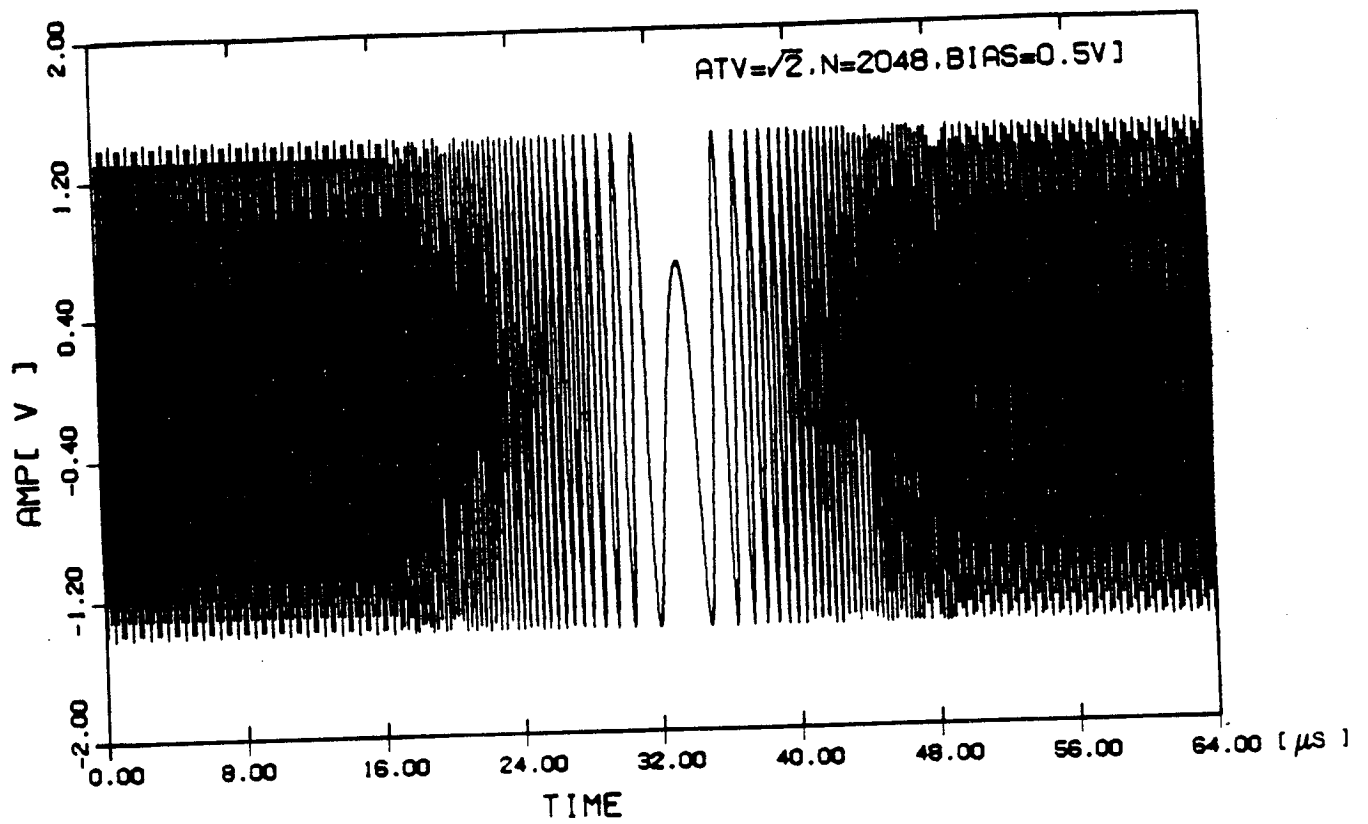


Figure 21. Transmitted FM-TV signal time plot (linear)

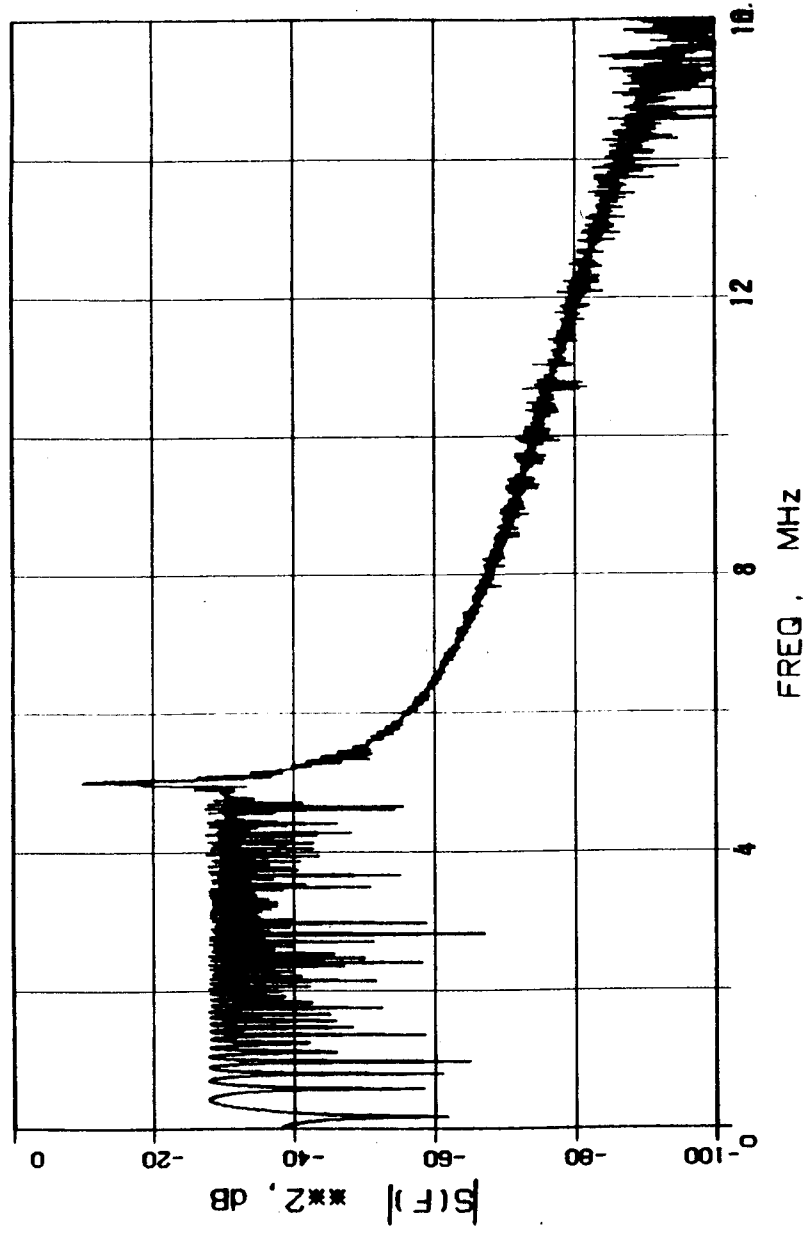


Figure 22. Frequency spectrum of figure 21 (linear)

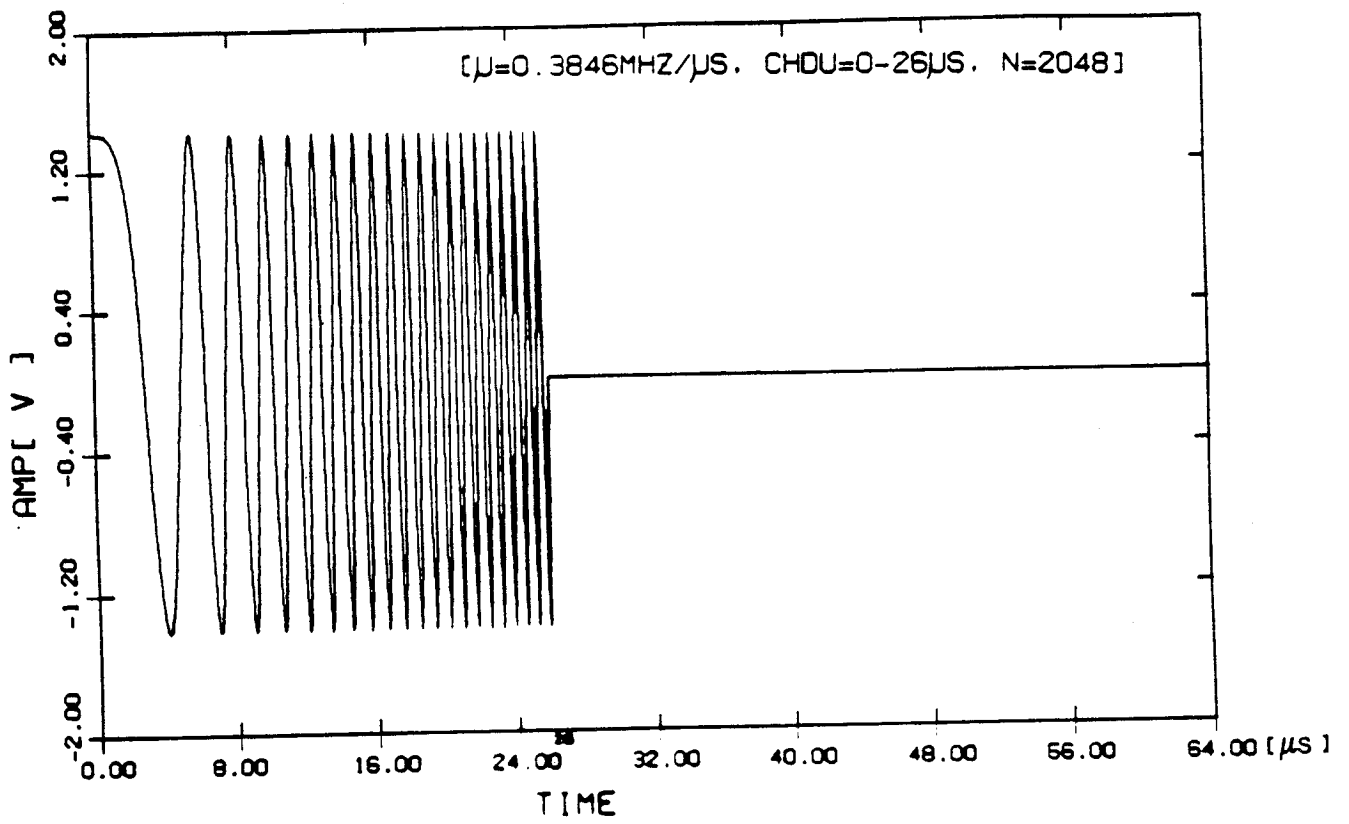


Figure 23. Transmitted chirp signal time plot

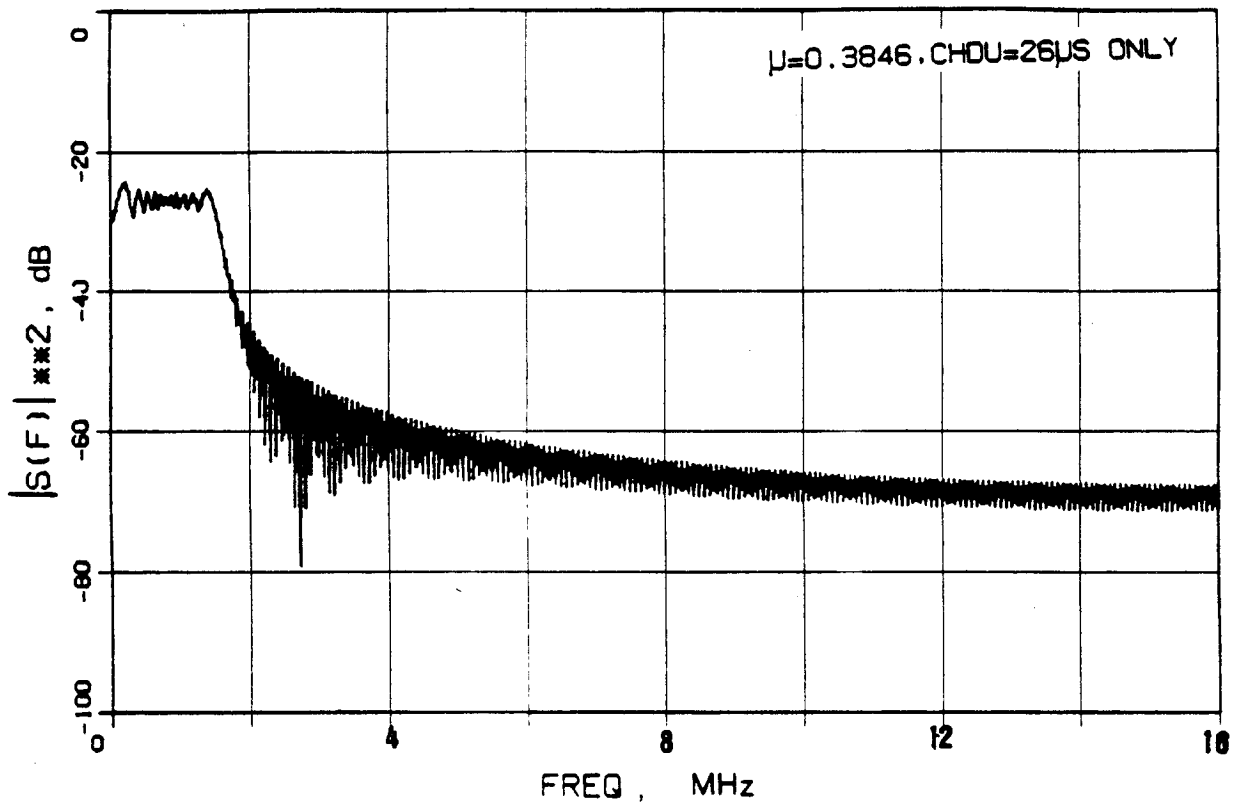


Figure 24. Frequency spectrum of Figure 23

6.3. Analog FM-television signal modeling II - with preemphasis

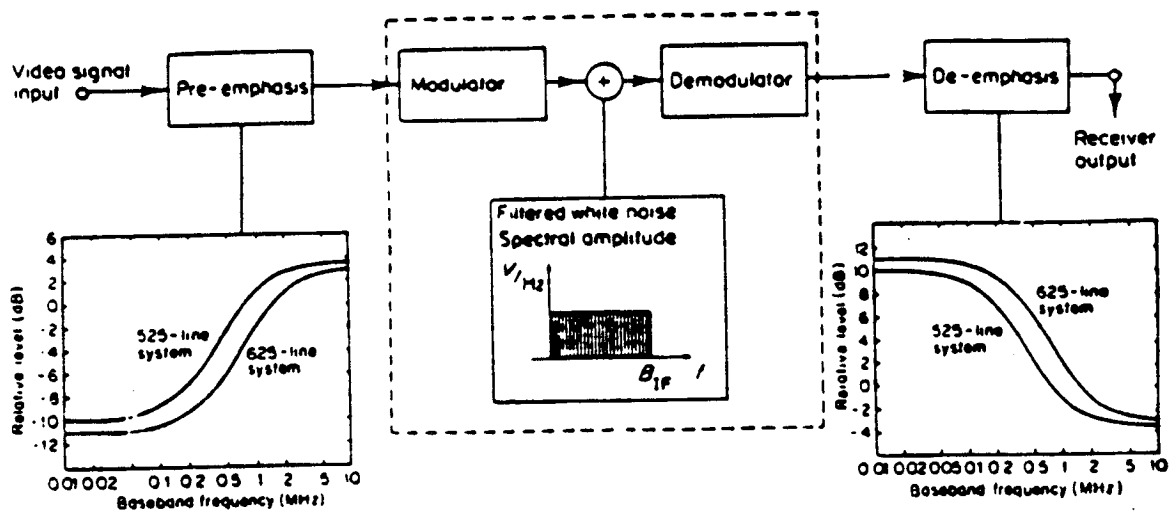
In the previous analysis, the models used for the FM-television video signal did not include preemphasis before modulation of the carrier. However, most practical FM systems employ preemphasis and deemphasis. Therefore, to get a more practical simulation result, preemphasis filtering of the analog FM television signal is necessary. Theoretically, a deemphasis filter also must be included after the television signal demodulation. But in the simulation performed here, especially the interference analysis at the input of the IF filter, it is not thought to be necessary, because deemphasis is achieved with a low pass filter which simply eliminates the residual interference spike after demodulation. The deemphasis filter can be eliminated from the simulation without losing validity of the simulation result. Fig. 25 illustrates an example of a NTSC FM television modem block diagram which employs preemphasis and deemphasis, along with typical frequency response curves of each filter.

6.3.1. Preemphasis Characteristics - NTSC 525 line/simulation

The characteristics of typical preemphasis filters can be found in relevant references. Janskey and Jeruchim [33] describes the CCIR Pre-Emphasis technique in detail, and Freeman [31] presents the various preemphasis curves under CCIR Recommendation 405. For more detailed information see CCIR Report 464 [34].

Fig. 26 illustrates the preemphasis characteristic curves for 405, 525, 625 and 819 line television systems. Here, in the simulation, we have confined our analysis to the 525 line NTSC system. Fig. 27 shows the 525 line NTSC preemphasis curve which we used as a model for simulation. An algorithm was developed by trial and error variation of the parameters of the usual expression for preemphasis. Fig. 28 shows our simulated preemphasis characteristic curve. Although there are

some differences between Rec 405 and the simulated curve, the error is within ± 1 dB over most of the frequency range.



(Pre-emphasis characteristic CCIR Rec. 405)

Figure 25. Typical NTSC modem structure with preemphasis/ deemphasis

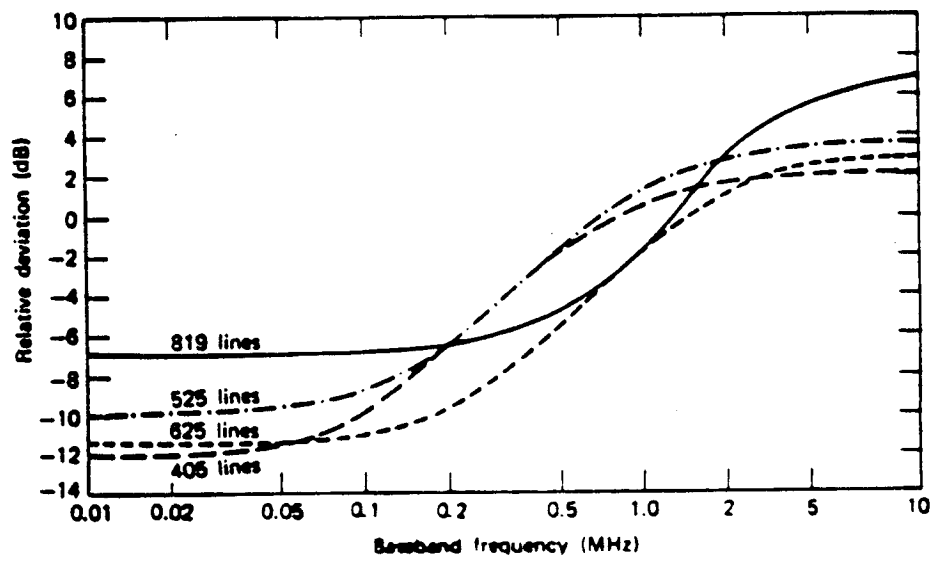


Figure 26. TV preemphasis characteristics (525, 625, 819 and 405 lines)

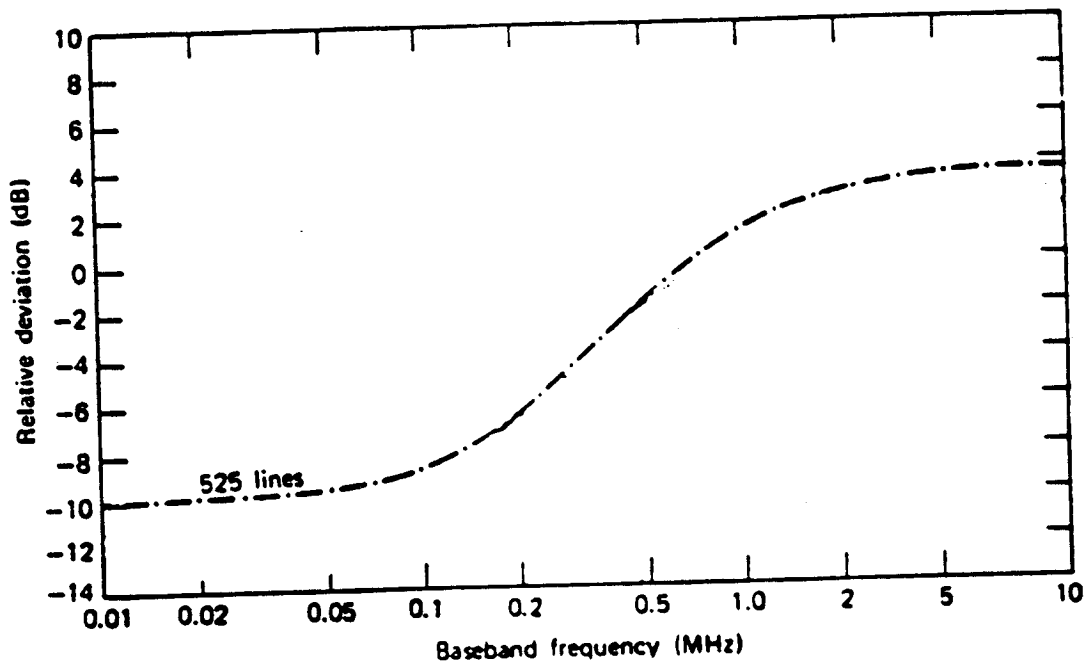


Figure 27. NTSC 525 line-CCIR Rec.405 preemphasis characteristic

ORIGINAL PAGE IS
OF POOR QUALITY

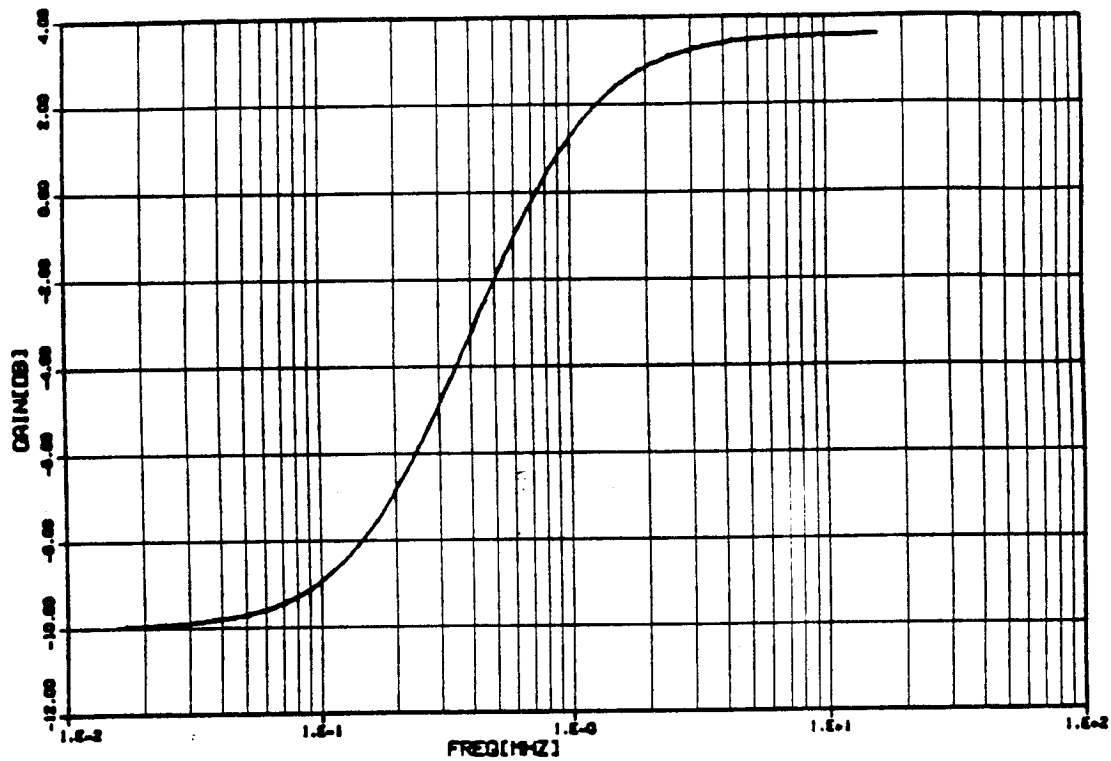


Figure 28. Simulated preemphasis filter for NTSC 525 line TV system

6.3.2. Modeling of FM-television video signal - With preemphasis

Basically, there cannot be any differences in the simulation models defined in Section 6.1.A and 6.1.B, because only a filtering operation has been added before frequency modulation of the wideband television signal. But for the convenience of simulation, some changes are needed because of the complex valued form of signal used in the filter process. The active luminance signal duration was changed from $17 \sim 51 \mu\text{s}$ to $18 \sim 50 \mu\text{s}$, which should not cause significant difference in the spectral domain. The other difference from the model in Section 6.1.B (random amplitude function of television video) was the number of random amplitude steps. It is necessary to keep the same number of time or frequency samples throughout the overall simulation procedure, and the filtering routine was made to accept data in this way. There are 2048 samples over the $64 \mu\text{s}$ duration of a single horizontal scanning line; a section lasting $32 \mu\text{s}$ ($18 \mu\text{s}$ to $50 \mu\text{s}$) which contained 1024 samples, was selected as having random amplitude. Therefore, instead of selecting and generating 256 random numbers, 1024 random numbers were generated in this simulation for the preemphasis version.

Fig. 29 shows the video signal with random amplitude before preemphasis, and Fig. 30 shows its preemphasized version. Because of the gain factor in the preemphasis filter at higher frequencies, the random portion has enhanced amplitude compared with the non-preemphasized case shown in Fig. 29. The other signal model was simulated by a staircase function. Fig. 31 illustrates the video message before preemphasis, and Fig. 32 shows the preemphasis version. In Fig. 32, a transient spike at $50\mu\text{s}$ is caused by the large level shift in the original message signal from -0.5V to 0.5V .

ORIGINAL PAGE IS
OF POOR QUALITY

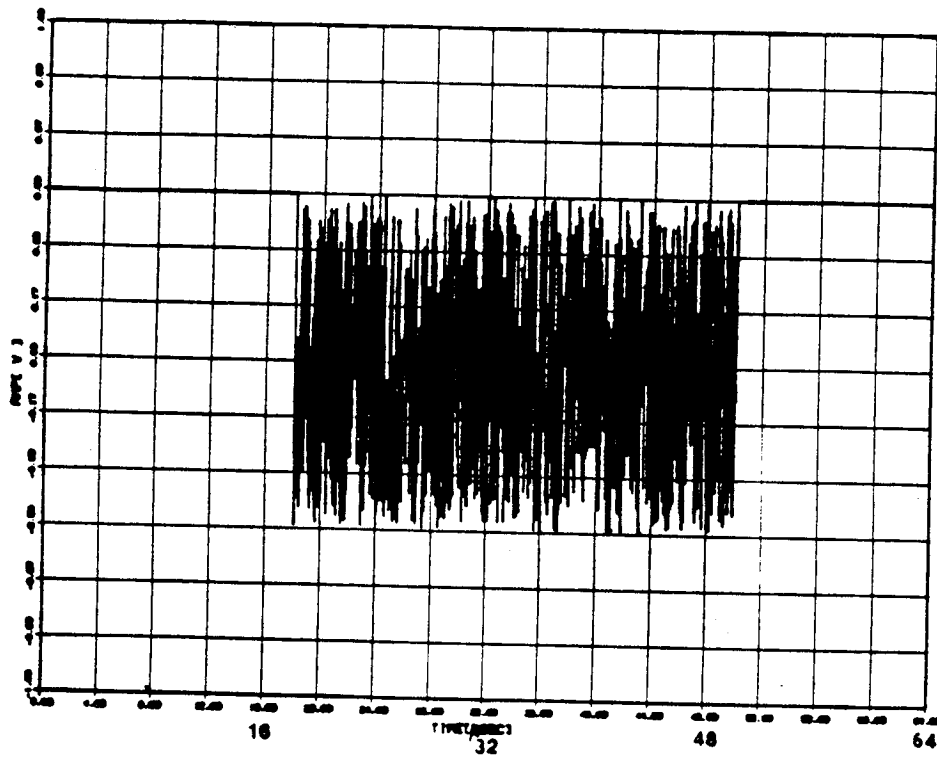


Figure 29. TV message $m(t)$ before preemphasis (time plot) ; random amplitude

ORIGINAL PAGE IS
OF POOR QUALITY

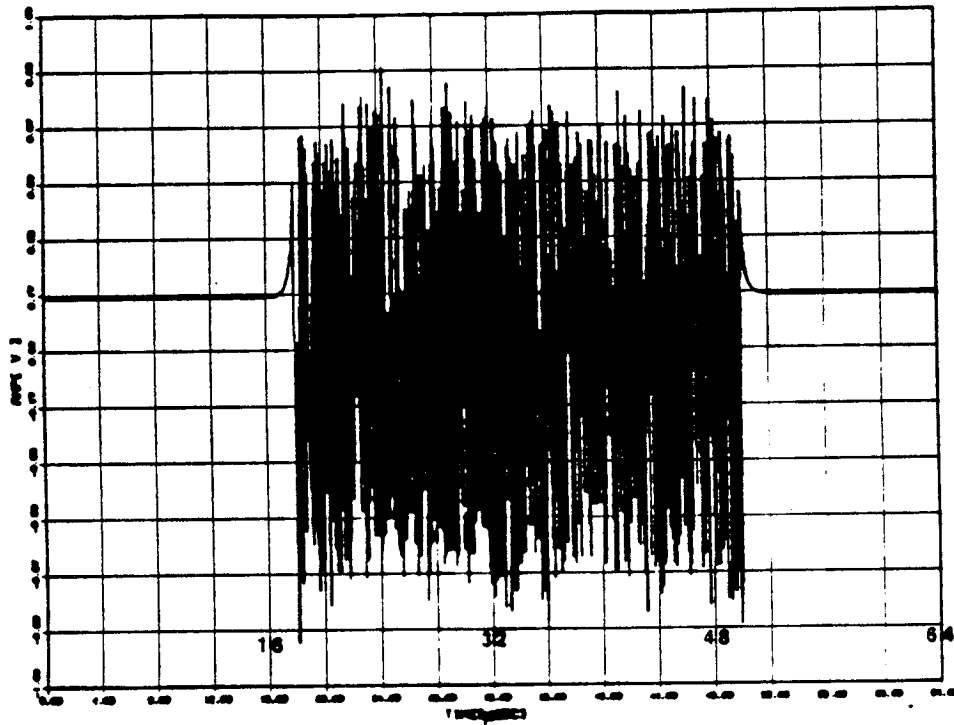


Figure 30. TV message $m(t)$ after preemphasis (time plot) ; random amplitude

ORIGINAL PAGE IS
OF POOR QUALITY

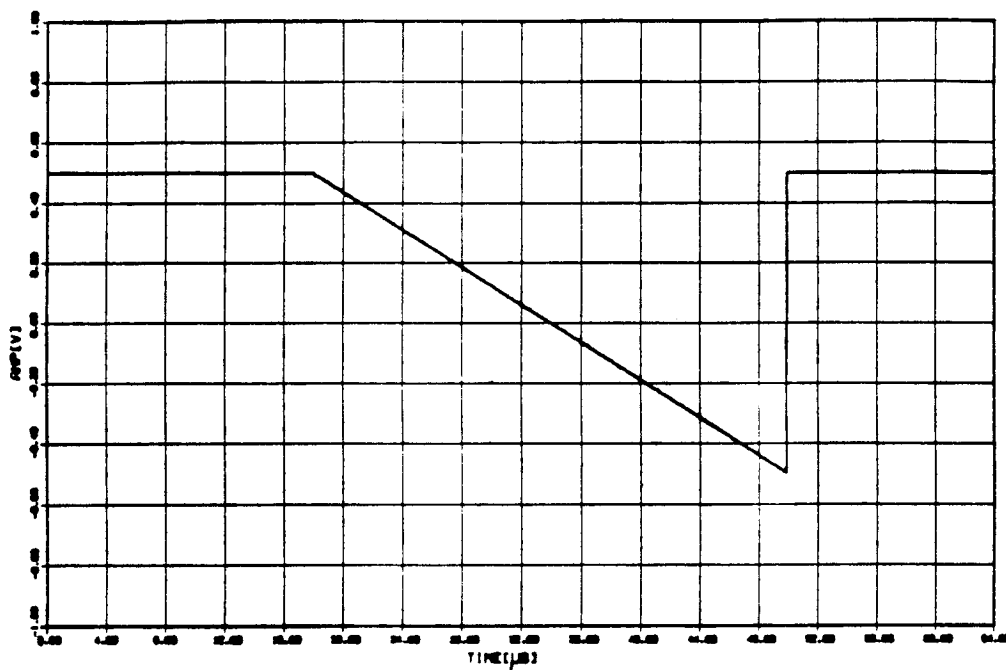


Figure 31. TV message $m(t)$ before preemphasis (time plot); linear staircase function

ORIGINAL PAGE IS
OF POOR QUALITY

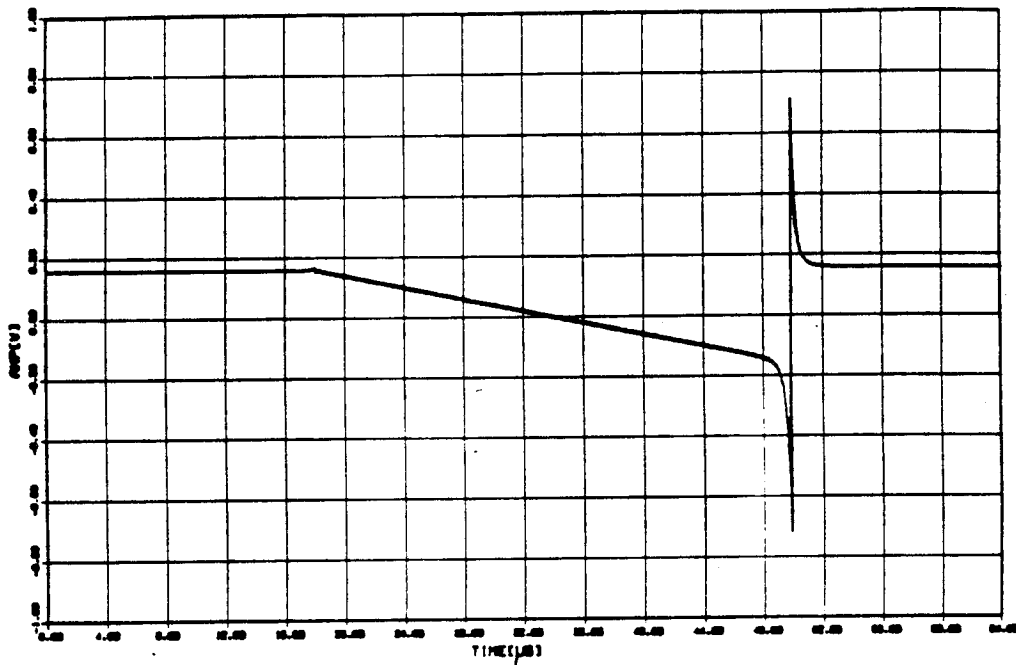


Figure 32. TV message $m(t)$ after preemphasis(time plot); linear staircase function

6.4. Wideband FM television signal simulation II-- with preemphasis

The computer simulation was repeated using the same procedures as were described in Section 6.2, but with the preemphasized video information (message) signals depicted in Fig. 30 and Fig. 32 of the previous section. Fig. 34 shows the frequency spectrum of the transmitted FM-television signal for baseband simulation when the video signal is a preemphasized 200 step staircase function. Fig. 33 illustrates the frequency spectrum of a transmitted FM-television signal for baseband simulation when the video signal is a preemphasized 1024 step random amplitude function. When we compare the transmitted wideband FM television spectra which were preemphasized (Fig. 33 and Fig. 34) with non-preemphasized ones (Fig. 20 and Fig. 22) (i.e., comparing Fig. 20 and Fig. 33 and comparing Fig. 22 and Fig. 34), we can observe that the average power density level at higher frequencies in the preemphasized spectra are raised relative to the non-preemphasis cases. The reason for this can be attributed to the gain factor in the preemphasis curve at the higher frequencies. However, the total average power is the same in all cases because the carrier amplitude of $\sqrt{2}$ is the same for all signals. In an FM signal, the transmitted power depends solely on the carrier amplitude, regardless of the modulating signal.

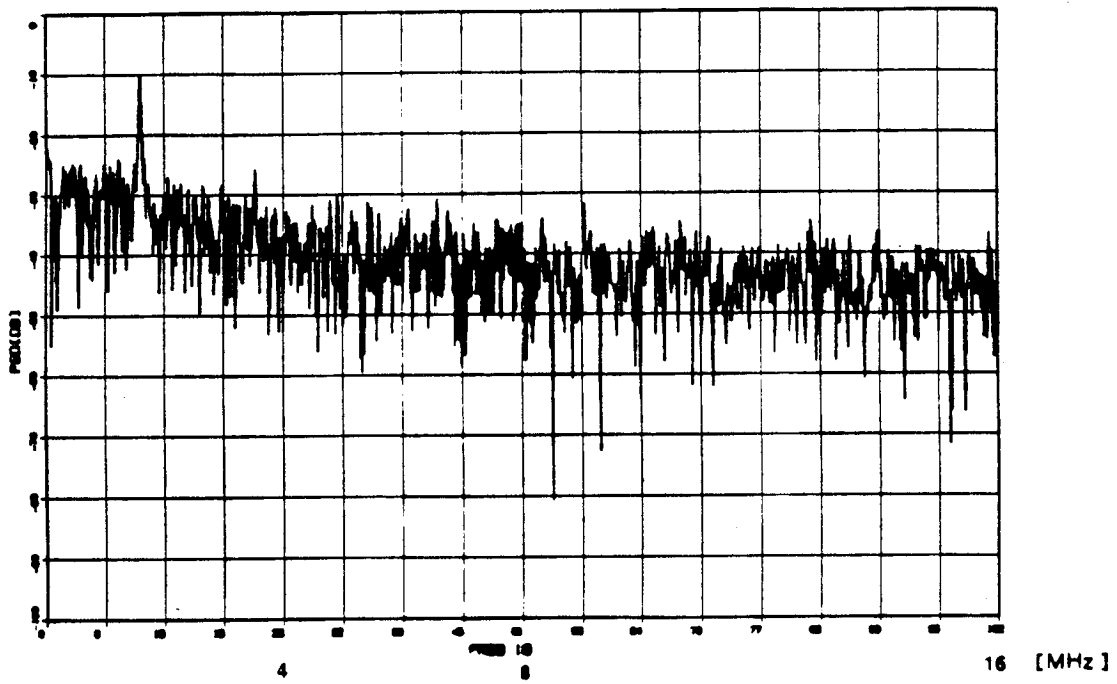


Figure 33. Transmitted FM-TV spectrum ($m(t)$ = random, preemphasis version)

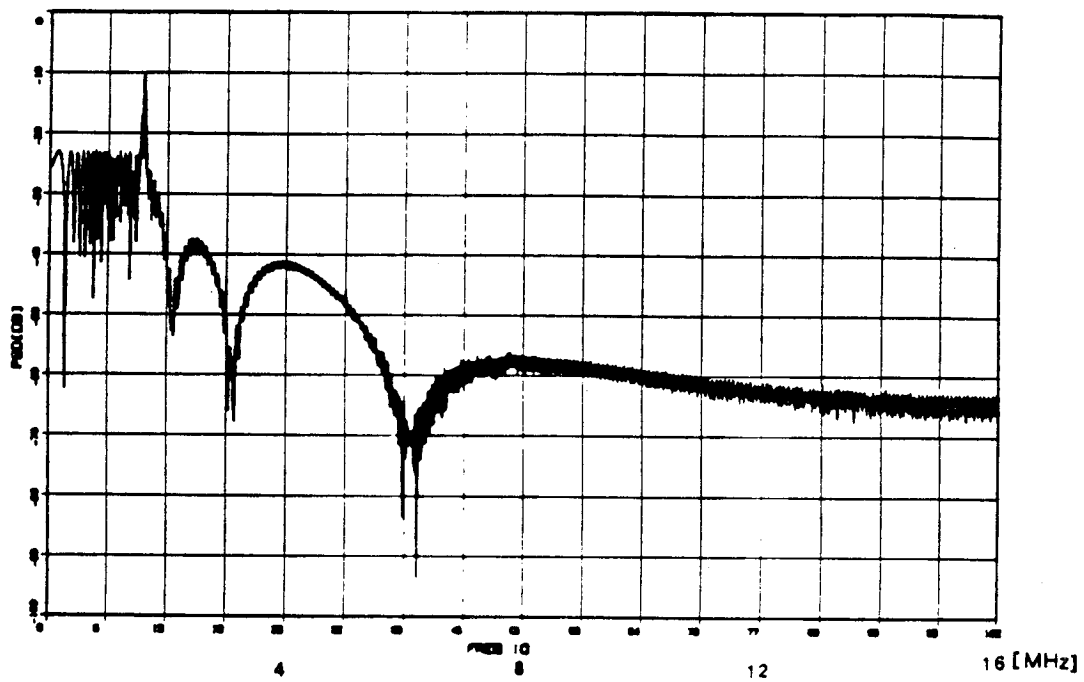


Figure 34. Transmitted FM-TV spectrum (multi-linear, preemphasis version)

6.5 Overlay System Link Analysis

In the previous section, 6.2, we have simulated the transmitted television signal and chirp signal at baseband, and found that a sufficient amount of suppression of the chirp signal permits the overlay of a chirp signal on top of a television signal, and proper compression gain in the chirp demodulator can guarantee successful chirp demodulation. The determination of the parameters in a given system must be obtained through a link analysis.

The major difference between television transmission and chirp via a satellite lies in the power limitation of the earth station in the case of the chirp signal because of the small antenna size and low transmitter power which are assumed for chirp transmission. The other major difference is the receiver bandwidth. Compared to the large IF bandwidth used for FM television, a comparatively narrow IF bandwidth (about 5 MHz) is anticipated for chirp. From this point of view, appropriate selection of the chirp carrier frequency in the 36 MHz transponder bandwidth used for television transmission plays an important role in deciding the carrier to interference ratios (C/I ratio). The final performance measure of the proposed coded multiple chirp s.s. system is the probability of bit (chip) error or word (code) miss probability. For the FM-TV service, the C/I ratio is a measure of degradation caused by chirp overlay.

In this analysis, a typical link using the Galaxy II satellite in C band was used as an example of overlay service. Some key parameter values of "Galaxy II" are listed below.

Galaxy II Parameters [Based on FM-TV Transmission with Chirp Overlay]

Satellite Transponder Parameters

EIRP	34 dBW
G/T	-3 to +3 dBK ⁻¹

Bandwidth 36 MHz

Earth Station Parameters

Antenna Diameter	9.0 m or 2.4 m (for Chirp only)
Aperture Efficiency	65
System Noise Temperature	100K (120K for chirp)
FM-TV Receiver IF BW	32 MHz (5.0 MHz for Chirp)

Desired Performance

Analog FM-TV Down Link	$C/N \geq 10 \text{ dB}$
Chip Error Probability	$P_e \leq 10^{-4}$

The proposed overlay service can be briefly explained here. The high power television signal at 6 GHz is transmitted by a 9 meter antenna and is received by a smaller antenna (2.4 meter in diameter) via the 4 GHz downlink. At the same time, the chirp signal with relatively low power is transmitted through a 2.4 meter antenna and received by the 9 meter antenna. The next two tables shows the FM-television and chirp s.s system link analyses in C-Band.

6.5.1. FM-TV Overlay Link Analysis

Based on the Galaxy II parameters and desired performance crieteria, the link analysis of FM-TV operating in C-band is listed in following Table 1.

Table 1. FM-TV Overlay Link -- C band

Uplink Parameters

Max Transmitter Power	20 dBW (100W)
Antenna Gain (9 m)	53.2 dB
EIRP	73.2 dBW
Path Loss (6 GHz, Clear Air)	200.2 dB
Rain Attenuation	Y dB

Satellite Parameters

Flux Density	-85.0 dBW/m ²
G/T	3.0 dBK ⁻¹
C/N	(30.96- Y) dB

Downlink Parameters

EIRP	37.0 dBW
TWTA Output Backoff	3.0 dB
Path Loss (4 GHz, Clear Air)	196.3 dB
Rain Attenuation	X dB
Rx Antenna Gain (2.4 m)	38.18 dBK ⁻¹
G/T	17.28 dBK ⁻¹
C/N	(8.64- X) dB

6.5.2. Chirp S.S Overlay Link Analysis

As the other phase, chirp spread spectrum overlay link was analyzed as in Table 2. Parameters in this table were found under the assumption that chirp's transmitted EIRP is lower than FM-TV uplink EIRP by 36 dB.

Table 2. Chirp Overlay Link -- C band

Uplink Parameters

Max Transmitter Power	-4.52 dBW (350mW)
Antenna Gain (2.4 m)	41.7 dB
EIRP	37.2 dBW
Path Loss (6 GHz, Clear Air)	200.2 dB
Rain Attenuation	XX dB

Satellite Parameters

Flux Density	-121.0 dBW/m ²
G/T	3.0 dBK ⁻¹
C/N (IF BW = 5.0 MHz)	(1.58 - XX) dB
C/N (IF BW = 40 KHz)	(22.6 - XX) dB

Downlink Parameters

EIRP	[1.0 + (X - XX)] dBW
TWTA Output Backoff	3.0 dB
Path Loss (4 GHz, Clear Air)	196.3 dB
Rain Attenuation	YY dB
G/T	29.66 dBK ⁻¹
Chirp Carrier Power	[-148.6 + (X-XX)-YY] dBW
C/N (IF BW = 5.0 MHz)	-7.04 dB
C/N (IF BW = 40 KHz)	13.94 dB

Probability of Chip Error

1.76×10^{-6}

Note.

1. 36 dB attenuation is given under 36 dB compression gain of chirp
2. the probability of Chip error is base on the formula in sec.3.2.4

7. Performance Analysis of Overlay Service I--Without Preemphasis

In the overlay link analysis in previous section, when the chirp signal EIRP is -36 dB below the FM-television signal EIRP, the final chip error probability for the chirp system is around 1.0×10^{-4} , assuming 2400 bps(hence corresponding chip rate is around 40K chips/sec using 16 bit codewords). However, the link analysis done in previous section does not consider the interference factor when calculating C/N ratio; it cannot be a sufficient proof that the overlay service is safe from mutual interference. Calculation of the C/I ratio is needed, so that we can recalculate the final C/N ratio both in the FM-television demodulator output and in the dechirper output, which will finally give the codeword error(miss) probability.

In the analysis procedure, the signal powers of the television and chirp are calculated first at the earth station receivers. The FM-television signal power and chirp signal power at the receiving earth station are calculated when each signal works as the interfering signal in the overlay service. Finally the C/I ratios for both cases are found and plotted for comparison. Because we dealt with two cases, the preemphasis case and the no-preemphasis case, the analyses will be done separately, then the final results will be compared.

7.1. Signal Power Calculation

A. FM-Television Power

FM-television signal power was set to one watt and it can be calculated by

$$P_{tv} = \frac{1}{2}(A_{tv})^2 = \frac{1}{2}(\sqrt{2})^2 = 1.0 \text{ W}$$

when the transmitted FM-TV signal is expressed by

$$W(t) = \sqrt{2} \cos[\omega_c t + 2\pi f_d \int^t m(\alpha) d\alpha]$$

where $\omega_c = 0$ in the baseband, $f_d = 10$ MHz/Volt, $m(\alpha)$ is a staircase function or random amplitude function. In simulation, once the power spectral density of each data point is obtained, the total power for 2048 samples is the summation of the spectral density over all frequencies, i.e.,

$$P_{tv} = \sum_{i=1}^{n=2048} |x(i)|^2$$

where $|x(i)|^2$ is the power spectral density at the i 'th sample(frequency) point.

The resulting FM-TV signal power calculated by summing spectral density values was:

case1; video signal is 256 step random amplitude function

$$P_v = 1.00537 \text{ W}$$

case2; video signal is 200 step staircase function

$$P_v = 0.97927 \text{ W}$$

When we compare the simulated FM-TV power with theoretical power, they are almost same (within 2.1%).

B. Chirp Signal Power

Let the transmitted chirp signal be given by

$$i(t) = \sqrt{2} \cos[\omega_c t + \frac{1}{2}\mu t^2]$$

then theoretical power is set to one watt:

$$P_{\text{chirp}} = \frac{1}{2}(A_{\text{chirp}})^2 = 1.0\text{W}$$

By computer simulation, we get the simulated chirp power as

$$P_{\text{chirp}} = 0.42213\text{W}$$

The simulated chirp power is 3.7 dB lower than the theoretical value. But, this is expected because the chirp signal is applied only 26 μs of the 64 μs scanning period. Thus, $26/64 = 0.406$ Watt is the correct value. Because the simulated power is within 4% error, it was assumed that the simulation was correct.

C. 36 dB Attenuated Chirp Power

In the link analysis, a chirp signal EIRP of -36 dB relative to FM-TV transmitted EIRP was assumed. Therefore, if we choose a simulated FM-TV power of 1.00537 watt in section A, -36 dB attenuated chirp power would be $1.00537 \times 10^{-3.6} = 0.0002528$ watt. Figure.35 illustrates this attenuated chirp spectrum; in this case, relative to the FM-TV signal of which the video signal is a 256 step random amplitude.[see Figure.24 for comparison.]

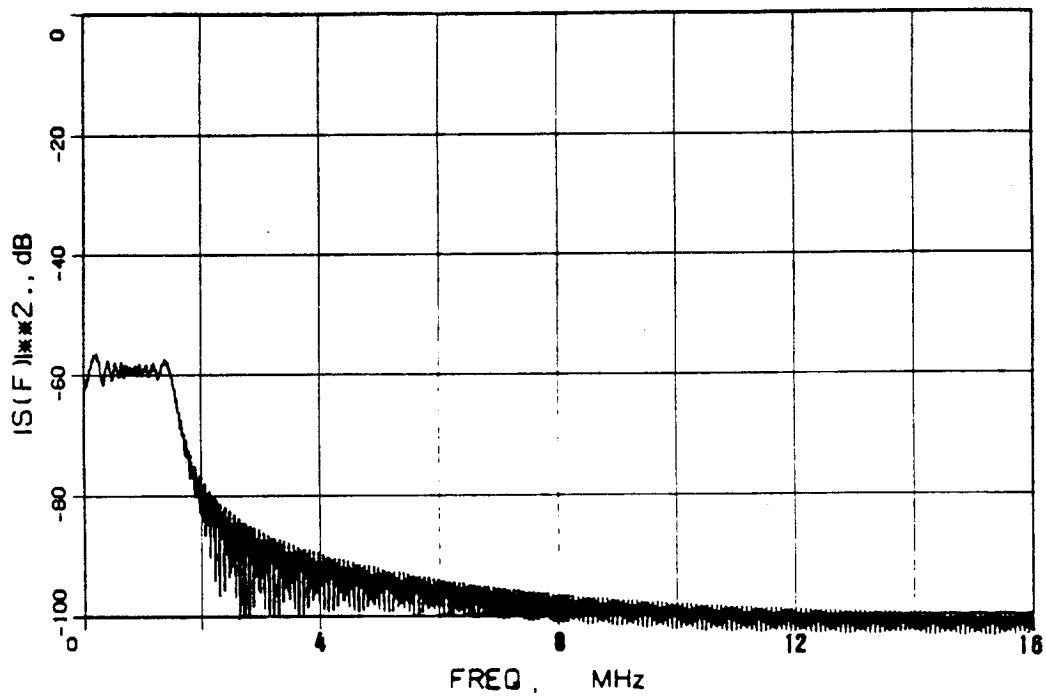


Figure 35. 36 dB attenuated chirp signal spectrum

7.2. Interference Power Calculation

In section 7.1, FM-TV signal power and chirp power at the earth station receiver were found both in theory and by computer simulation. As the second step, we calculated the mutual interference power I , and thus the C/I ratio, when we overlapped the chirp's attenuated spectrum onto the FM-TV signal transponder bandwidth and vice versa.

7.2.1. Chirp Interference to FM-TV

As mentioned earlier, FM-TV signals use the whole 36 MHz transponder bandwidth. but the overlaying signal, in this case the chirp signal, uses a relatively narrower bandwidth. We have already fixed the chirp signal bandwidth at 5.0 MHz in the overlay link analysis. However, because of a restriction of the FFT routine permitting only 2^n number of samples in frequency, a 32 MHz TV bandwidth was assumed. Because of this difference in bandwidth, to calculate the chirp interference into the FM-TV channel, it is necessary to find the power spectral density of chirp signals over a 5 MHz bandwidth. Fortunately the chirp spectrum has a relatively high level and a flat portion below 2.5 MHz. Therefore it is not required to move a 5.0 MHz bandwidth unit to and from the entire 32 MHz (two sided) bandwidth of the spectral plot. [Note: All the spectral plots are drawn only for positive frequency, and the maximum frequency in those plots is 16 MHz.]

We already know that the low power chirp signal has a power of 0.00025W relative to the FM-TV signal of one watt. When we calculated the single sided power of the chirp signal from 0 to 2.5 MHz bandwidth, we got 0.00012W. therefore the total power in a frequency bandwidth of -2.5 MHz to 2.5 MHz is almost the same as 0.00025W. We can conclude that at least 99% of the power in the chirp signal is in the -2.5 MHz to 2.5 MHz range.

7.2.1.A FM-Television C/I Ratio

From the result that almost all of chirp power is in the -2.5 MHz to +2.5 MHz band, with a total power of 0.00025W, there is no difference in C/I ratio if the chirp carrier frequency is located anywhere in the 32 MHz bandwidth used by the FM television signal. In addition, chirp interference is an all pass signal in the wideband television IF filter, so interference power from the chirp loses nothing. Therefore,

$$\frac{C}{I} = \frac{1.000537[\text{W}]}{0.00025[\text{W}]} = 36\text{dB}$$

7.2.1.B Net C/N of FM-TV under chirp Interference.

By the result of 7.2.1.A, C/I is 36 dB. It is necessary to recalculate the C/N for the TV signal because the interference adds to thermal noise and affects the C/N. Because the chirp signal power is 36 dB attenuated relative to the TV signal, the interference power of the chirp signal is calculated as -163.12 dBW at the receiver, based on the FM-TV link analysis. If we regard the interference as another form of noise, the net noise power is -132.76 dBW. Therefore the net C/N under chirp interference is 8.636 dB. When we compare this C/N with the C/N defined in the link analysis, which does not consider the interference, there is almost no difference. Therefore we can conclude that the effect of interference on FM-TV is negligible.

7.2.2. FM-Television Interference on Chirp

As the reverse case of section 7.2.1, interference from FM-TV into the chirp channel, the high powered FM-TV signal is the interference into the chirp channel. Before starting the analysis, the following must be noted:

1. Compared to the wide bandwidth of FM-TV (32 MHz assumed), the chirp bandwidth is narrower at 5 MHz.
2. By (1), contrary to the previous case, only a 5.0 MHz bandwidth portion of the FM-TV power spectrum is interfering with the chirp signal.
3. By (2), there can be a large difference in interference level depending on the IF center frequency offset between the chirp and the TV signal center frequency, within the 32 MHz bandwidth.

7.2.2.A. Chirp C/I Ratio Calculation.

From the result that almost all of chirp power (36 dB attenuated) is located in the -2.5 MHz to 2.5 MHz range, we set the chirp power in a 5.0 MHz bandwidth as $C_{\text{chirp}} = 0.00025W$.

The C/I ratio for the chirp channel depends, in part, on the center frequency used for the chirp signal relative to the center frequency of the FM-TV signal. Figure 36 showing the spectrum of the FM-TV signal indicated that the TV signal has a much higher power spectral density close to the carrier than well away from it. To determine the C/I ratio as a function of frequency offset between the chirp and TV signal carrier frequencies, we shifted the center frequency for the chirp carrier across the 32 MHz band of the FM-TV signal in 0.5 MHz steps, and calculated the power from the TV signal in a 5 MHz bandwidth centered at the chirp carrier.

Table 3 lists all the necessary information when the FM-TV video signal is modeled by a 256 step random amplitude function and when the FM-TV video signal is modeled by a 200 step staircase function. As can be seen from Table 3, when the IF offset frequency approaches the positive maximum (or negative maximum) (far from the center frequency), the C/I ratio gets better. In addition, when the FM-TV signal is modeled by a staircase function, the C/I ratio is much better than that of the random amplitude function. This is expected because the spectrum of the FM-TV signal in this case (staircase function model) is decaying faster than that of the random amplitude case. Figure 36 and Figure 37 show the overlaid spectral plots of the FM-TV spectrum modeled by a staircase function (Figure 36)

and the FM-TV spectrum modeled by a random amplitude (Figure 37), with a 36 dB attenuated chirp spectrum. As a graphical representation, the C/I ratio vs IF offset frequency for both cases of FM-TV interference signal are drawn in Figure 38. Based on Table 3, when the chirp IF center frequency is located at 12.5 MHz from the center frequency of the FM-TV signal, the corresponding C/I ratio is -5.56 dB. The reason why the best C/I ratio is selected from Table 3, where the message signal (video) model is a random amplitude function, is that this should be a worst case analysis. Then the net C/N (E_b/N_o) recalculated for the existence of FM-TV interference, is -9.37 dB. When we compare this value with the C/N ratio in the earlier link analysis, about 1 dB degradation occurs because of the FM-TV interference. Finally, if we assume 23 dB compression gain, the C/N ratio after the compression filter will be +14dB, the corresponding probability of chip (bit) error will be around 5×10^{-6} . In this case, the data rate is around 25 kbps.

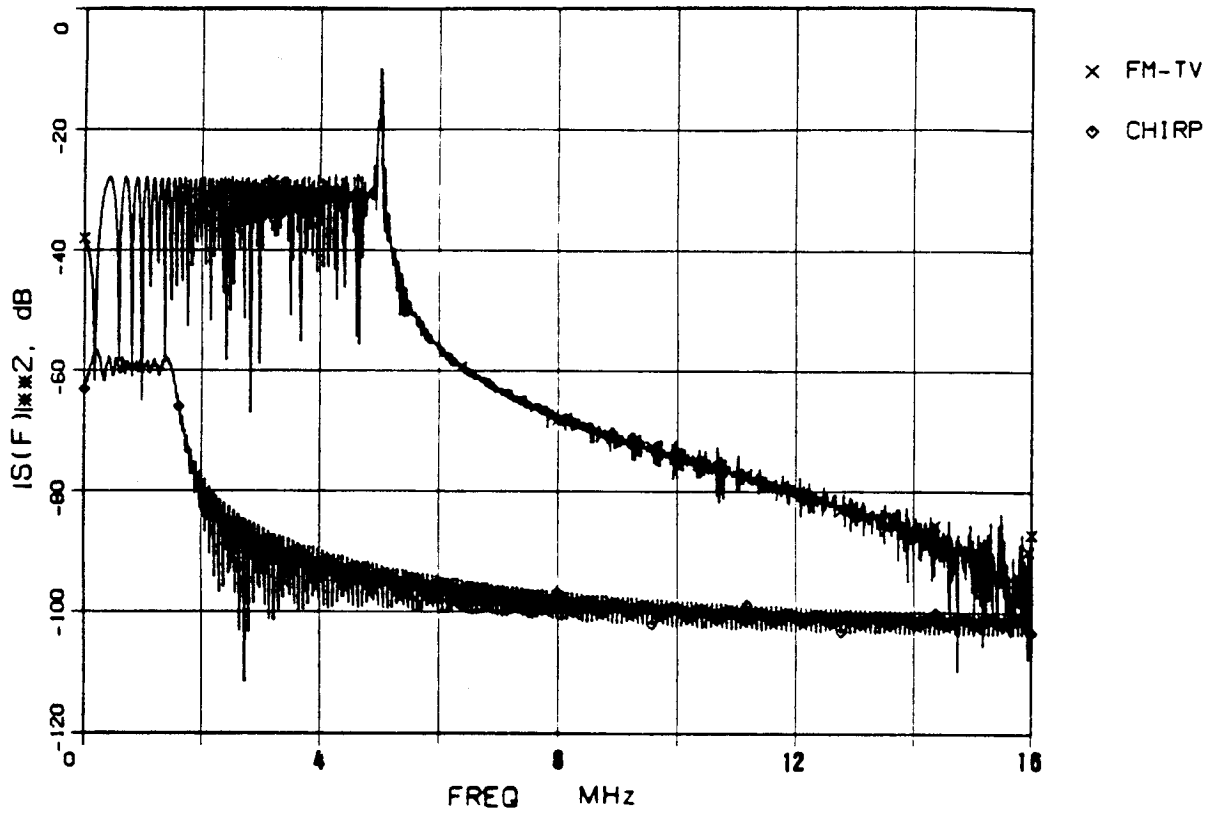


Figure 36. Overlapped spectrum of FM-TV (m(t) = linear stair) and 36 dB attenuated chirp

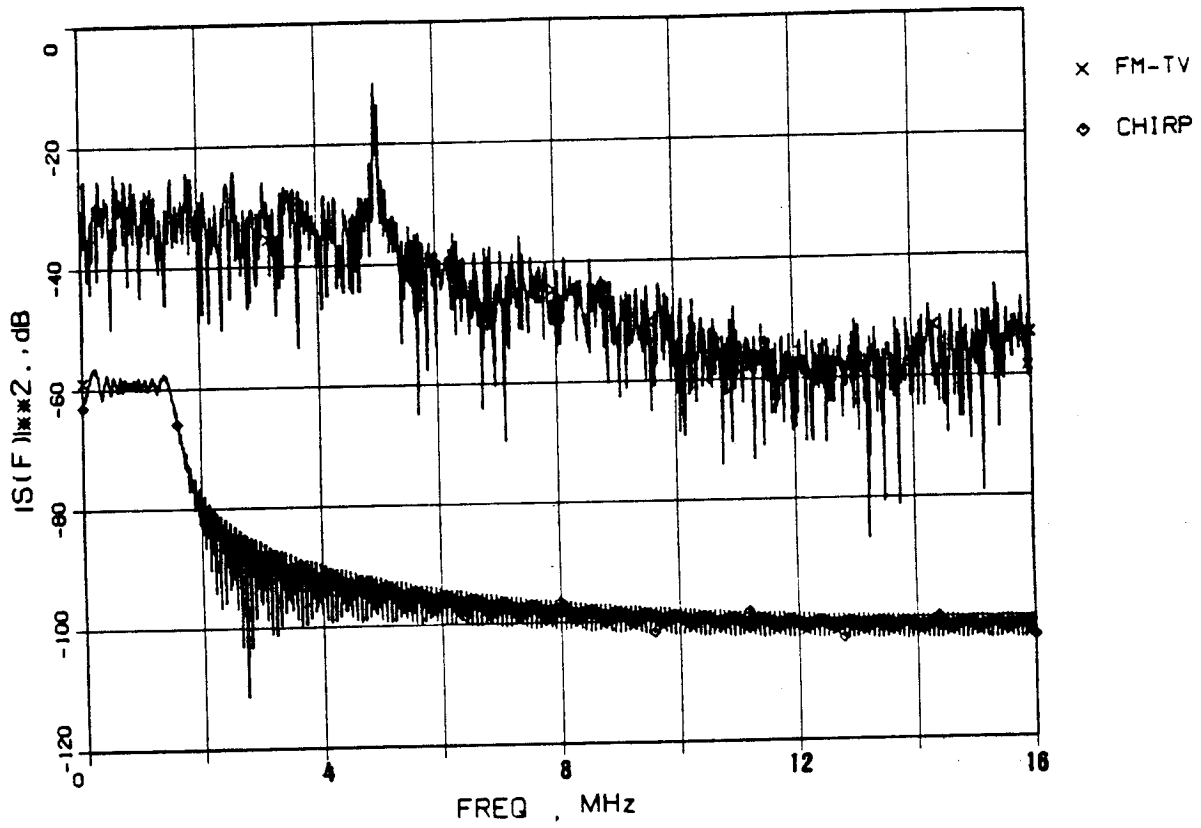


Figure 37. Overlapped spectrum of FM-TV ($m(t)$ = random amplitude) and 36 dB attenuated chirp

Table 3. C/I ratio vs IF offset for FM-TV spectrum [No preemphasis] [m(t): 256 step random function and 200 step linear step function]

Leading freq [MHz]	Trailing freq [MHz]	Offset freq [MHz]	256 step random		200 step linear	
			5 MHz BW TV POWER [w]	C/I [dB]	5 MHz BW TV POWER [w]	C/I [dB]
2.5	-2.5	0.0	0.289	-30.6	0.240	-29.8
3.0	-2.0	0.5	0.287	-30.6	0.239	-29.8
3.5	-1.5	1.0	0.274	-30.3	0.238	-29.8
4.0	-1.0	1.5	0.275	-30.4	0.238	-29.8
4.5	-0.5	2.0	0.253	-30.0	0.242	-29.8
5.0	0.0	2.5	0.414	-32.2	0.387	-31.9
5.5	0.5	3.0	0.459	-32.6	0.471	-32.8
6.0	1.0	3.5	0.426	-32.3	0.449	-32.5
6.5	1.5	4.0	0.407	-32.1	0.422	-32.2
7.0	2.0	4.5	0.375	-31.8	0.396	-32.0
7.5	2.5	5.0	0.353	-31.5	0.369	-31.7
8.0	3.0	5.5	0.332	-31.2	0.344	-31.4
8.5	3.5	6.0	0.307	-30.9	0.318	-31.0
9.0	4.0	6.5	0.285	-30.5	0.292	-30.6
9.5	4.5	7.0	0.272	-30.4	0.266	-30.3
10.0	5.0	7.5	0.086	-25.4	0.103	-26.1
10.5	5.5	8.0	0.013	-17.4	0.000	0.0
11.0	6.0	8.5	0.010	-16.1	0.0002	4.4
11.5	6.5	9.0	0.007	-14.6	0.0001	6.9
12.0	7.0	9.5	0.005	-13.7	---	---
12.5	7.5	10.0	0.004	-12.2	---	---
13.0	8.0	10.5	0.003	-10.8	---	---
13.5	8.5	11.0	0.002	-9.4	---	---

14.0	9.0	11.5	0.001	-7.4	---	---
14.5	9.5	12.0	0.001	-6.6	---	---
15.0	10.0	12.5	0.001	-5.6	---	---
15.5	10.5	13.0	0.001	-5.7	---	---
16.0	11.0	13.5	0.001	-5.9	---	---

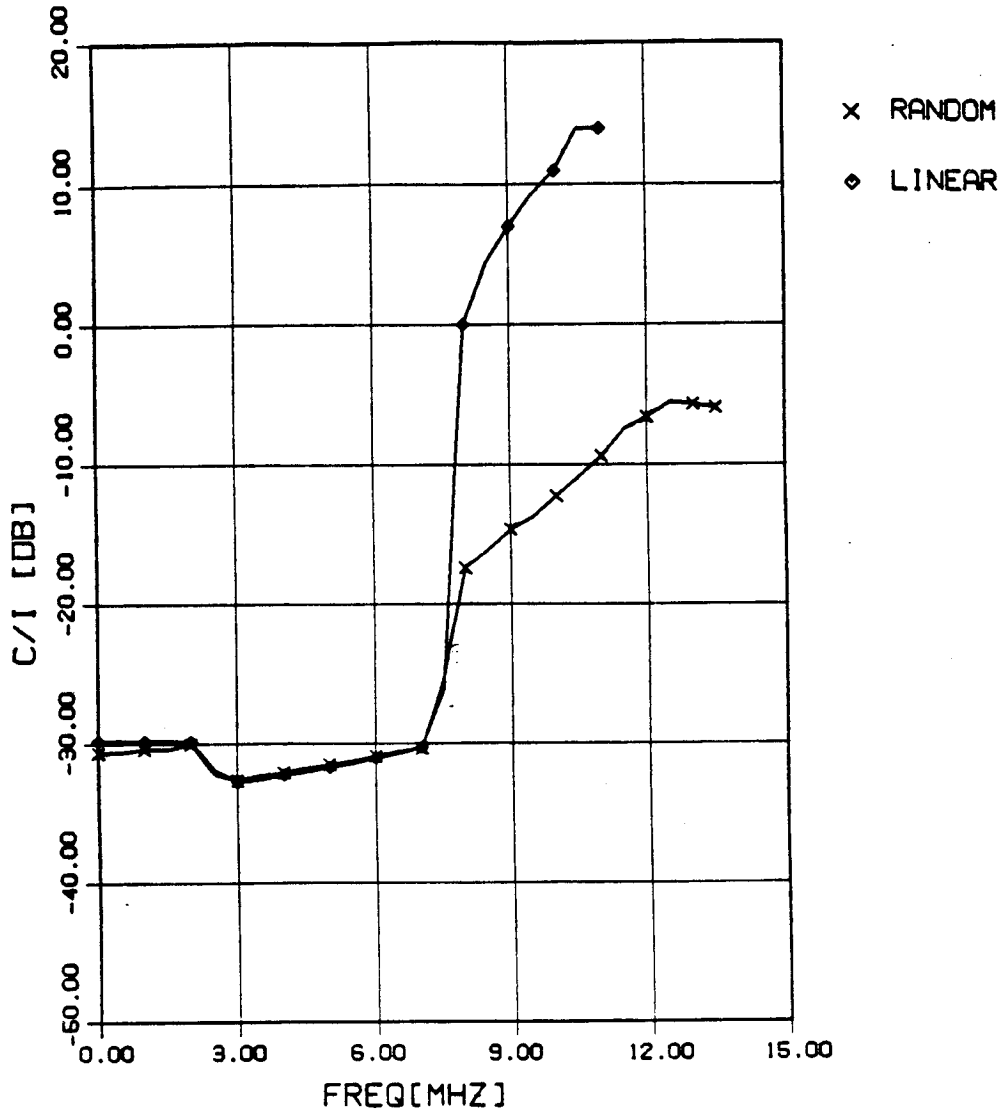


Figure 38. C/I ratio vs IF offset frequency (message are linear stair and random amplitude)

8. Performance Analysis of Overlay Service II- With Preemphasis

In chapter 7, we have analyzed the interference effects in an overlay service, but without preemphasis filtering at the input video signal to the FM-TV modulator. In this section, the same procedures as in section 4 are repeated for the case when preemphasis is considered. Based on the spectrum and time plots of the transmitted wideband signal in section 6.4, the chirp signal is also attenuated by 36 dB relative to the FM-TV signal spectrum. Figure 39 and Figure 40 show the overlapped spectra of chirp and FM-TV signals. For simplicity and to avoid repetitive explanation, only the result of the calculations are described here.

8.1. Signal Power

1. FM-TV signal power (by simulation)

- <Case 1> when video signal is modeled by random amplitude, the TV power is 1.00507 W

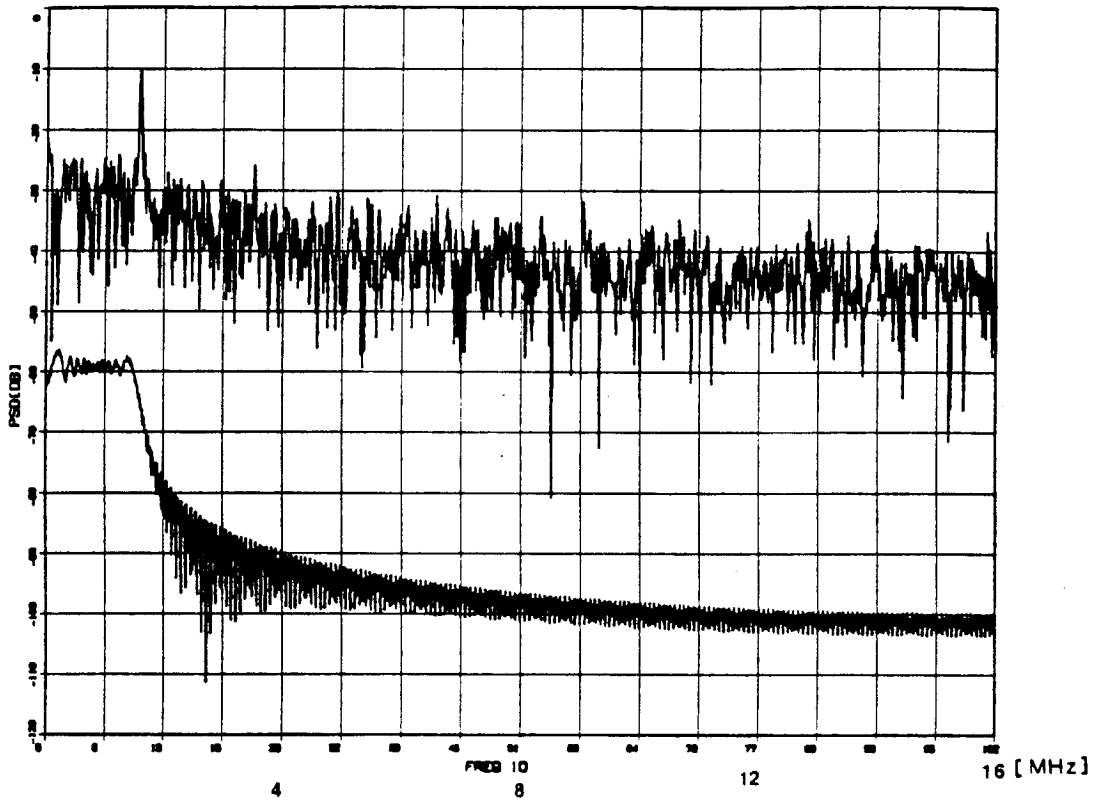


Figure 39. Overlapped spectrum of FM-TV (preemphasis) and 36 dB attenuated chirp(random)

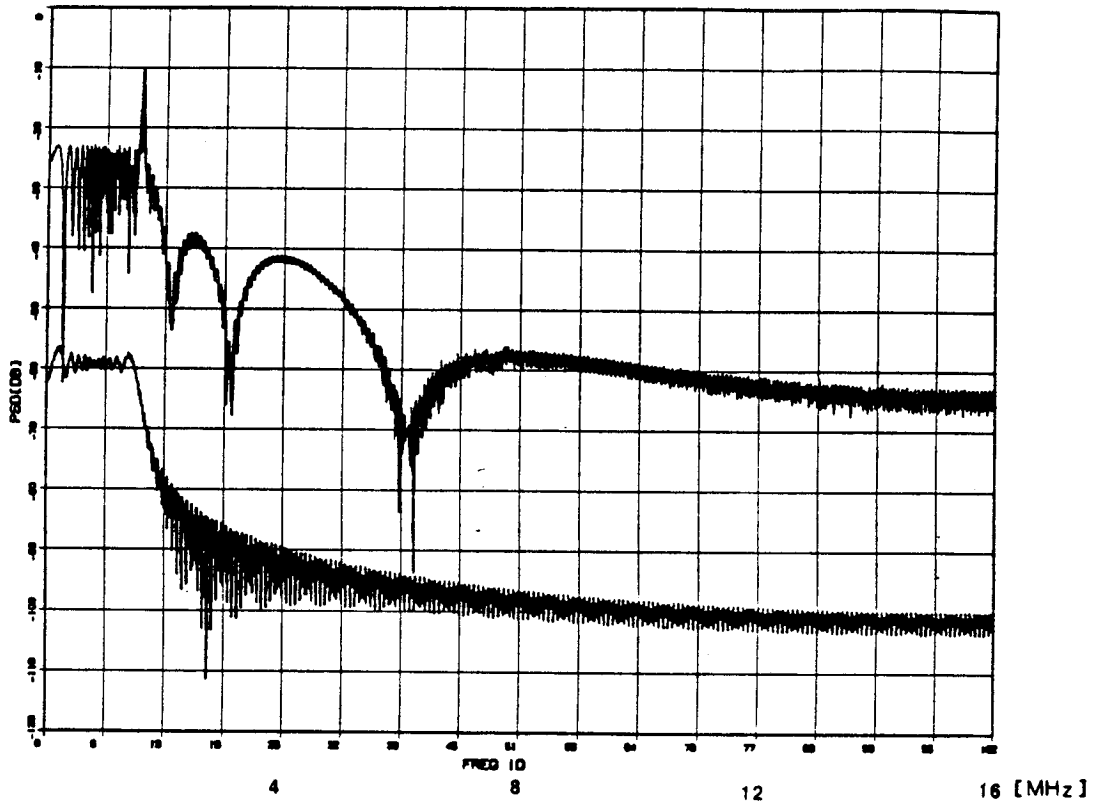


Figure 40. Overlapped spectrum of FM-TV (preemphasis) and 36 dB attenuated chirp(linear stair)

- <Case 2> when video signal is modeled by staircase function, the TV power is 1.02763 W
2. Chirp signal power is same as before because preemphasis is not applied to the chirp signal. However after 36 dB attenuation, it turn out to be 0.00025 W. Because the simulated TV power is within 1% error from the theoretical value of 1.0W, we need no normalization of the FM-TV spectrum. In addition, the 36 dB attenuated chirp power can be used as before.

8.2 Interference of Chirp to FM-TV

By using the same procedures in section 6.2.2.A, almost all the chirp power is in the -2.5 MHz to 2.5 MHz bandwidth. Therefore, $I=0.00025$ W and $C=1.00537$ W, and the C/I ratio will be 36 dB. In addition, the net C/N ratio of FM-TV under chirp interference is the same as before because the C/I ratio is the same as before.

8.3 Interference of FM-TV into chirp channel.

By following the same procedure as in section 6-2-3, Table 4 can be obtained for the case when the FM-TV video signal is modeled by random amplitude function and the FM-TV video signal is modeled by the staircase function, respectively. Figure 41 illustrates the C/I ratios versus IF offset frequencies for the different video signal models. Figure 42 depicts the four cases of C/I ratio vs IF offset frequencies. One pair is for the cases when preemphasis is used and the other pair is for the cases when no preemphasis is used. In Figure 42, the C/I ratio still maintains the trend that C/I ratio gets better as the TV carrier frequency goes away from the chirp IF center frequency. In Figure 42, we can observe the effect of preemphasis. The use of preemphasis in the FM-TV video signal,

regardless of the modulation applied, degrades the C/I ratio approximately 15-20 dB in general. Figure 43 shows the calculated chip error rate when the C/N of the chirp signal is found for the case of FM-TV signal interference. From the result for FM-TV interference, the final C/N ratio of the chirp signal is found to be -20 dB before compression. If 23 dB compression gain is provided, the probability of chip error is around 10^{-1} . When this is compared to the case for no preemphasis in chapter 6, about 10^5 times more error can occur in the preemphasis case. However, the compression gain can be arbitrarily increased up to 10000 using recent advanced technology, although the cost may be a critical factor. Around 5-10 dB increase in processing gain can be used to compensate for this degradation caused by preemphasis filtering.

Table 4. C/I ratio vs IF offset for FM-TV spectrum[With Preemphasis] [m(t): 256 step random function and 200 step linear step function]

Leading freq [MHz]	Trailing freq [MHz]	Offset freq [MHz]	256 step random		200 step linear	
			5 MHz BW TV POWER [w]	C/I [dB]	5 MHz BW TV POWER [w]	C/I [dB]
2.5	-2.5	0.0	0.788	-34.5	1.001	-36.1
3.0	-2.0	0.5	0.788	-34.5	1.001	-36.1
3.5	-1.5	1.0	0.551	-33.4	0.752	-34.8
4.0	-1.0	1.5	0.523	-33.2	0.682	-34.4
4.5	-0.5	2.0	0.497	-33.0	0.605	-33.8
5.0	0.0	2.5	0.442	-32.5	0.511	-33.1
5.5	0.5	3.0	0.393	-32.0	0.417	-32.2
6.0	1.0	3.5	0.365	-31.6	0.339	-31.1
6.5	1.5	4.0	0.332	-31.2	0.266	-30.3
7.0	2.0	4.5	0.087	-25.4	0.011	-16.1
7.5	2.5	5.0	0.069	-24.5	0.007	-14.8
8.0	3.0	5.5	0.061	-23.9	0.005	-13.4
8.5	3.5	6.0	0.052	-23.1	0.005	-13.0
9.0	4.0	6.5	0.043	-22.3	0.003	-11.0
9.5	4.5	7.0	0.041	-22.1	0.001	-7.4
10.0	5.0	7.5	0.035	-21.5	0.0005	-3.5
10.5	5.5	8.0	0.033	-21.1	0.0003	-1.5
11.0	6.0	8.5	0.031	-20.9	0.0003	-1.5
11.5	6.5	9.0	0.028	-20.5	0.0004	-1.7
12.0	7.0	9.5	0.025	-20.1	0.0004	-1.7
12.5	7.5	10.0	0.024	-19.8	0.0003	-1.2
13.0	8.0	10.5	0.022	-19.4	0.0003	-1.2
13.5	8.5	11.0	0.021	-19.2	0.0002	-0.1

14.0	9.0	11.5	0.020	-19.2	0.0002	0.5
14.5	9.5	12.0	0.018	-18.6	---	---
15.0	10.0	12.5	0.018	-18.7	---	---
15.5	10.5	13.0	0.017	-18.2	---	---
16.0	11.0	13.5	0.015	-17.9	---	---

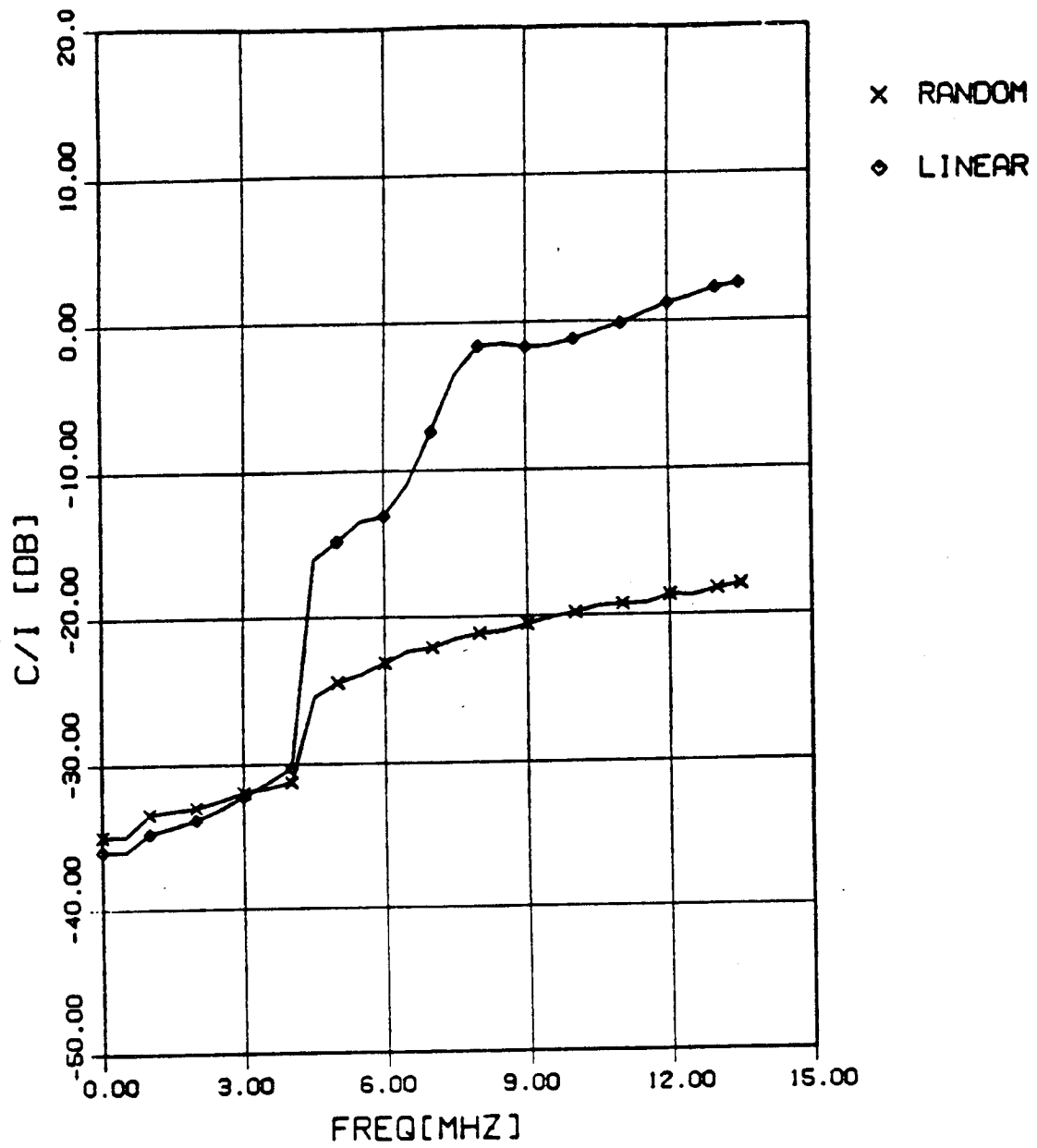


Figure 41. C/I ratio vs IF offset frequency (preemphasis case)

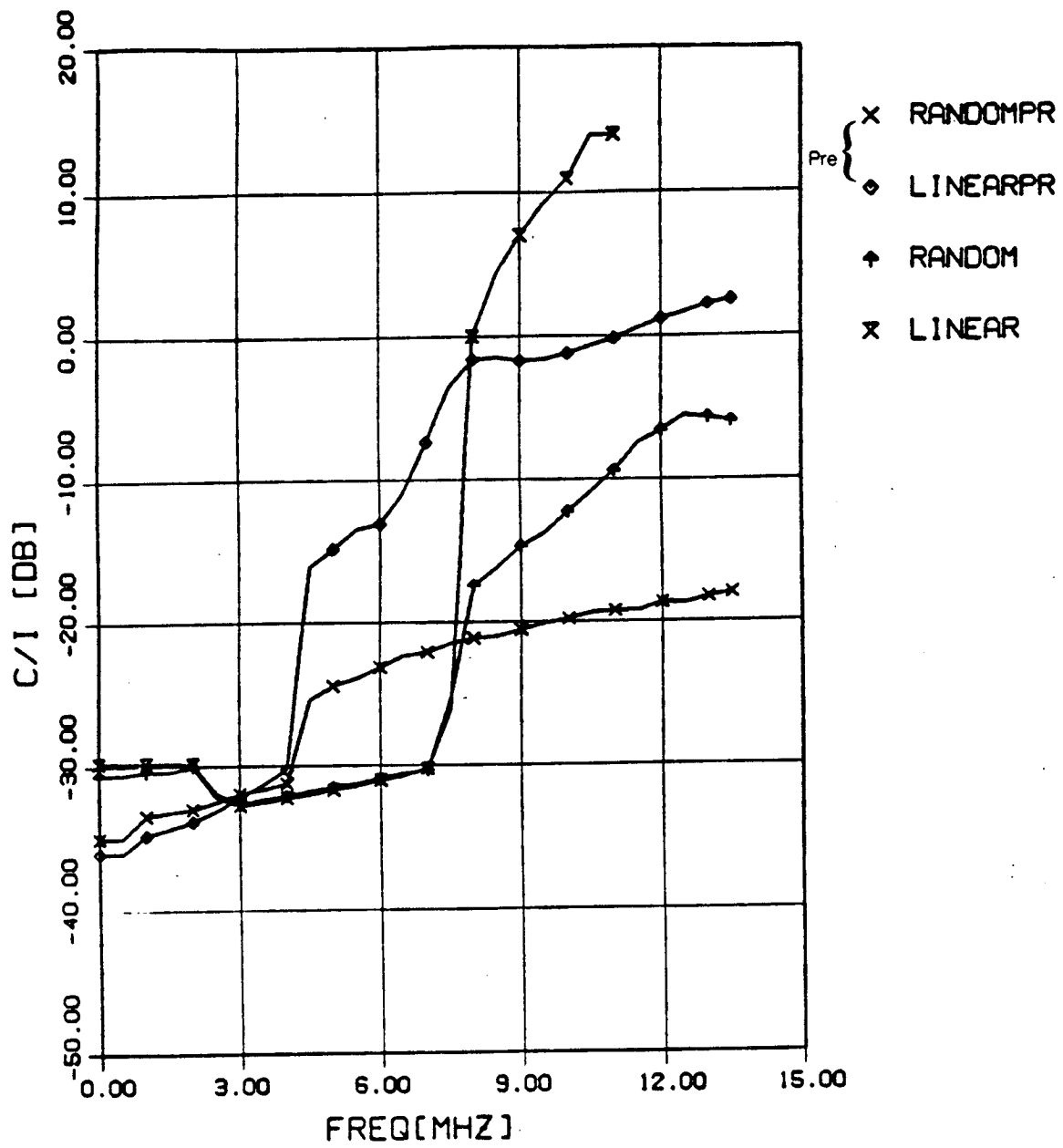


Figure 42. C/I ratio vs IF offset frequency(preemphasis case and no preemphasis case)

ORIGINAL PAGE IS
OF POOR QUALITY

Data Rate
x CO-21DB : 39.7 kbps
♦ CO-23DB : 25.1
♦ CO-27DB : 10
x CO-30DB : 5
x CO-33DB : 2.5

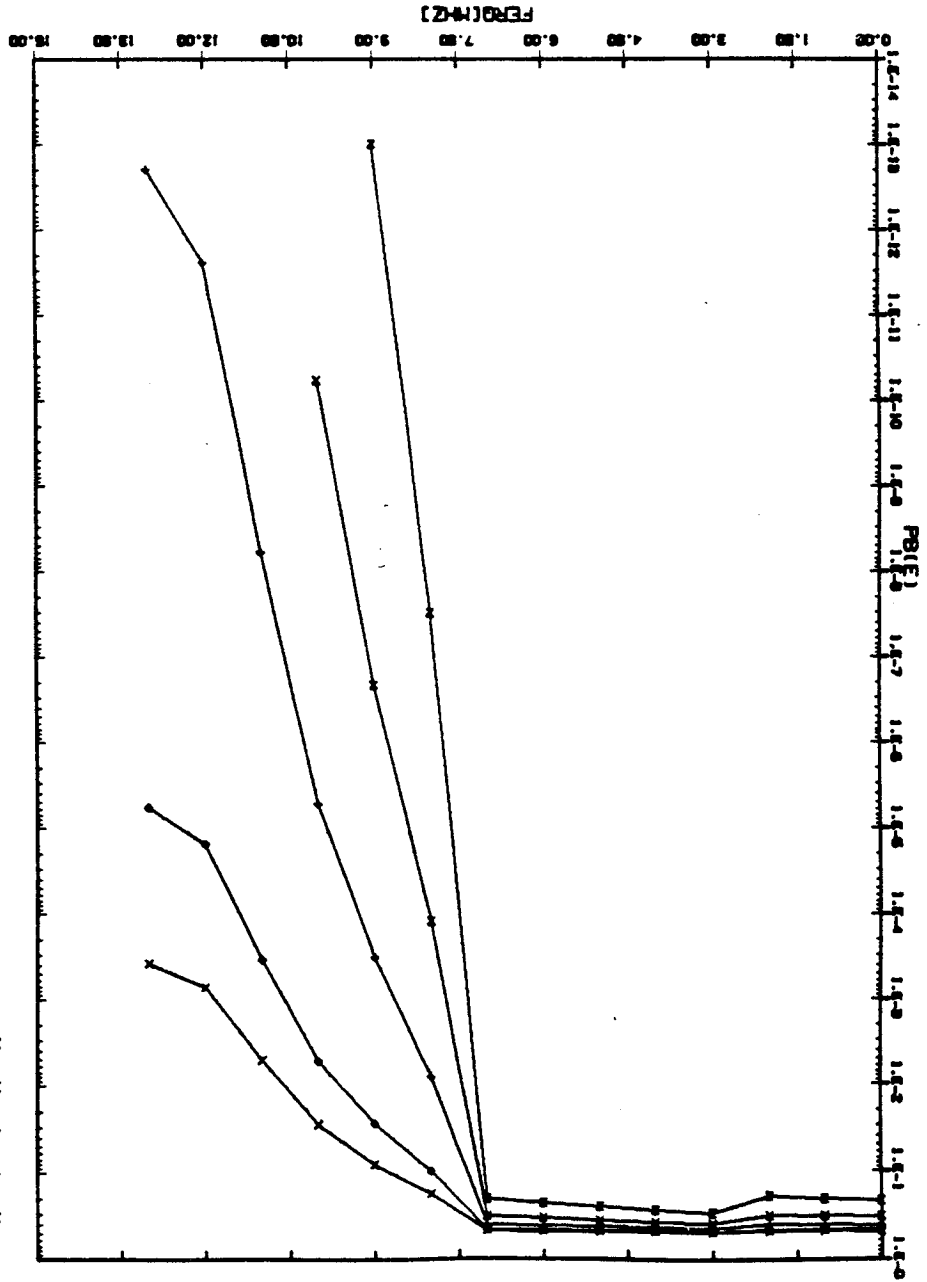


Figure 43. Offset(F) frequency vs chip error rate for some compression gains

9. Conclusions

Multiple-coded chirp has been proposed as a valuable spread spectrum communication technique for low data rate services. It avoids the difficult and lengthy synchronization process of all direct sequence spread spectrum systems, making it especially valuable for low duty-cycle applications.

Chirp can be used to overlay an FM-TV channel provided the chirp center frequency is offset from the TV carrier. Study of a satellite channel carrying a TV signals shows that two chirp signals with data rate up to 25 kbps could be overlaid in a 36 MHz transponder without significant mutual interference.

Performance estimates for a VSAT earth station operating at C-band show that a 2.4 meter antenna and 300 mW transmitter could send a 2.4 kbps signal to a large central earth station over an occupied channel.

10. References

1. J. R. Klauder, et al. "The Theory and Design of Chirp Radars," Bell System Technical Journal, vol. 29, No. 4, July 1960.
2. V. Ramanan, "An Asynchronous Multiple Access Scheme for Satellite Communications," Ph.D. Dissertation, Department of Electronic and Electrical Engineering, University of Birmingham, England, June 1983.
3. R. S. Berkowitz, "Modern Radar," John Wiley, New York, NY, 1965.
4. C. E. Cook, M. Bernfeld, "Radar Signals", Academic Press, New York, NY, 1967.
5. H. O. Ramp, E. R. Wingrove. "Principles of Pulse Compression," IRE Trans. Military Electronics, vol. MIL-5, April 1961, pp. 109-116.
6. R. C. Dixon, "Spread Spectrum Systems," John Wiley, New York, NY, 1976.
7. M. R. Winkler, "Chirp Signals for Communications," IEEE WESCON Convention Record, 1962.

8. E. K. Holland-Moritx, J. C. Dute, and D. R. Brundage, "Swept Frequency Modulation," Proc. Nation. Electron. Conf. vol. 22, 1966, pp. 469-474.
9. A. J. Berni, W. D. Gregg, "On the Utility of Chirp Modulation for Digital Signaling," IEEE Trans. Comm., vol. COM-21, June 1973, pp. 748-751.
10. W. Hirt, S. Pasupathy, "Continuous Phase Chirp (CPC) Signals for Binary Data Communications," IEEE Trans. Comm. vol. COM-29, June 1981, pp. 836-858.
11. D. S. Dayton, "Coming to Grips with Multipath Ghosts," Electronics, vol. 40, Nov. 1967, pp 104-108.
12. G. F. Gott, J. P. Newsome, "HF Data Transmission Using Chirp Signals," Proc. Inst. Elec. Eng., vol. 118, pp. 1162-1166, Spet 1971.
13. G. W. Barnes, D. Hirst, D. J. James, "Chirp Modulation System in Aeronautical Satellite," AGARD Conf. Proc., No. 87, Avionics in Spacecraft, Royal Aircraft Establishment, Rome, Italy, 1971.
14. Max Kowatsch, J. T. Lafferl, "A Spread-Spectrum Concept Combining Chirp Modulation and Pseudonoise Coding," IEEE Trans., vol. COM-30, No. 10, Oct. 1983, pp. 1122-1142.
15. P. W. Baier, R. Simons, H. Waibel, "Chirp-PN-PSK Signale als Spread - Spectrum - Signalformen geringer Dopplerempfindlichkeit and grosser Signalformvielhalt," NTZ Archiv. vol. 3, pp. 29-33. Feb. 1981.
16. M. Kowatsch, F. J. Siefert, J. Lafferl, "Comments on Transmission System Using Pseudonoise Modulation of Linear Chirps," IEEE Trans. Aerosp. Electron. System, vol. AES-17, pp. 300-303, Mar. 1981.
17. R. Gold, "Characteristic Linear Sequences and Their Coset Functions," J. Soc. Ind. Appl. Math. May 1965.

18. T. Kasami, "Weight Distribution Formula for Some Class of Cyclic Codes," University of Illinois, Urbana, Rept. R-265, Apr. 1966.
19. C. E. Cook, "Pulse Compression - Key to More Efficient Radar Transmission," Proc. of IRE, vol. 48, pp. 310-316, Mar. 1960.
20. B. A. Carlson, "Communications Systems, McGraw Hill," 1975
21. M. Cohn, W. L. Eastman, "A Class of Balanced Binary Sequence with Optimal Autocorrelation Properties" IEEE Trans. Inform. Theory, vol. IT-23, pp.38-42, 1977.
22. D. V. Sarwate, M. B. Pursley, "Crosscorrelation Properties of Pseudorandom and Related Sequences," Proc. of IEEE, vol. 68m No. 5, pp. 593-619, May 1980.
23. D.V. Sarwate, "Bound on cross-correlation and autocorrelation of sequences," IEEE Trans. Inform. Theory, vol. IT-25, pp 720-724, 1979.
24. S. Stein, "Unified Analysis of Certain Coherent and Non-Coherent Binary Communications Systems," IEEE Trans. Inform. Theory, vol. IT-10, pp. 43-51, Jan. 1964
25. C. W. Helstrom, "Resolution of Signals in White Gaussian Noise," Proc. IRE, vol. 43, pp. 1111-1118. Sept. 1955.
26. L. W. CouchII, "Digital and Analog Communication Systems," pp. 362-364, MacMillan, New York, NY 1983.
27. T. Pratt, C. W. Bostian, "Satellite Communications," John Wiley, Inc., New York, NY 1986. pp. 241-242.
28. R. M. Gagliardi, "Satellite Communications," Lifetime Learning Publications, Belmont, CA. 1983. pp. 248.

29. K. Feher, "Digital Communications," Prentice-Hall, NJ, 1983, pp. 375-379.
30. F. G. Stremler, "Introduction to Communication Systems," Addison- Wesley, 1982, pp.338-341.
31. R. L. Freeman, "Telecommunication Transmission Handbook," John Wiley, Inc., Boston NY 1981, pp.194.
32. M. A. Maggenti, "Spread Spectrum Multiple Access and Overlay Service," M.S. Thesis, VPI&SU, Mar 1987.
33. D. M. Jansky, M. C. Jeruchim, "Communication Satellite in Geostationary Orbit," Artech House, 1983, pp.482-485.
34. CCIR: XIV'th Plenary Assembly, Kyoto, Japan, vol.4, Report 464 on "Pre-emphasis Characteristics for Frequency Modulation Systems for FDM Telephony in the Fixed Satellite Service," Genova, 1978.

